

NASA Contractor Report 3439

Wind Tunnel Force and Pressure Tests of a 13% Thick Medium Speed Airfoil With 20% Aileron, 25% Slotted Flap and 10% Slot-Lip Spoiler

W. H. Wentz, Jr.
Wichita State University
Wichita, Kansas

Prepared for
Langley Research Center
under Grant NSG-1165

NASA

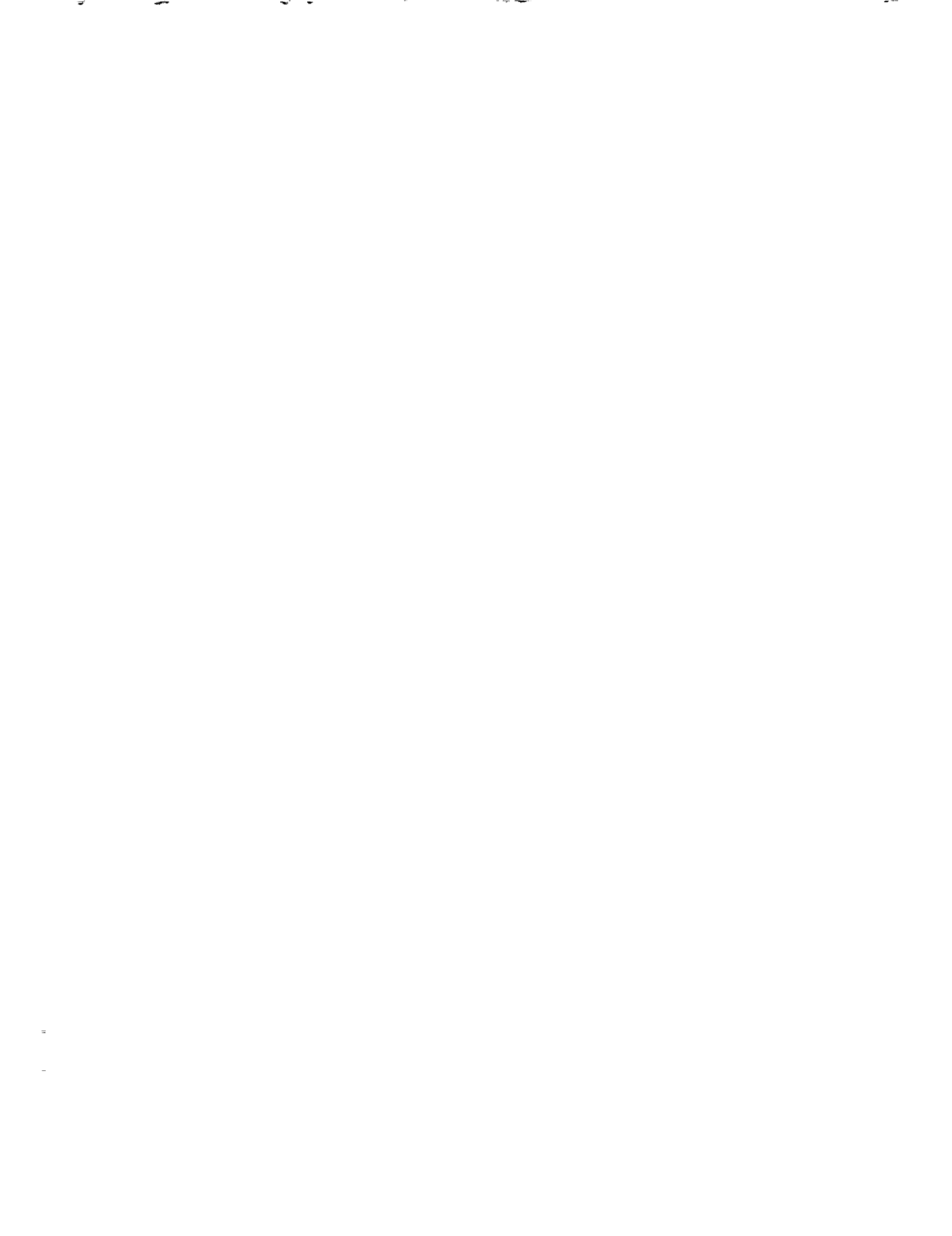
National Aeronautics
and Space Administration

**Scientific and Technical
Information Branch**

1981

SUMMARY

Force and surface pressure distributions have been measured for a 13% medium speed (NASA MS(1)-0313) airfoil fitted with 20% aileron, 25% slotted flap and 10% slot-lip spoiler. All tests were conducted in the Walter Beech Memorial Wind Tunnel at Wichita State University at a Reynolds number of 2.2×10^6 and a Mach number of 0.13. Results include lift, drag, pitching moments, control surface normal force and hinge moments, and surface pressure distributions. The basic airfoil exhibits low speed characteristics similar to the GA(W)-2 airfoil. Incremental aileron and spoiler performance are quite comparable to that obtained on the GA(W)-2 airfoil. Slotted flap performance on this section is reduced compared to the GA(W)-2, resulting in a highest $c_{l_{\max}}$ of 3.00 compared to 3.35 for the GA(W)-2.



INTRODUCTION

As part of NASA's recent program for developing new airfoil sections (Ref. 1), Wichita State University is conducting flap and control surface research for the new airfoils. One of the new airfoils designed for medium (subsonic) Mach number cruise conditions is the NASA MS(1)-0313 airfoil. The present report documents two-dimensional wind tunnel tests of this airfoil with 20% aileron, 25% slotted flap and 10% slot-lip spoiler.

All experimental tests reported herein were conducted in the Walter Beech Memorial Wind Tunnel at Wichita, at a Reynolds number of 2.2×10^6 and a Mach number of 0.13. NASA tests of this airfoil at higher Reynolds number and Mach number have been reported in reference 2.

SYMBOLS

The force and moment data have been referred to the .25c location on the flap-nested airfoil. Dimensional quantities are given in International (SI) Units. Measurements were made in U.S. Customary Units. Conversion factors between the various units may be found in reference 3. The symbols used in the present report are defined as follows:

- c Airfoil reference chord (flap-nested)
- c_d Airfoil section drag coefficient, section drag/
(dynamic pressure x c)

c_f Flap chord
 c_h Control surface hinge moment coefficient, section moment about hingeline/(dynamic pressure x control surface reference chord²)
 c_l Airfoil section lift coefficient, section lift/(c x dynamic pressure)
 c_m Airfoil section pitching moment coefficient with respect to the .25c location, section moment/(c² x dynamic pressure)
 c_{m_a} Airfoil forward section moment coefficient, moment about leading edge/(c² x dynamic pressure)
 c_{m_f} Flap moment coefficient, section moment about leading edge/(c² x dynamic pressure)
 c_n Airfoil normal force coefficient, section normal force/(c x dynamic pressure)
 c_{n_a} Airfoil forward section normal force coefficient, section normal force/(c x dynamic pressure)
 $c_{n_{ai}}$ Aileron normal force coefficient, section normal force/(c x dynamic pressure)
 c_{n_f} Flap normal force coefficient, section normal force/(c x dynamic pressure)
 c_p Coefficient of pressure, (p - p_∞)/dynamic pressure
 Δh Spoiler projection height normal to local airfoil surface
p Static pressure
RN Reynolds number
x Coordinate parallel to airfoil chord
z Coordinate normal to airfoil chord
 α Angle of attack, degrees
 Δ Increment
 δ_a Rotation of aileron from nested position, degrees
 δ_f Rotation of flap from nested position, degrees
 δ_s Rotation of spoiler from nested position, degrees

Subscripts:

- a Aileron
- f Flap
- p Pivot
- ∞ Remote free-stream value

TEST METHODS

Instrumentation, test procedure, tests facility and data correction methods have been described in reference 4.

Resolution values for the various instrumentation systems are given in Table 1.

Table 1 - Instrumentation Resolution

<u>Measurement</u>	<u>Resolution</u>	
	<u>Dimensional Form</u>	<u>Coefficient Form</u>
lift (force balance)	$\pm 0.9N$	$\pm 0.001 (\Delta c_l)$
drag (wake survey)	$\pm 0.06N$	$\pm 0.00009 (\Delta c_d)$
drag (force balance)	$\pm 0.2N$	$\pm 0.0003 (\Delta c_d)$
pitching moment (force balance)	$\pm 0.1N-m$	$\pm 0.0003 (\Delta c_m)$
hinge moment	$\pm 0.02N-m$	$\pm 0.006 (\Delta c_h)$
pressure transducers	$\pm 4.8N/m^2$	$\pm 0.004 (\Delta c_p)$
dynamic pressure	$\pm 4.8N/m^2$	---
angle of attack	$\pm 0.05^\circ$	---
flap and aileron angles	$\pm 0.5^\circ$	---
spoiler angle	$\pm 0.25^\circ$	---
flap longitudinal and vertical settings	$\pm 0.6mm$	$\pm 0.001c$

MODEL DESCRIPTION

The MS(1)-0313 airfoil section is a 13% maximum thickness section designed for high cruising efficiency at medium (≈ 0.72) Mach number. Model geometric details are given in figure 1. For tests in the WSU two-dimensional facility, models were sized with 91.4 cm span and 61.0 cm chord. The 20% chord aileron was designed with a 0.5% chord leading edge gap. The 25% slotted flap was designed with an airfoil forward section terminating at 87.5% chord. The 10% spoiler was arranged in a slot-lip configuration with the 25% slotted flap. The model was fitted with 2.5 mm wide transition strips of #80 carborundum grit located at 5% chord on the upper surface and at 10% chord on the lower surface. The more aft grit location on the lower surface was selected to place the transition strip aft of the stagnation point for high flap deflection conditions.

RESULTS AND DISCUSSION

Presentation of Results

Test results and comparisons with theory and other experimental results are shown in the figures as listed in Table 2.

Table 2 - List of Figures

<u>Configuration</u>	<u>Type Data</u>	<u>Comparisons</u>	<u>Figure</u>
airfoil, aileron, flap and spoiler	model geometry	---	1
basic section	C_l, C_d, C_m	data of Ref. 2	2
basic section	pressures	theory	3
basic section	tufts	---	4
20% aileron	C_l, C_d, C_m	---	5
20% aileron	$\Delta C_l, \Delta C_d, \Delta C_m, C_h$	---	6
20% aileron	pressures	---	7
25% flap	optimum flap settings	---	8
25% flap	$C_{l_{max}}$ contours	---	9
25% flap	C_l, C_d, C_m	theory	10
25% flap	flap effectiveness	GA(W)-2	11
25% flap	experimental pressures	---	12
25% flap	pressures	theory	13-16
25% flap	tufts	---	17-20
10% spoiler	effect of spoilers on lift for various flap settings	---	21
10% spoiler	incremental spoiler effectiveness and hinge moments	---	22

Discussion

Flap Nested: (figures 2 through 4). Comparisons of WSU data with NASA data show that the lift and pitching moment data agree quite well, even including stalling effects. The drag data do not compare as well. The agreement is good at low lift coefficients, but the WSU tests indicate somewhat higher drag levels at moderate lift coefficients. At near-stalling lift coefficients, the data again show reasonable agreement.

The pressure distributions show good agreement with the theoretical methods of reference 5 at angles of attack below separation. Separation predictions agree rather well with experiment, with separation appearing first at the trailing edge, and gradually progressing forward. At high angles of attack with massive separation, the discrepancies between experimental and theoretical pressure distributions are large.

Table 3 shows a comparison of this airfoil with the GA(W)-2 airfoil of reference 6.

Table 3 - Comparison of Section Properties
(RN = 2.2×10^6 , Mach = 0.13)

	GA(W)-2 (Ref. 6)	MS(1)-0313 (Present Tests)
thickness/chord	0.13	0.13
c_l @ $\alpha = 0^\circ$	0.43	0.31
c_m @ $\alpha = 0^\circ$	-0.107	-0.075
c_d @ $\alpha = 0^\circ$	0.0109	0.0100
$c_{l_{max}}$	1.67	1.66

These data show a reduction in c_{ℓ} @ $\alpha = 0^\circ$ and corresponding reduction in c_m @ $\alpha = 0^\circ$ for the MS(1)-0313 airfoil, as expected for the lower design lift coefficient. The $c_{\ell_{\max}}$ for the MS(1)-0313 is essentially the same as for the GA(W)-2, in spite of the reduction in design lift coefficient. The drag level for the MS(1)-0313 airfoil is essentially the same as the GA(W)-2 at the Reynolds number and Mach number of the present tests.

20% Aileron: (figures 5 through 7). Aileron characteristics for this airfoil are quite similar to the LS(1)-0421, GA(W)-1, and GA(W)-2 airfoils (given in refs. 4 and 6-9). Control effectiveness is somewhat non-linear but positive for all angles below stall. Integrations of pressure distributions are tabulated to provide individual component normal force coefficients for structural design purposes.

25% Flap: (figures 8 through 20). Optimum flap settings are quite similar to other airfoils (such as refs. 4 and 6-9). The theory of reference 10 under-predicts the lift for 10° flap, and over-predicts the lift for larger flap deflections and for zero flap. As reported earlier (ref. 4), the reasons for these trends are not understood. The highest $c_{\ell_{\max}}$ obtained for this airfoil-flap combination was 3.00, at a 30° flap deflection, compared to the value of 3.35 obtained with the GA(W)-2 airfoil with 25% chord flap deflected either 35° or 40° (ref. 6).

The flap effectiveness data show that the increments in $c_{\ell_{\max}}$ for high flap deflections are substantially lower than the increments in c_{ℓ} at $\alpha = 0^\circ$. The increments in $c_{\ell_{\max}}$ for the 25%

flap at high flap deflections with this airfoil are consistently lower than increments obtained with the GA(W)-2 airfoil. Increments in $c_{l_{\max}}$ with 20% plain flap are essentially the same as obtained with the GA(W)-2 airfoil. Limitations in $c_{l_{\max}}$ can only be understood by study of separation patterns.

Separated regions are observed from tuft photos and from interpretation of surface pressure distributions. Separation is evidenced in surface pressure distributions by two characteristics:

- a) Trailing edge pressure changes from $c_p \approx 0$ to $c_p = -0.1$ to -0.2 when separation occurs.
- b) Pressure becomes essentially constant from the trailing edge forward to the point of separation.

Integrations of pressure distributions are tabulated to provide individual component normal force coefficients. Comparisons of theoretical pressure distributions with experiment show good agreement except for cases where regions of separation are present. No theoretical results are shown for the case of 0° angle of attack with 10° flap deflection. With this geometry the computer program failed to run, in spite of repeated attempts and numerous checks of input geometry, flap nose geometry smoothing, etc.

Pressure distributions and tuft surveys indicate that for 25% flap deflections of 10° and 20° , initial separation takes place at the airfoil trailing edge, and moves progressively forward, while the flap flow remains attached. With 30° and 35° flap deflections, the flow over the flap was separated from about mid-flap chord aft for low angles of attack. At angles of attack near $c_{\ell_{\max}}$ the flap flow was attached, but flap separation reappeared rather quickly at angles just beyond $c_{\ell_{\max}}$, along with separation at the trailing edge of the main airfoil.

Studies of tuft photos and pressure distributions from the GA(W)-2 tests (refs. 6 and 9) show quite different separation characteristics than the MS(1)-0313 airfoil. The GA(W)-2 tuft and pressure studies show attached flow over the flap at all angles of attack for all flap deflections up to 30° . These differences in boundary layer separation and surface pressure distributions are entirely consistent with the lower $c_{\ell_{\max}}$ performance from force measurements of the MS(1)-0313 airfoil-flap combination.

The reduced flaps-down performance of the MS(1)-0313 airfoil is somewhat surprising, since tests of the GA(W)-2 and MS(1)-0313 airfoils show that both airfoils achieve the same $c_{\ell_{\max}}$ without flaps. Reference 2 confirms that the unflapped airfoils have the same $c_{\ell_{\max}}$ at a Reynolds number of 2×10^6 , but it should be noted that at higher Reynolds numbers the GA(W)-2 has higher $c_{\ell_{\max}}$ than the MS(1)-0313. The thickness distributions of these airfoils are nearly identical, so the principal difference between the airfoils is a reduction (average reduction $\approx 25\%$) in camber of the MS(1)-0313. This reduction in airfoil section camber reduces flow turning angles,

particularly in the region of 75% to 85% chord. This region forms the flap leading edge camber and the camber of the important flap slot lip. Comparable theoretical runs for the GA(W)-2 and MS(1)-0313 airfoils with 30° flap deflection and experimental optimum gap and overlap for each show that the GA(W)-2 should produce 0.14 higher c_{ℓ} , due to these added camber effects. The fact that the experimental increment in $c_{\ell_{\max}}$ is 0.35 is evidently a consequence of non-linear boundary layer behavior associated with conditions near separation. Evidently the difficulties in attaining attached flap flow for high deflection angles on the MS(1)-0313 airfoil are a consequence of this camber reduction.

10% Slot-Lip Spoiler: (figures 21 and 22). Spoiler control effectiveness and hinge moment characteristics are quite similar to those observed for slot-lip spoilers on similar airfoils in earlier research (refs. 4 and 6). Control effectiveness with flap nested is positive and nearly linear for normal angles of attack. At -8° angle of attack a lack of response (deadband) appears for small deflections, but this negative lift condition does not represent a realistic flight situation for normal operations. Control effectiveness increases as the flap is deflected, showing a strongly non-linear characteristic, but without reversal or deadband tendency.

CONCLUSIONS

1. The MS(1)-0313 basic section exhibits lift and drag characteristics similar to the GA(W)-2 section at $RN = 2.2 \times 10^6$ and $Mach = 0.13$. Pitching moments are reduced somewhat due to the reduced camber of the MS(1)-0313 section.

2. Aileron control effectiveness and hinge moments for the MS(1)-0313 are similar to comparable parameters for the GA(W)-2 section.

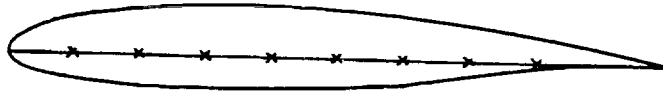
3. Incremental $c_{l_{max}}$ performance of a 25% slotted flap on the MS(1)-0313 section is somewhat lower than a similar flap applied to the GA(W)-2 section. Incremental performance of a 20% plain flap on this section is similar to a 20% plain flap applied to the GA(W)-2 section.

4. The highest $c_{l_{max}}$ for this airfoil flap combination is 3.00 compared to 3.35 for the GA(W)-2 airfoil with a similar flap.

5. Slot-lip spoiler control effectiveness on the MS(1)-0313 section is non-linear but positive for normal angles of attack and spoiler deflection angles. Spoiler incremental effectiveness and hinge moment values are similar to comparable values for the GA(W)-2 section.

REFERENCES

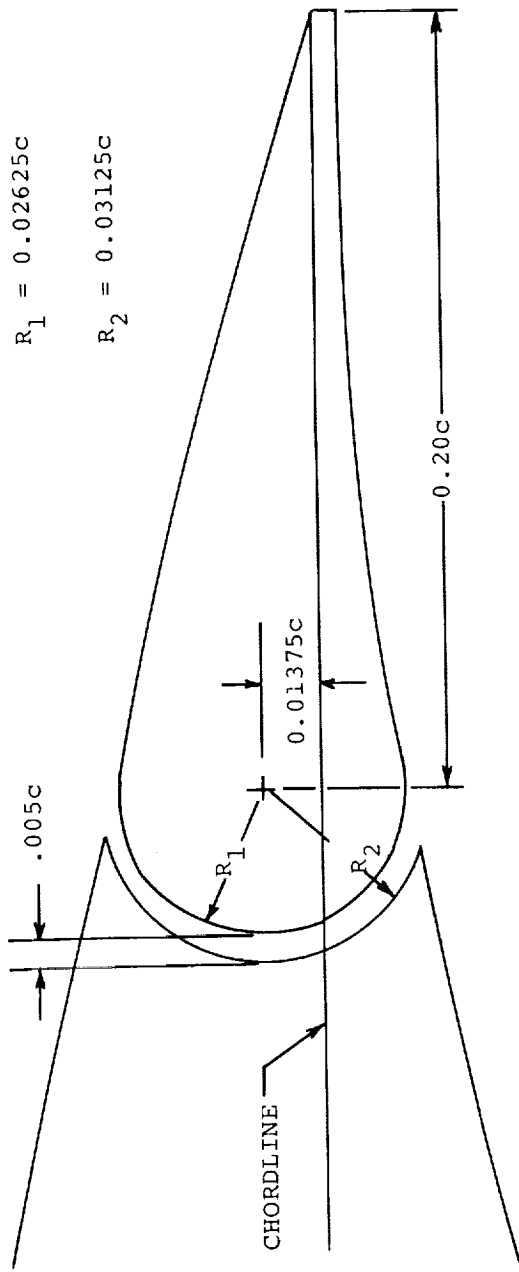
1. Pierpont, P.K.: Bringing Wings of Change. *Astronautics and Aeronautics Magazine*, October 1975.
2. McGhee, R.J., and Beasley, W.D.: Low-Speed Aerodynamic Characteristics of a 13-Percent-Thick Medium-Speed Airfoil Designed for General Aviation Applications. NASA Technical Paper 1498, Aug. 1979.
3. Mechtly, E.A.: The International System of Units--Physical Constants and Conversion Factors (Revised). NASA SP-7012, 1969.
4. Wentz, W.H. Jr., and Fiscsko, K.A.: Wind Tunnel Force and Pressure Tests of a 21% Thick General Aviation Airfoil with 20% Aileron, 25% Slotted Flap and 10% Slot-Lip Spoiler. NASA CR-3081, 1979.
5. Smetana, Frederick O., Summey, Delbert C., Smith, Neill S., and Carden, Ronald K.: Light Aircraft Lift, Drag, and Moment Prediction - A Review and Analysis. NASA CR-2523, 1975.
6. Wentz, W.H. Jr.: Wind Tunnel Tests of the GA(W)-2 Airfoil with 20% Aileron, 25% Slotted Flap, 30% Fowler Flap and 10% Slot-Lip Spoiler, NASA CR-145139, 1977.
7. Wentz, W.H. Jr., and Seetharam, H.C.: Development of a Fowler Flap System for a High Performance General Aviation Airfoil. NASA CR-2443, 1974.
8. Wentz, W.H. Jr., Seetharam, H.C., and Fiscsko, K.A.: Force and Pressure Tests of the GA(W)-1 Airfoil with a 20% Aileron and Pressure Tests with a 30% Fowler Flap. NASA CR-2833, 1977.
9. Wentz, W.H. Jr., and Fiscsko, K.A.: Pressure Distributions for the GA(W)-2 Airfoil with 20% Aileron, 25% Slotted Flap, and 30% Fowler Flap. NASA CR-2948, 1978.
10. Stevens, W.A., Goradia, S.H., and Braden, J.A.: Mathematical Model for Two-Dimensional Multi-Component Airfoils in Viscous Flow. NASA CR-1843, July 1971.



UPPER SURFACE		LOWER SURFACE	
x/c	z/c	x/c	z/c
0.0000	0.0010	0.0000	0.0010
.0020	.0095	.0020	-.0063
.0050	.0151	.0050	-.0099
.0125	.0243	.0125	-.0153
.0250	.0345	.0250	-.0206
.0375	.0418	.0375	-.0244
.0500	.0474	.0500	-.0275
.0750	.0552	.0750	-.0323
.1000	.0606	.1000	-.0361
.1250	.0648	.1250	-.0392
.1500	.0682	.1500	-.0418
.1750	.0709	.1750	-.0440
.2000	.0733	.2000	-.0458
.2250	.0752	.2250	-.0473
.2500	.0767	.2500	-.0485
.2750	.0780	.2750	-.0494
.3000	.0789	.3000	-.0501
.3250	.0796	.3250	-.0506
.3500	.0801	.3500	-.0509
.3750	.0803	.3750	-.0511
.4000	.0803	.4000	-.0509
.4250	.0800	.4250	-.0505
.4500	.0795	.4500	-.0498
.4750	.0787	.4750	-.0488
.5000	.0777	.5000	-.0475
.5250	.0765	.5250	-.0459
.5500	.0748	.5500	-.0440
.5750	.0729	.5750	-.0418
.6000	.0706	.6000	-.0393
.6250	.0679	.6250	-.0364
.6500	.0649	.6500	-.0333
.6750	.0615	.6750	-.0300
.7000	.0577	.7000	-.0266
.7250	.0537	.7250	-.0231
.7500	.0494	.7500	-.0196
.7750	.0449	.7750	-.0160
.8000	.0402	.8000	-.0128
.8250	.0353	.8250	-.0098
.8500	.0303	.8500	-.0073
.8750	.0252	.8750	-.0051
.9000	.0201	.9000	-.0035
.9250	.0149	.9250	-.0026
.9500	.0098	.9500	-.0025
.9750	.0047	.9750	-.0035
1.0000	-.0005	1.0000	-.0061

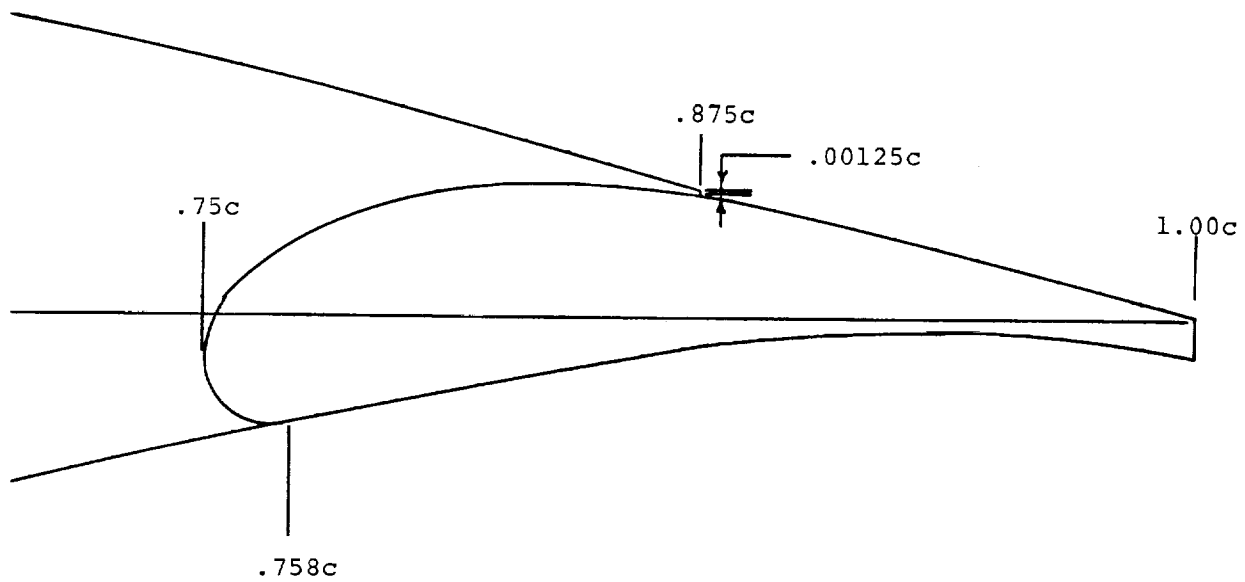
(a) Basic MS(1)-0313 Airfoil

Figure 1 - Geometry.



(b) 20% Aileron

Figure 1 - Continued.



Flap Upper Surface

x/c	z/c
0.7500	-.0053
.7531	.0030
.7562	.0068
.7594	.0097
.7625	.0122
.7750	.0192
.7875	.0231
.8000	.0251
.8125	.0259
.8250	.0262
.8375	.0260
.8500	.0254
.8625	.0248
.8750	.0239

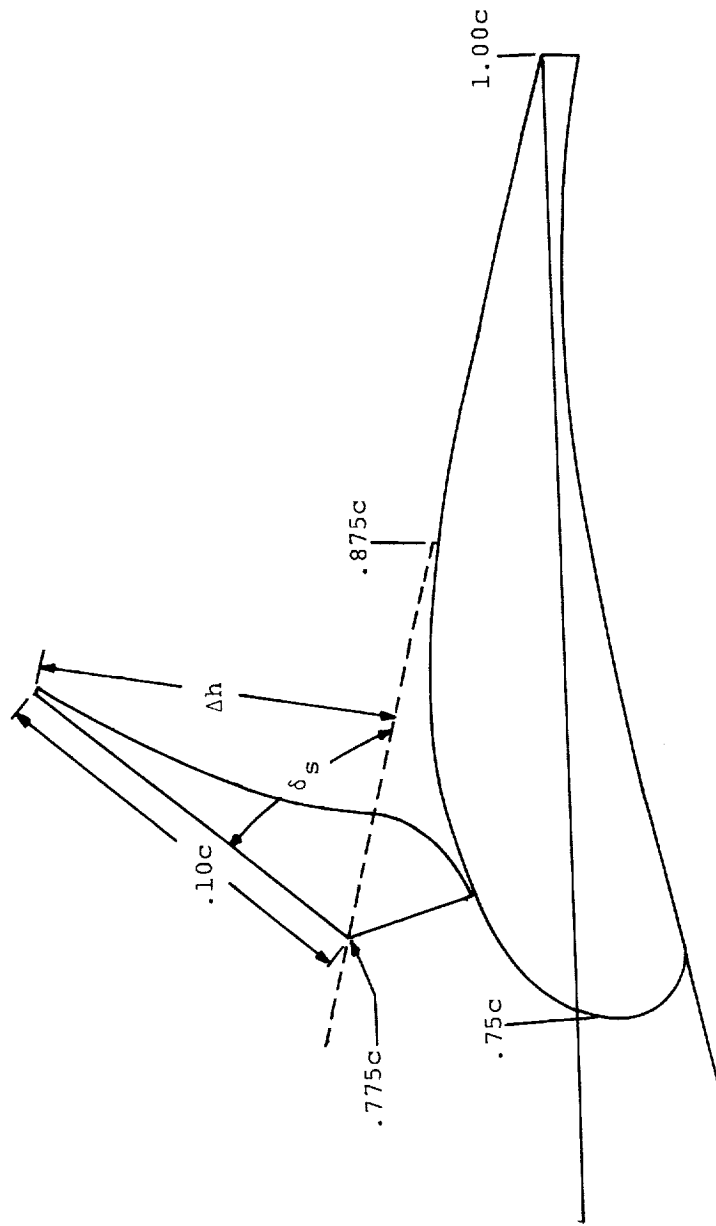
Nose Radius = $.012c$

Nose Radius Location
 $(x/c, z/c) = (0.7620, -0.0054)$

Note: Remainder of flap contour
 matches basic airfoil.

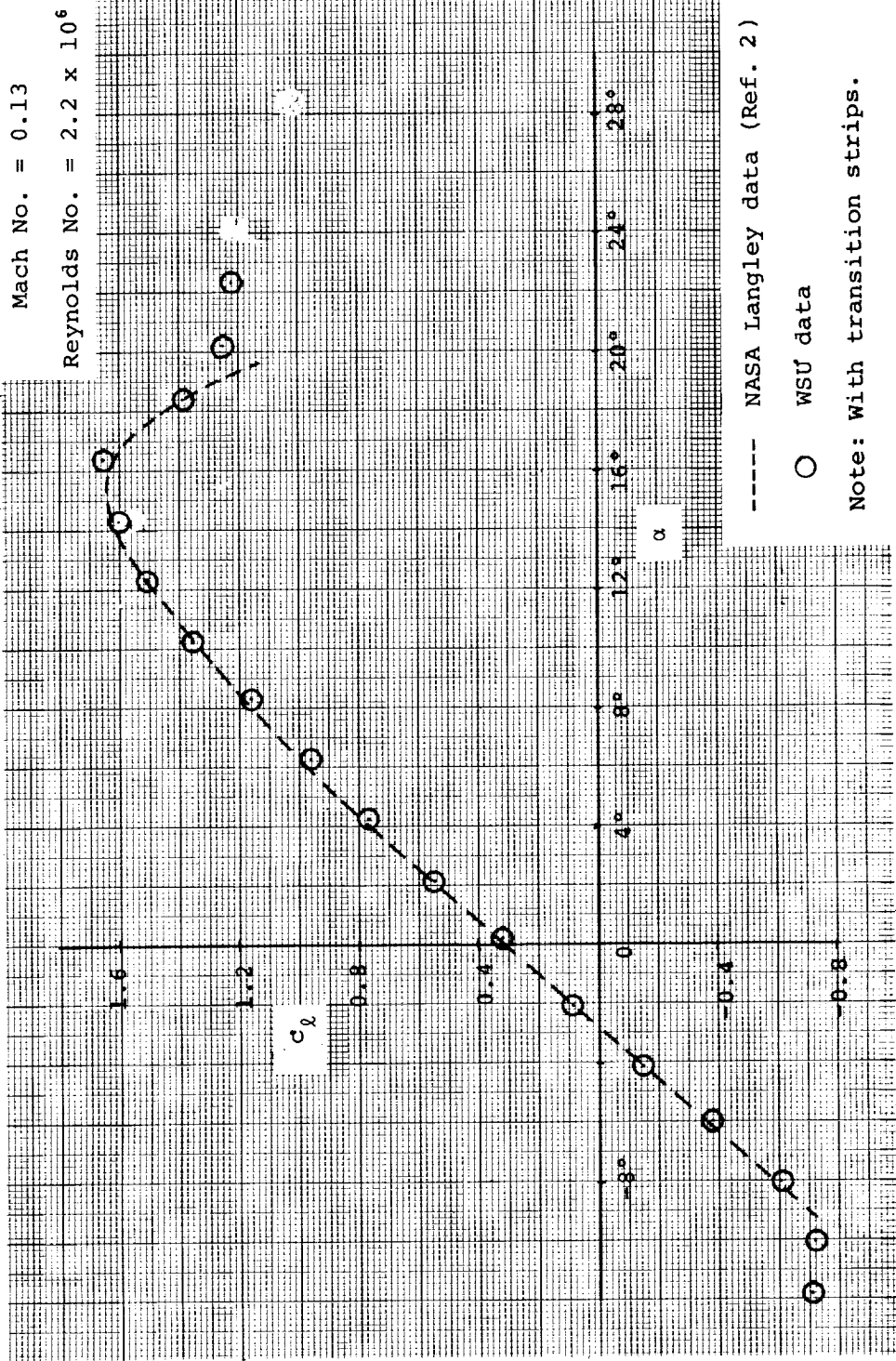
(c) 25% Flap Geometry.

Figure 1 - Continued.



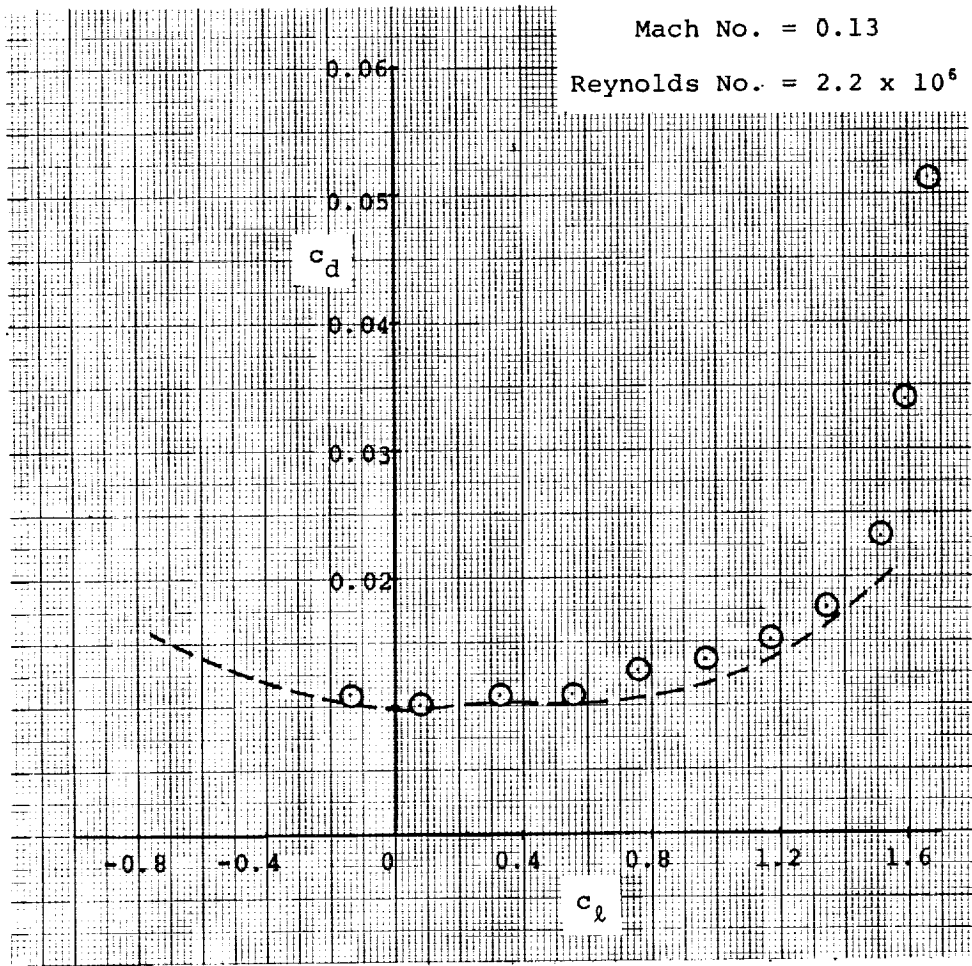
(d) 10% slot Lip Spoiler.

Figure 1 - Concluded.



(a) Lift

Figure 2 - Basic Airfoil Data - Comparisons with NASA Data.



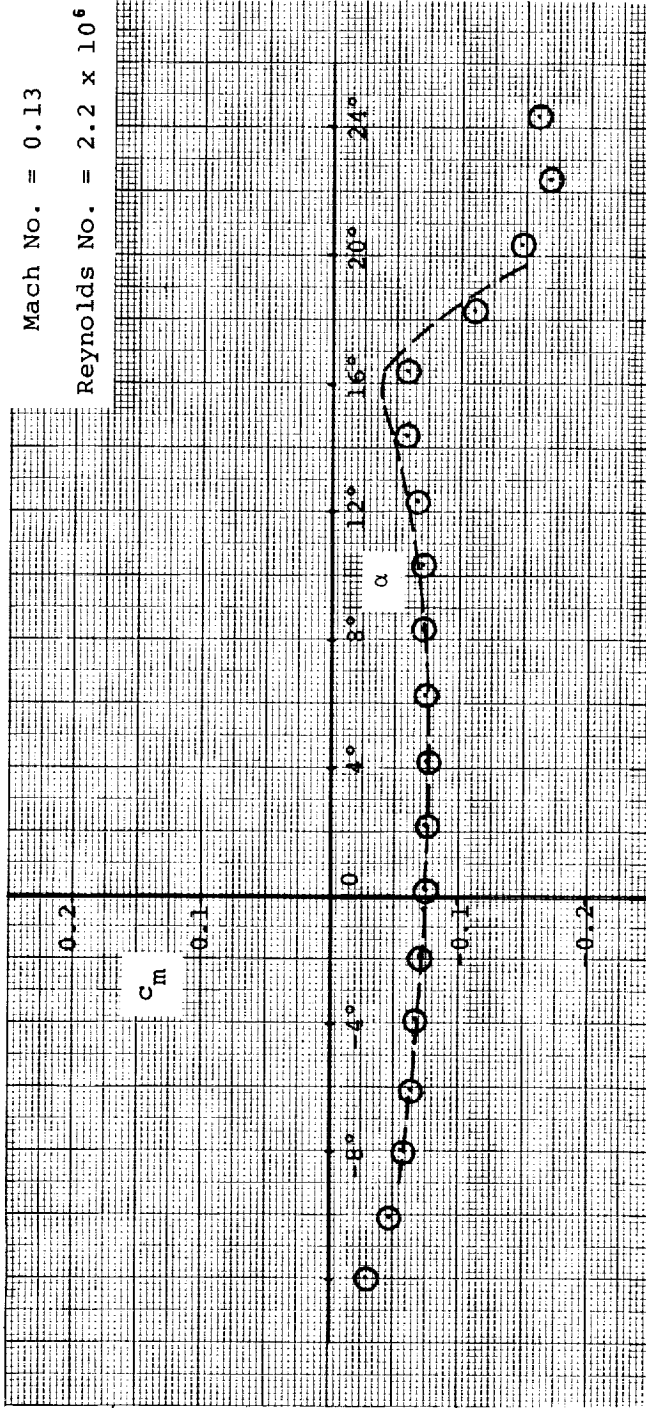
---- NASA Langley data (Ref. 2)

○ WSU data

Note: With transition strips.

(b) Drag

Figure 2 - Continued.



--- NASA Langley data (Ref.2)

○ WSU data

Note: With transition strips.

(c) Moment.

Figure 2 - Concluded.

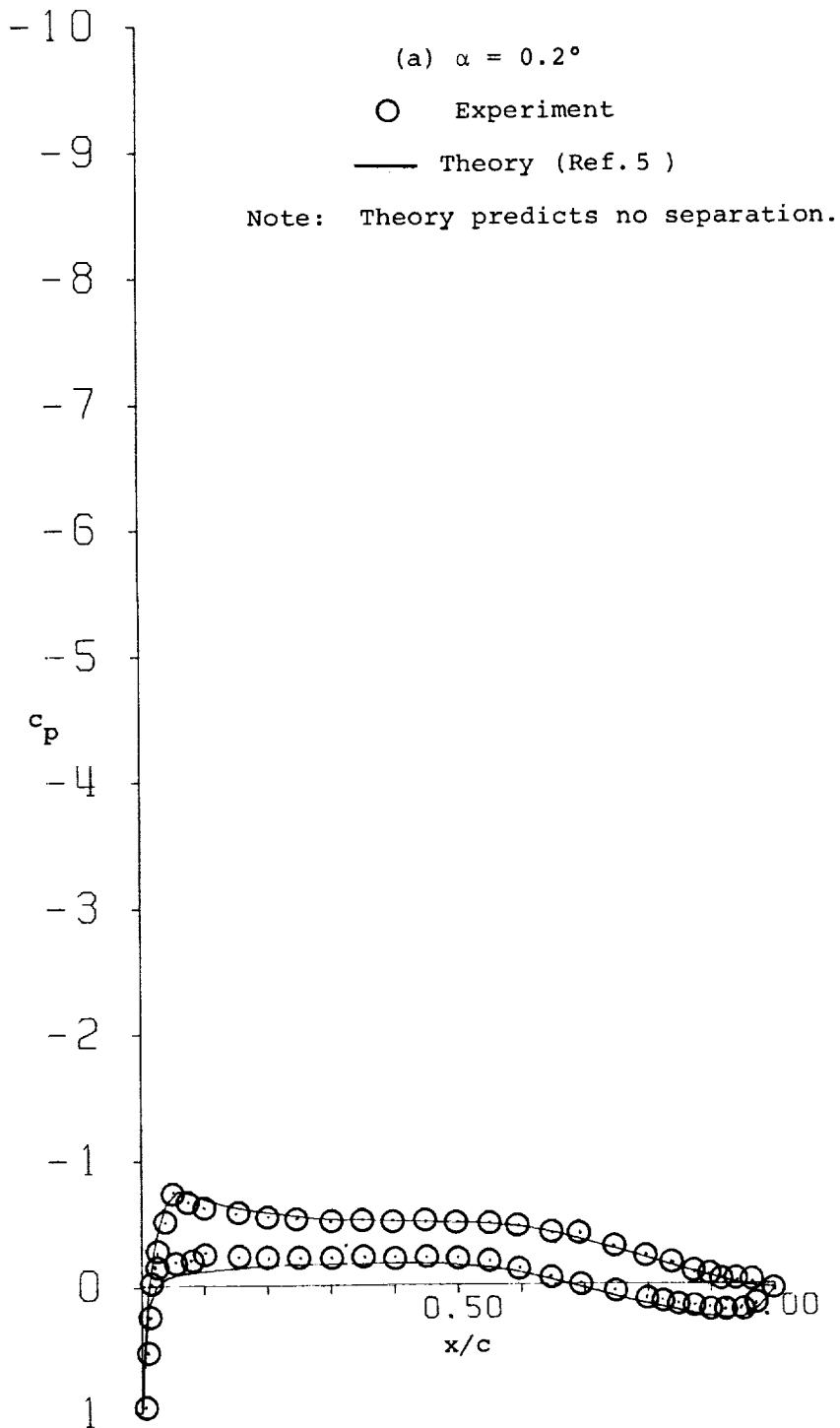


Figure 3 - Pressure Distribution for the Basic Section.

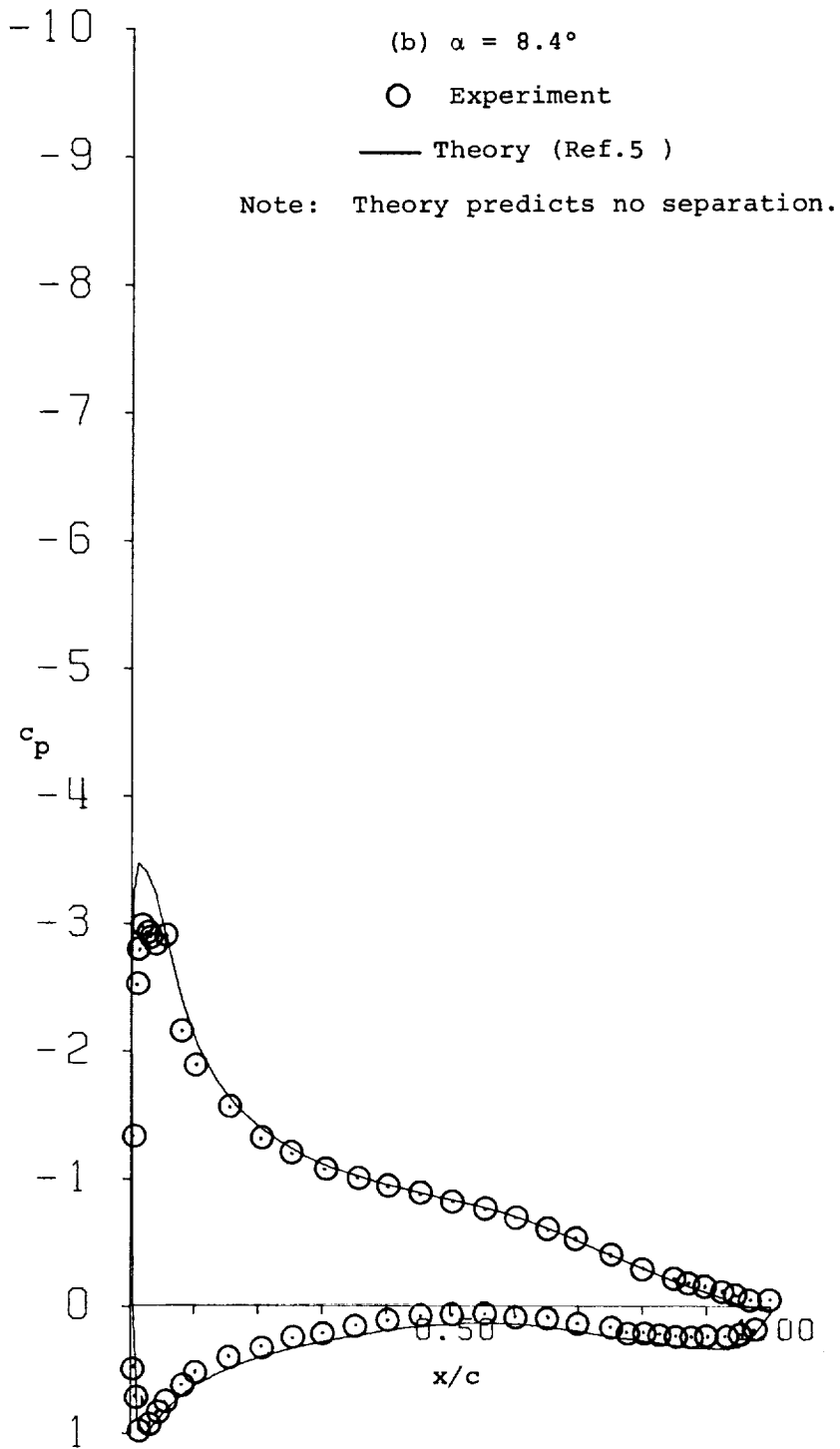


Figure 3 - Continued.

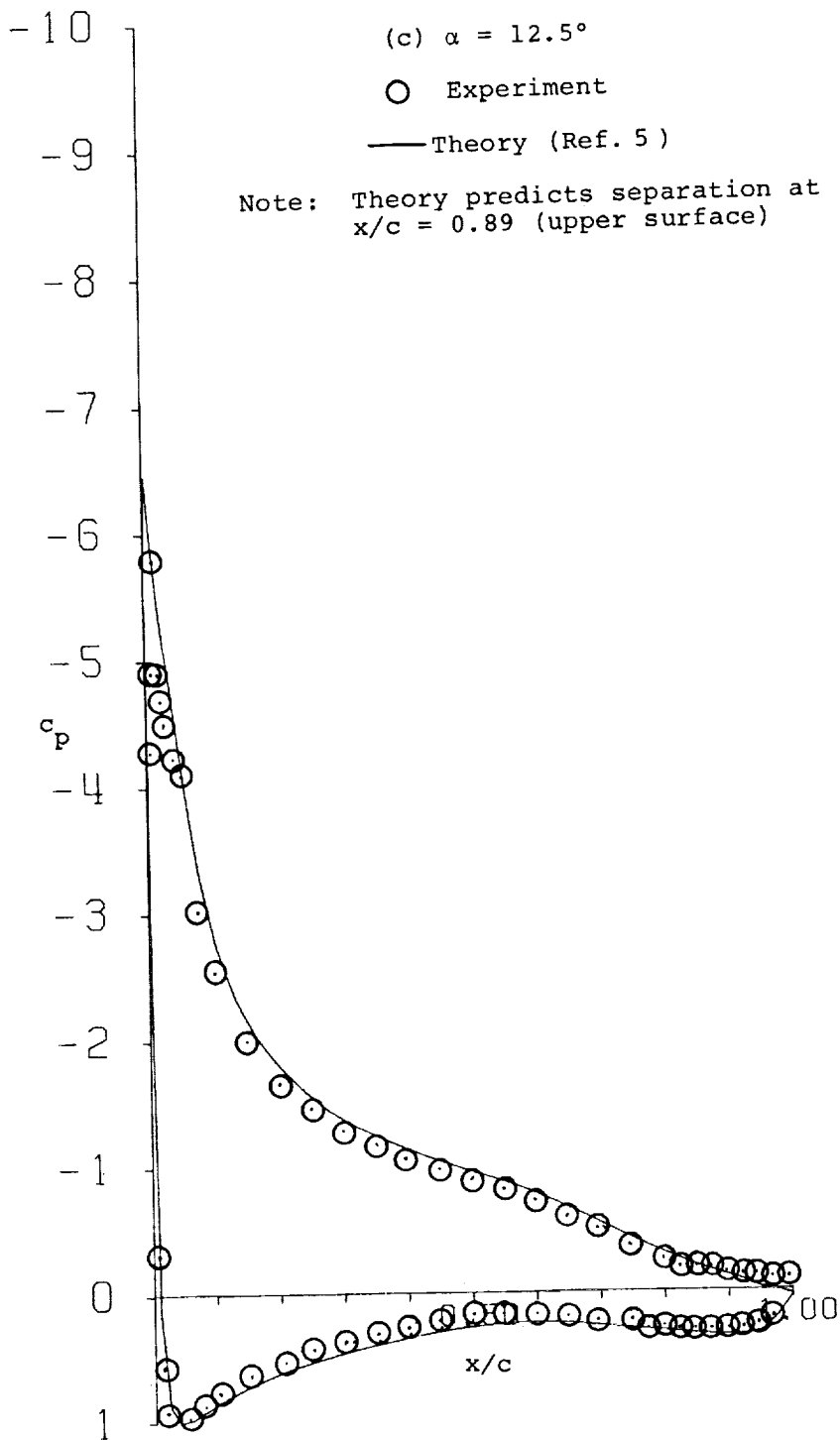


Figure 3 - Continued.

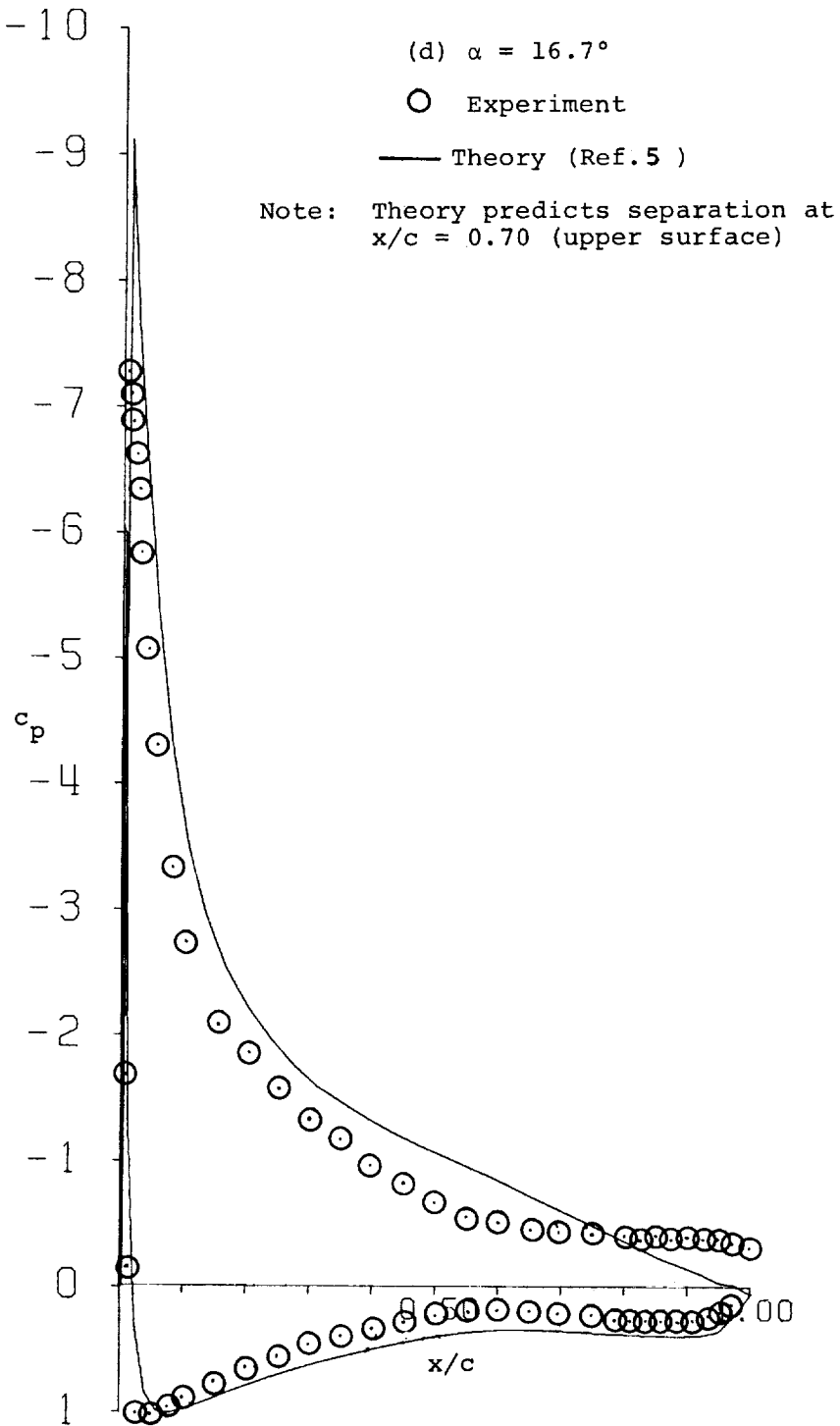


Figure 3 - Continued.

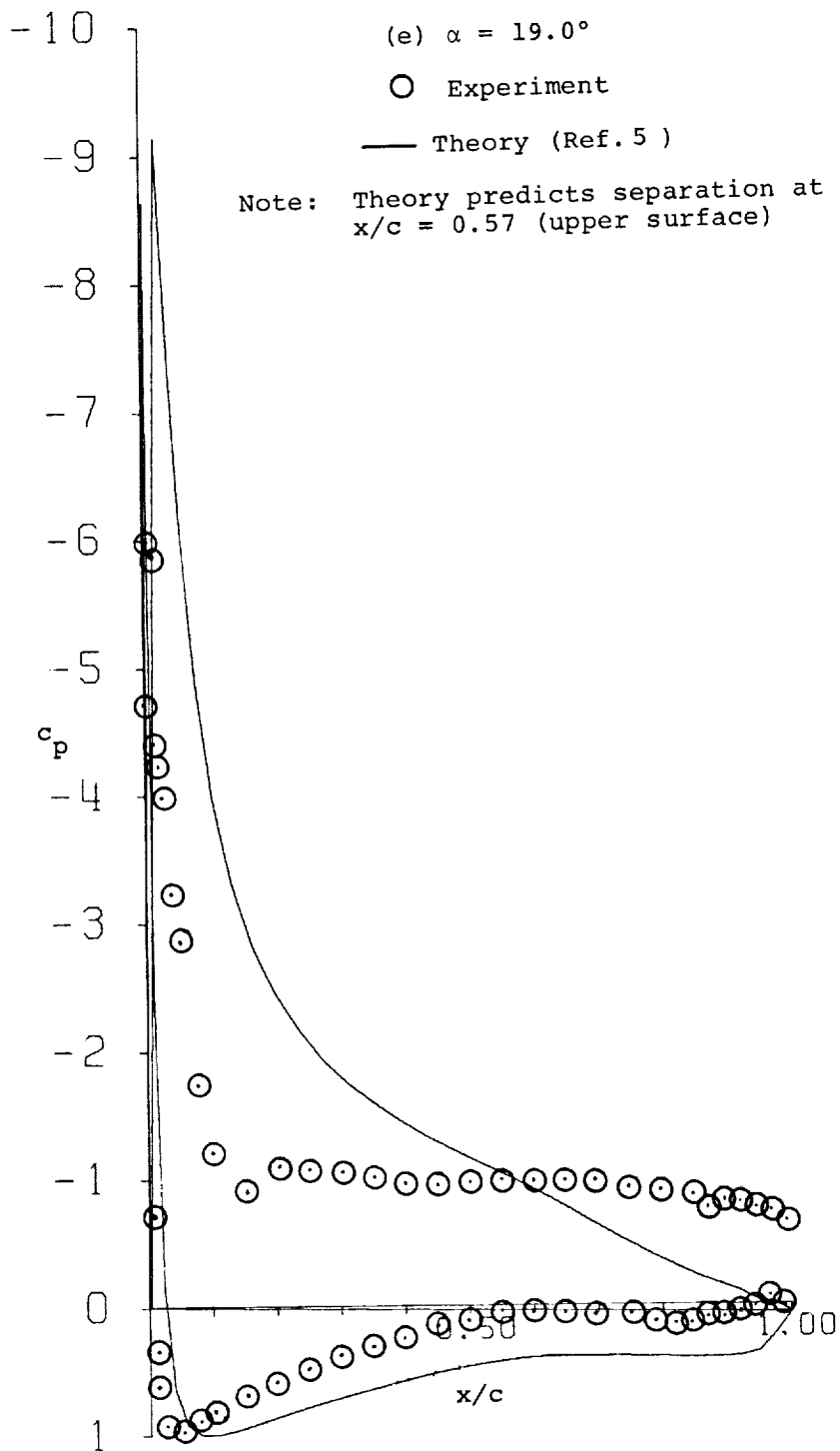
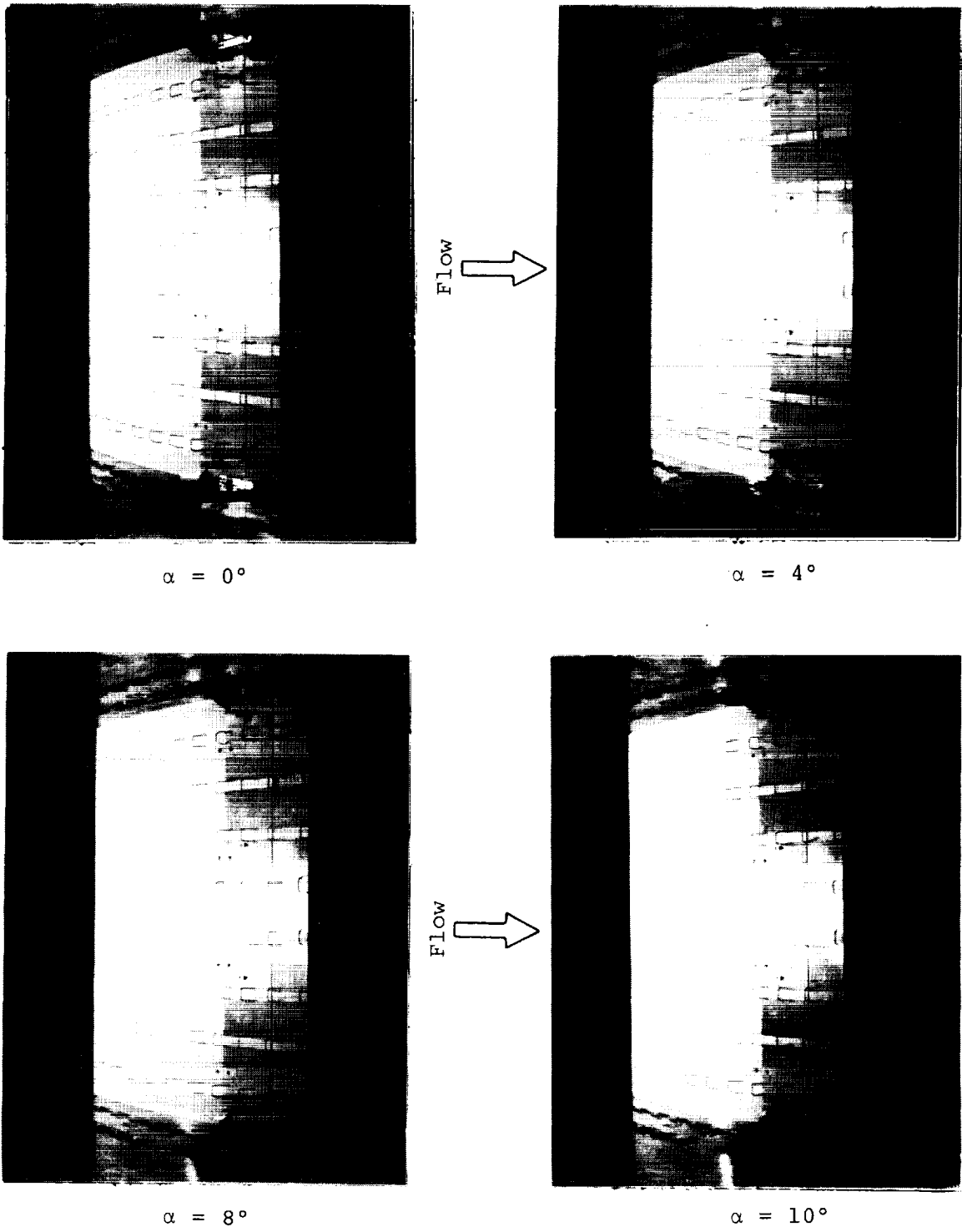
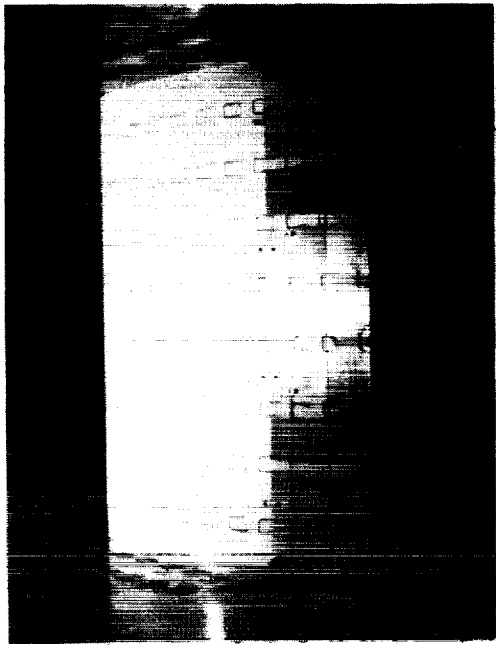


Figure 3 - Concluded.



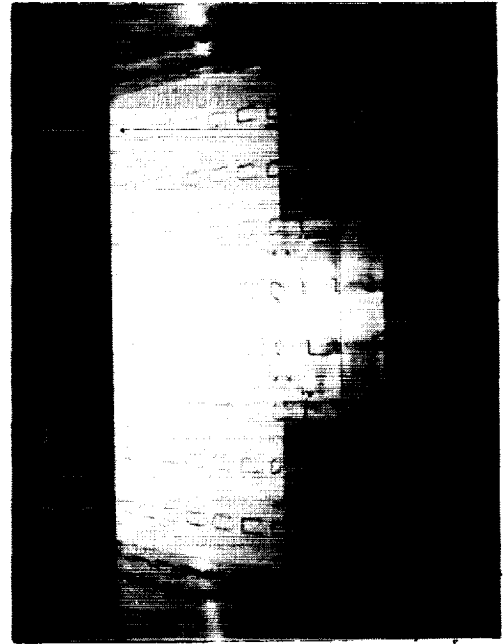
(a) Low angles of attack

Figure 4 - Tuft Patterns with 25% Slotted Flap, 0° Flap Deflection.

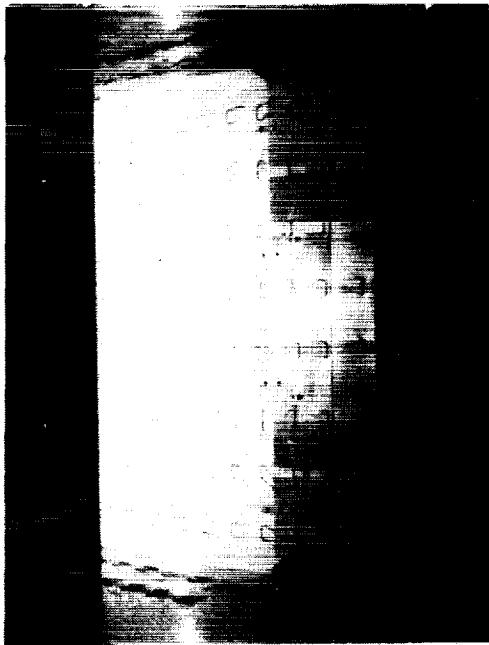


$\alpha = 12^\circ$

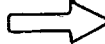
FLOW 

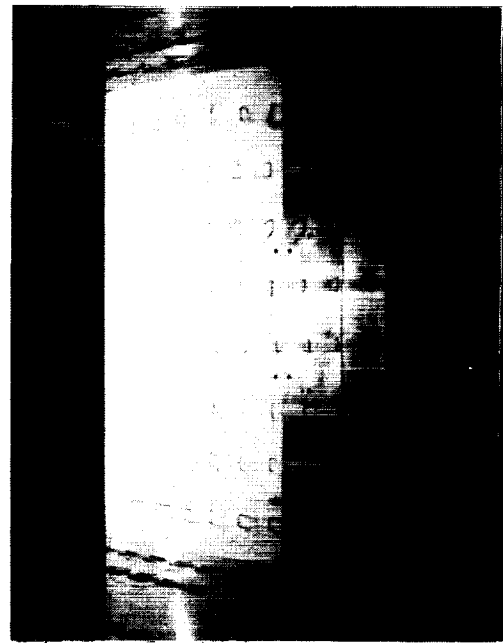


$\alpha = 14^\circ$



$\alpha = 16^\circ$

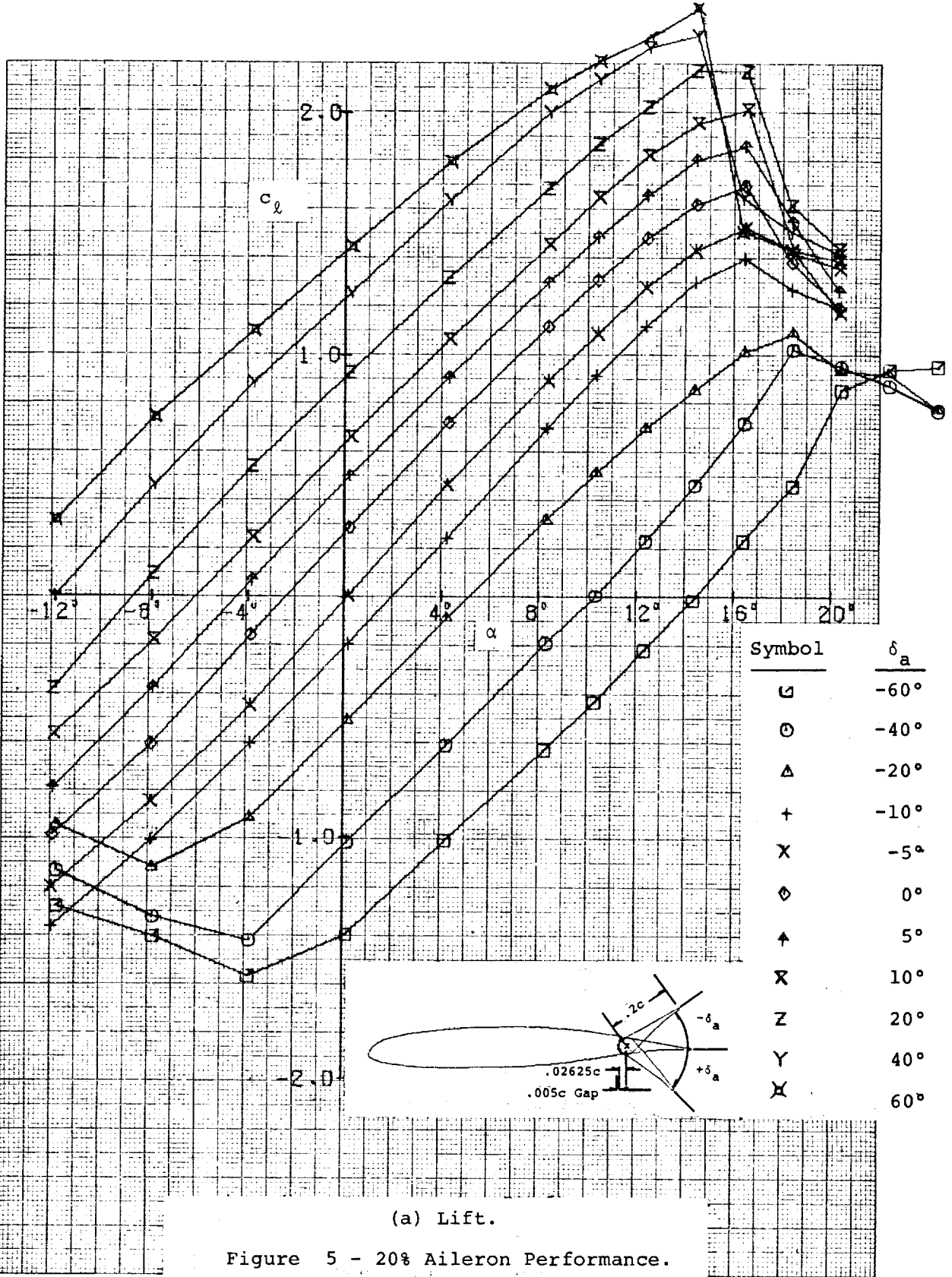
FLOW 



$\alpha = 18^\circ$

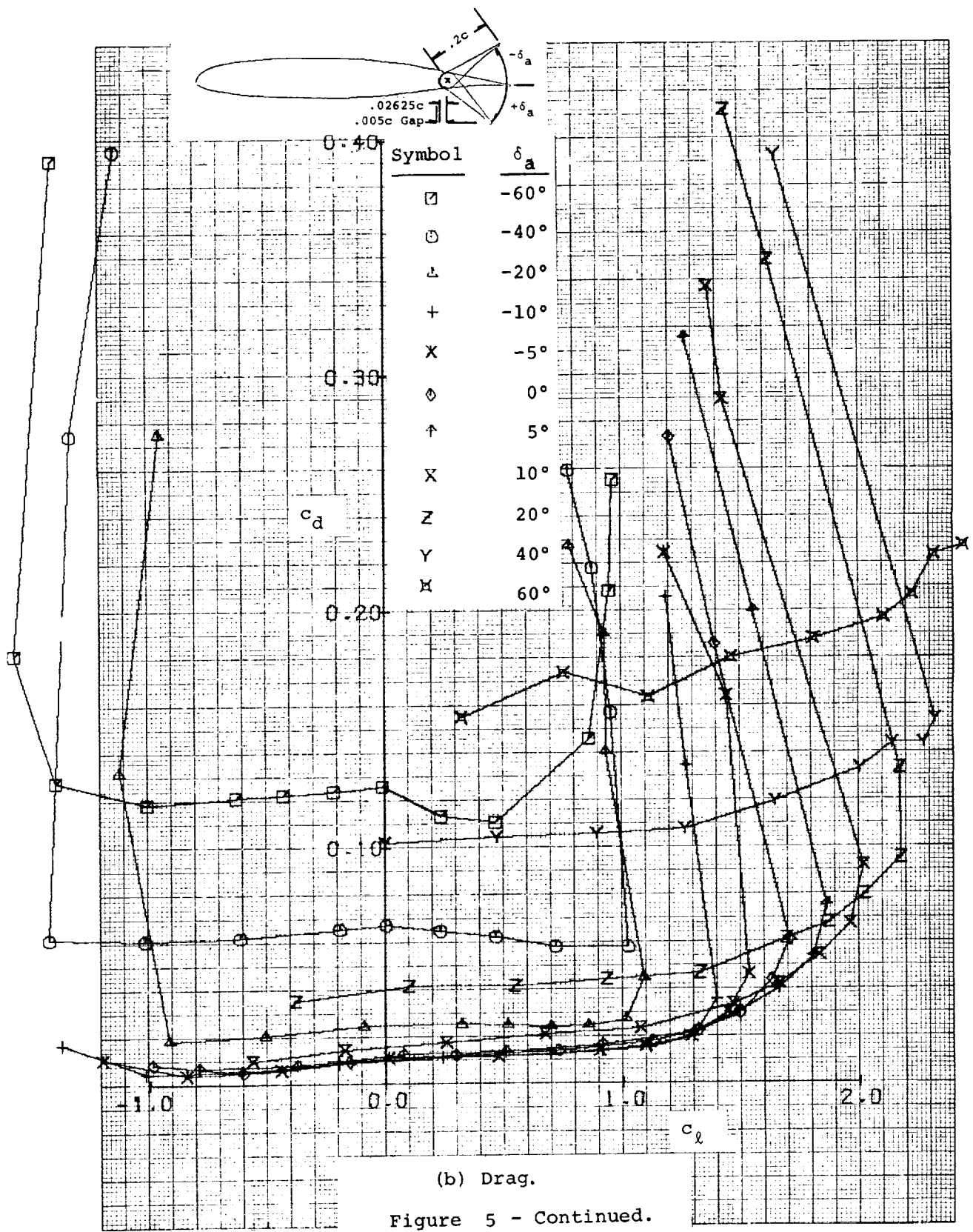
(b) High angles of attack

Figure 4 - Concluded.



(a) Lift.

Figure 5 - 20% Aileron Performance.



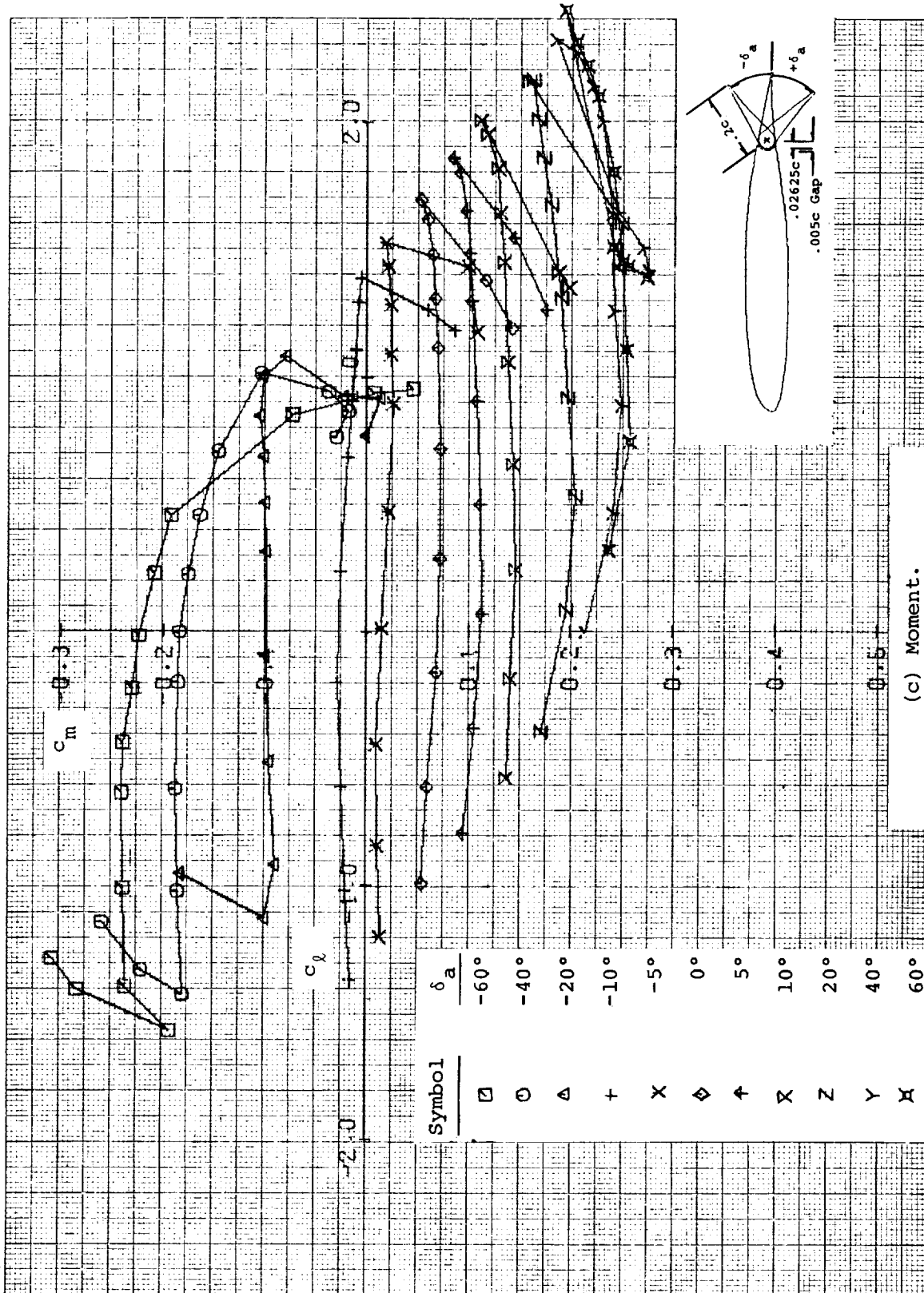
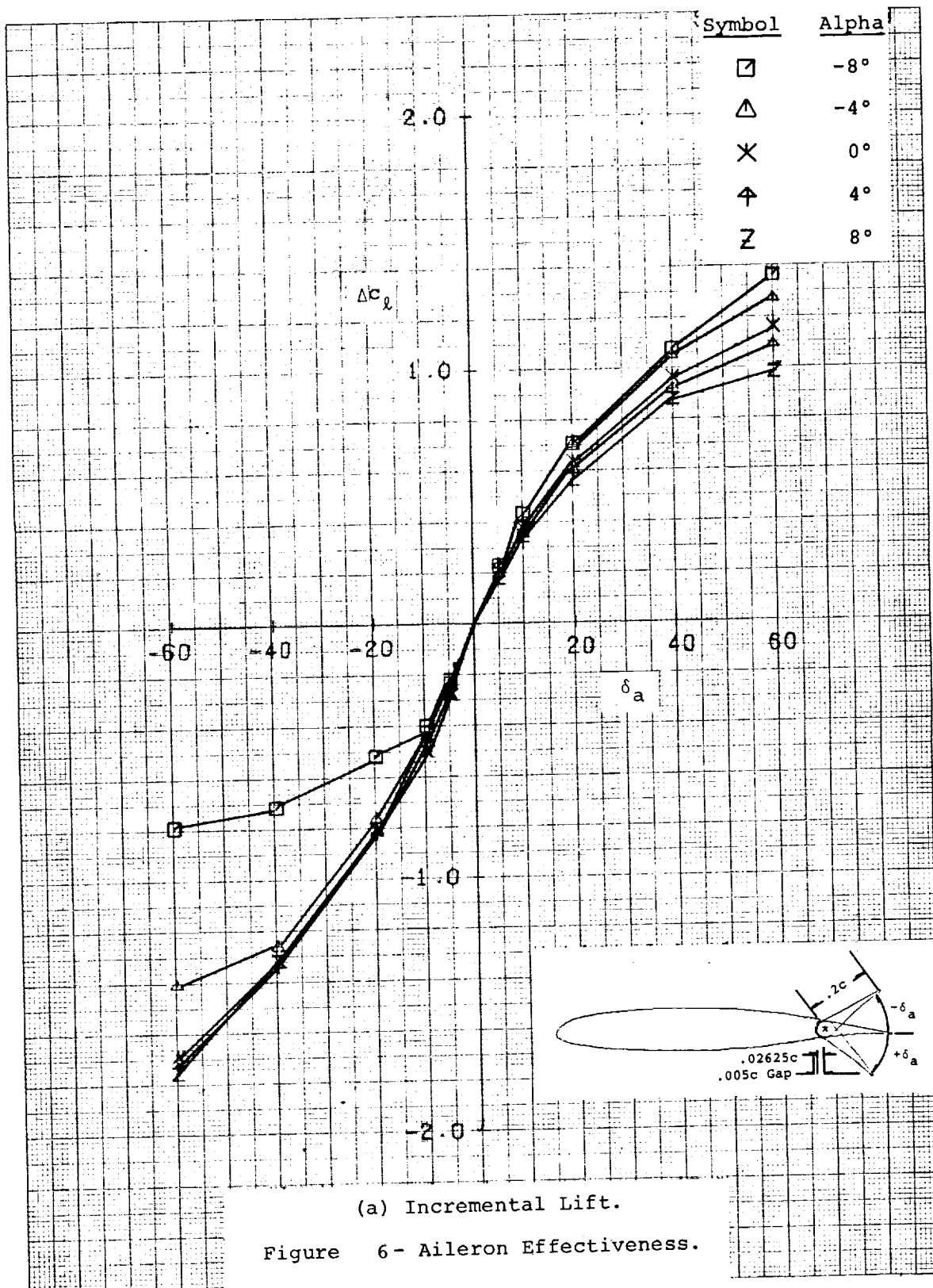
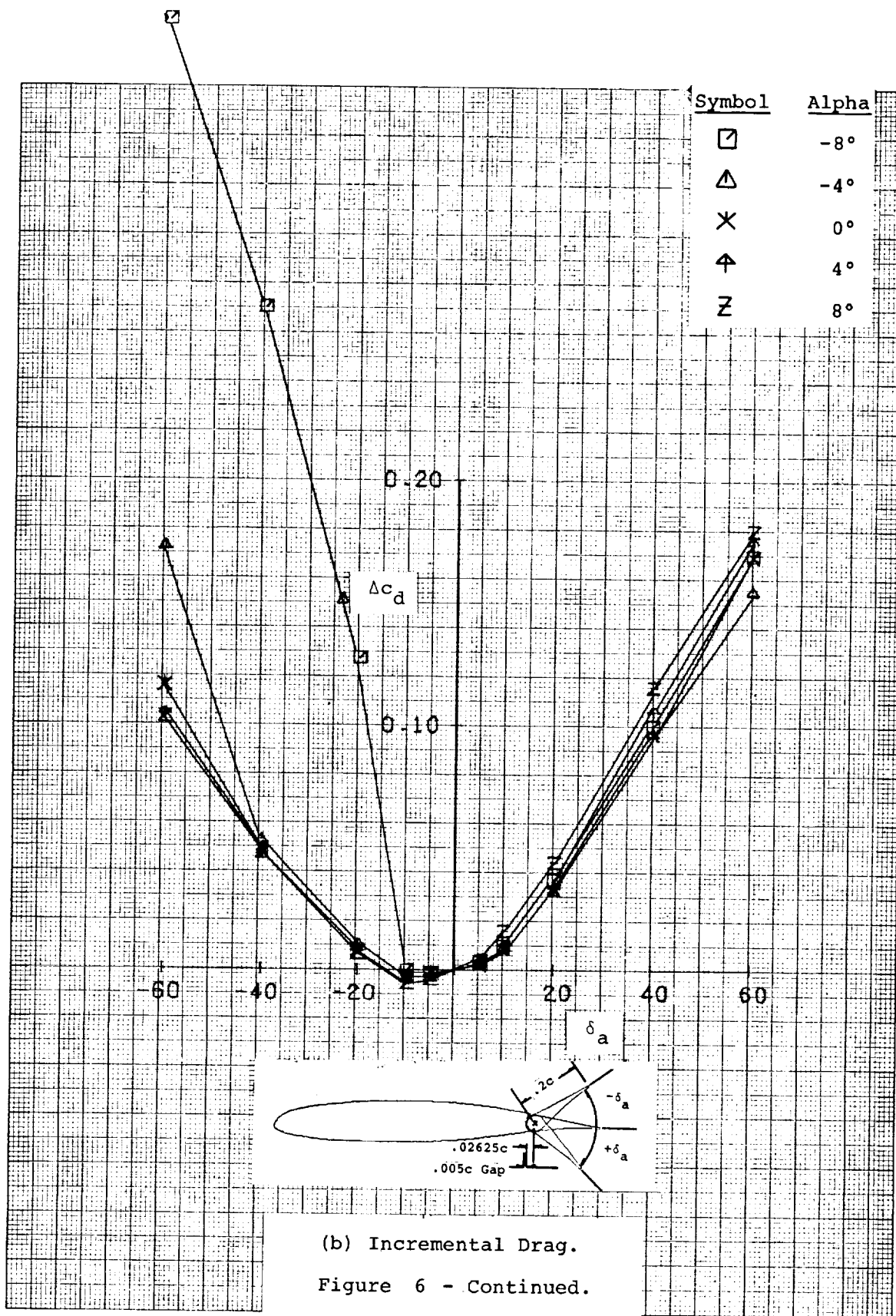
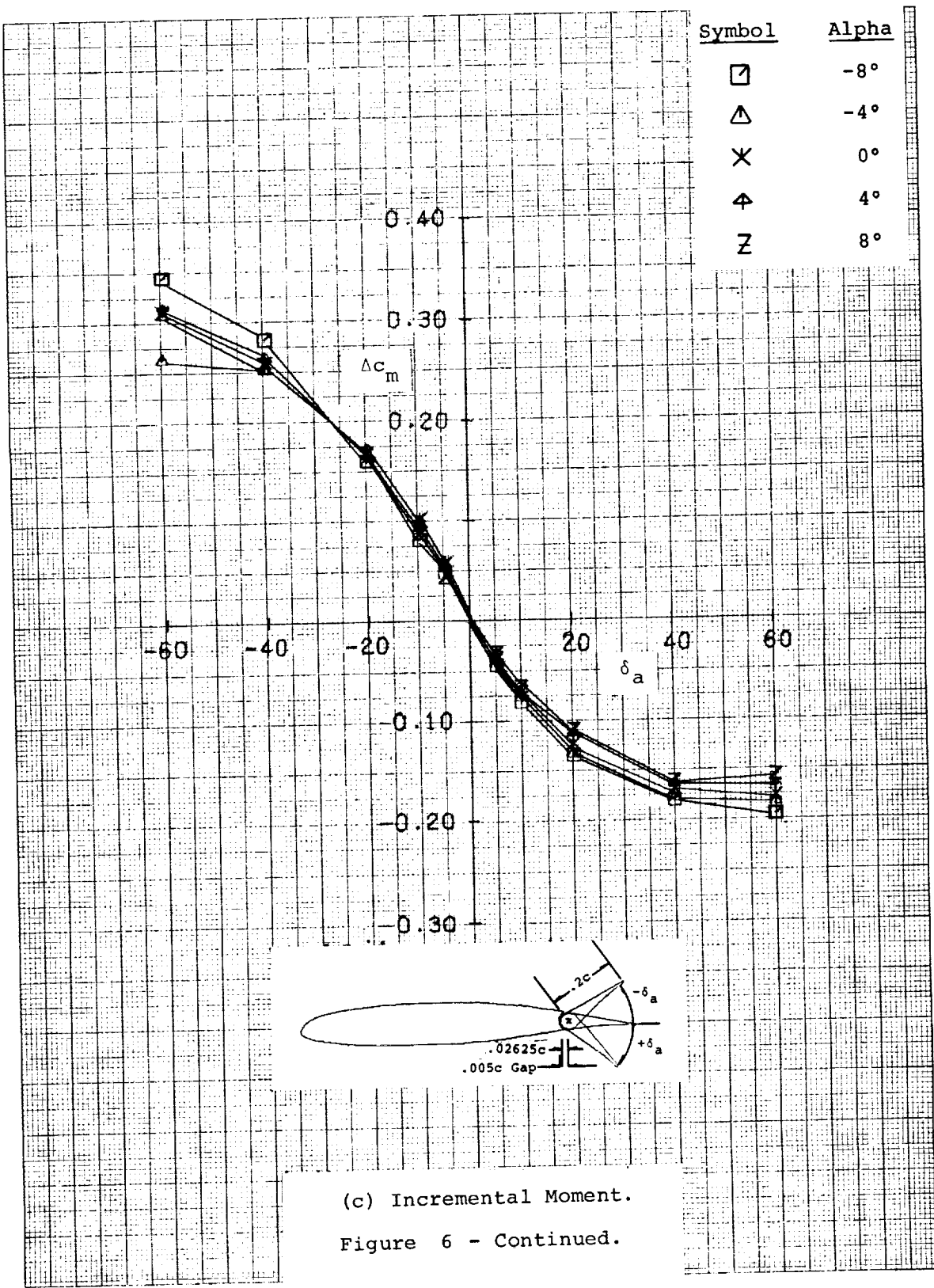
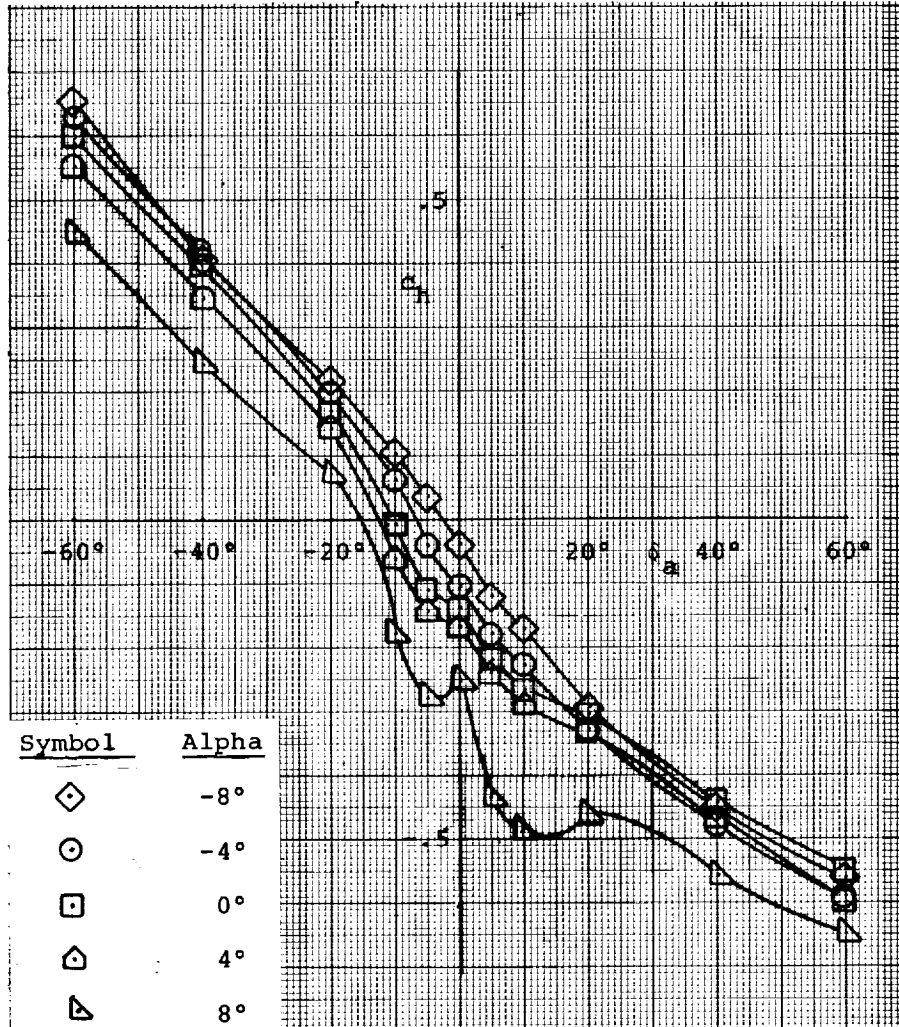
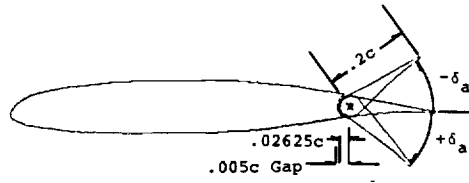


Figure 5 - Concluded.









(d) Hinge Moment.

Figure 6 - Concluded.

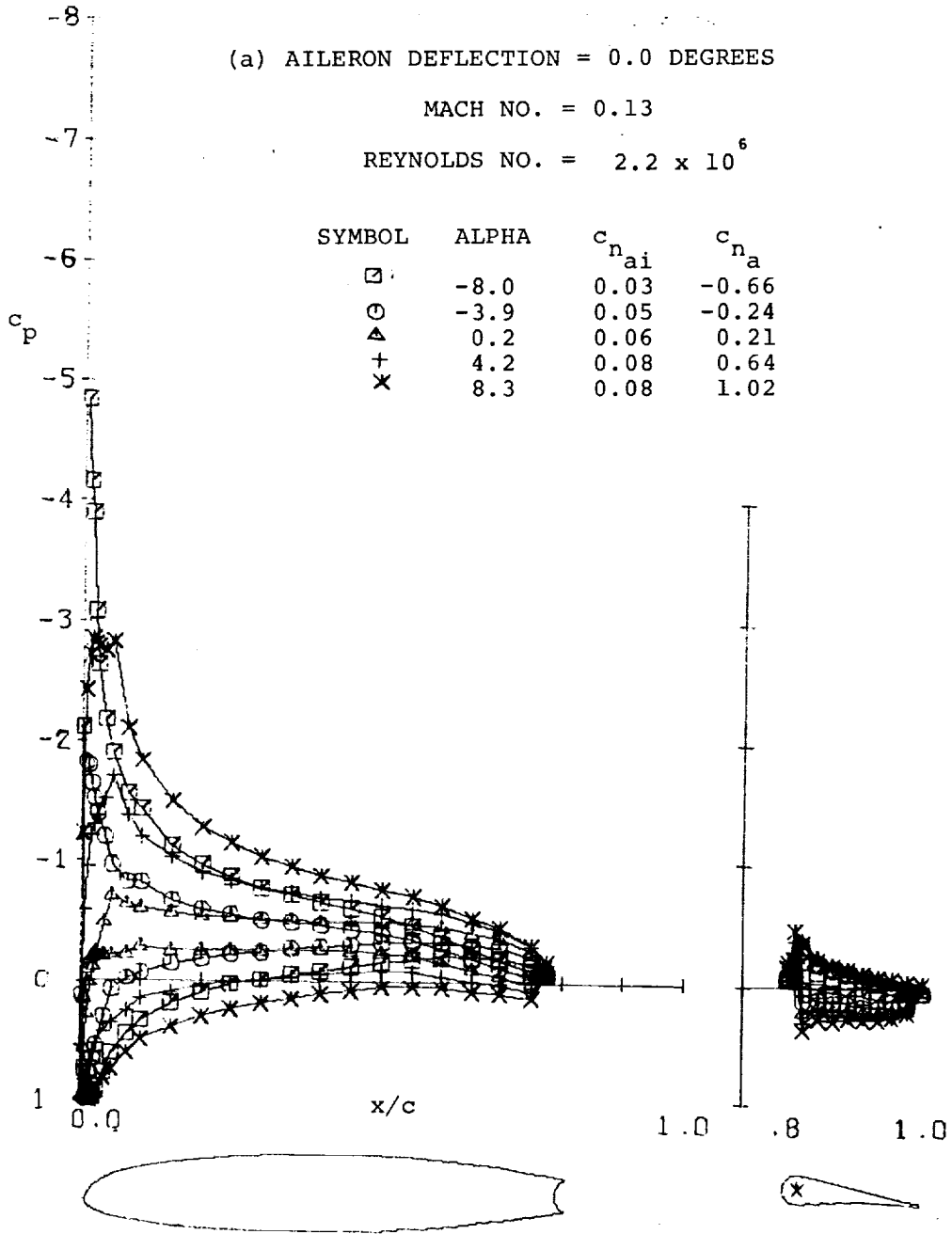


Figure 7 - Pressure Distribution with 20% Aileron.

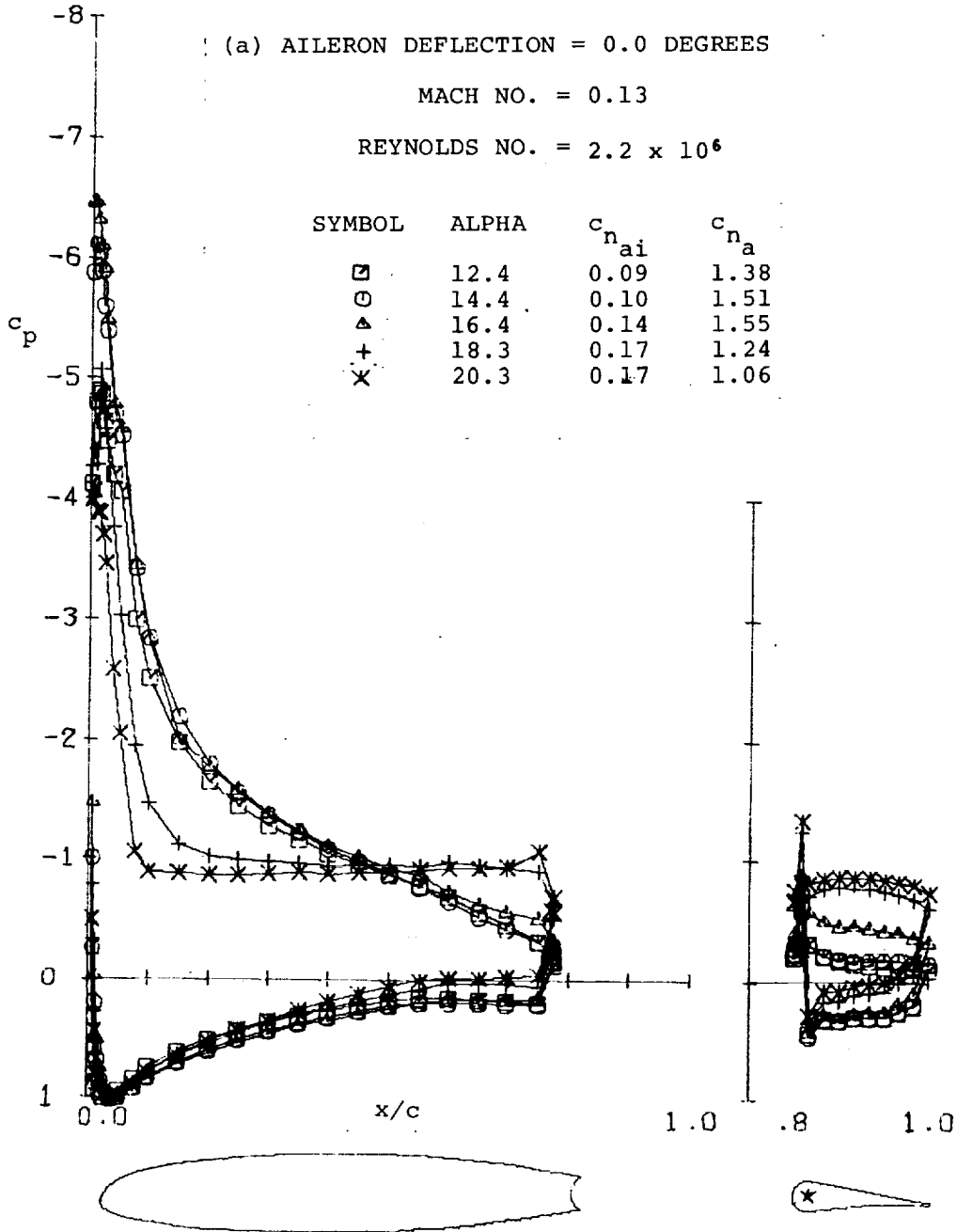


Figure 7 - Continued.

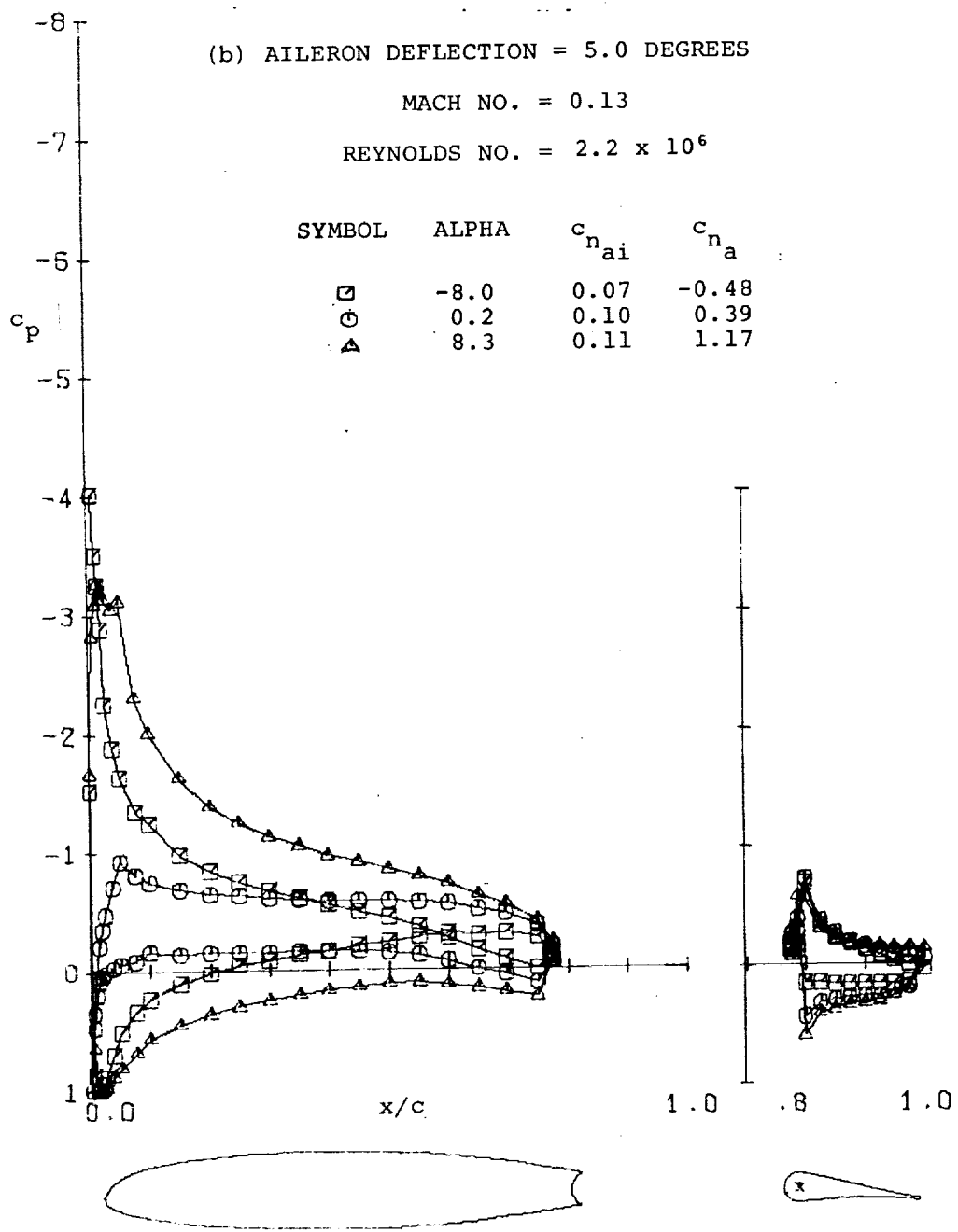


Figure 7 - Continued.

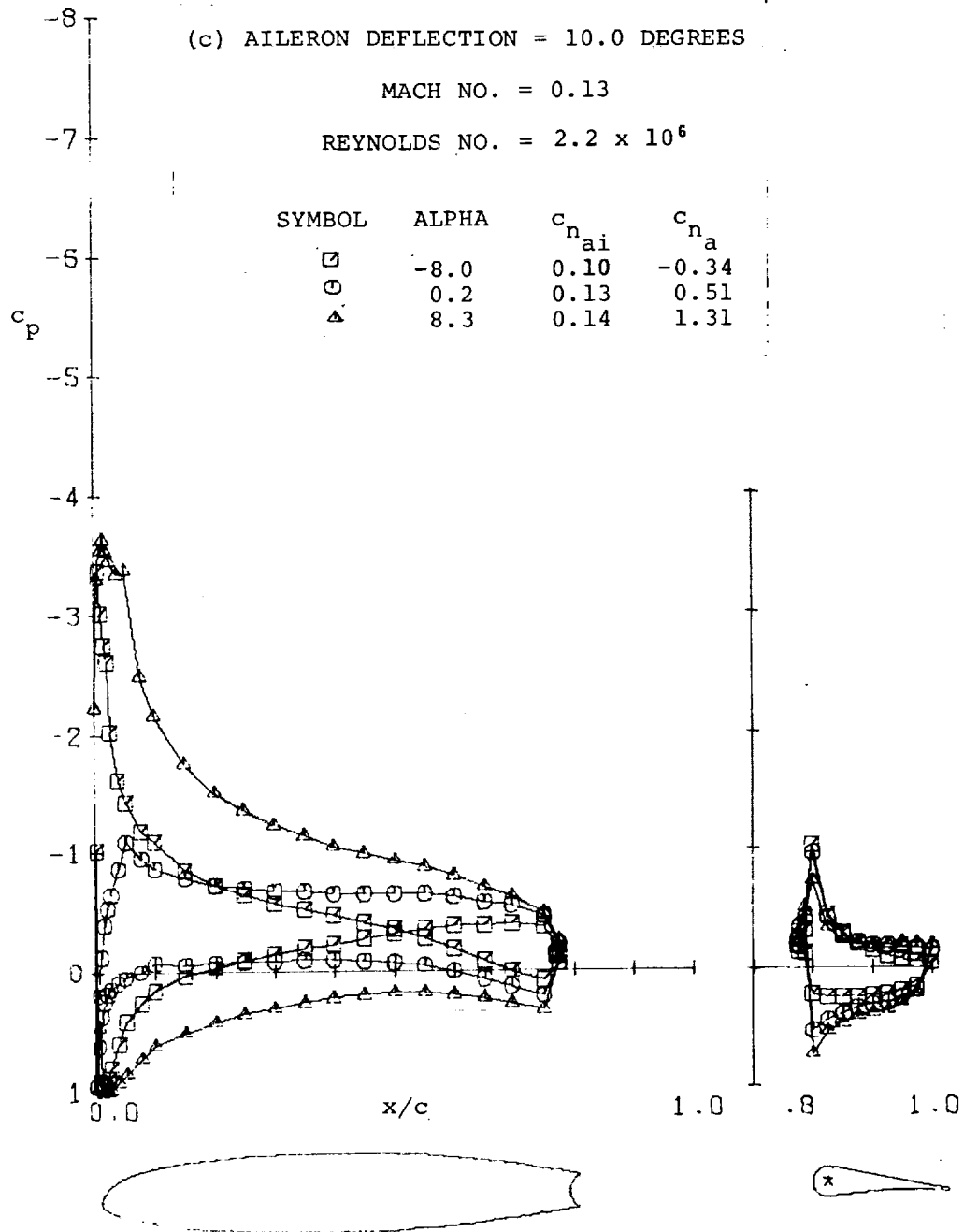


Figure 7 - Continued.

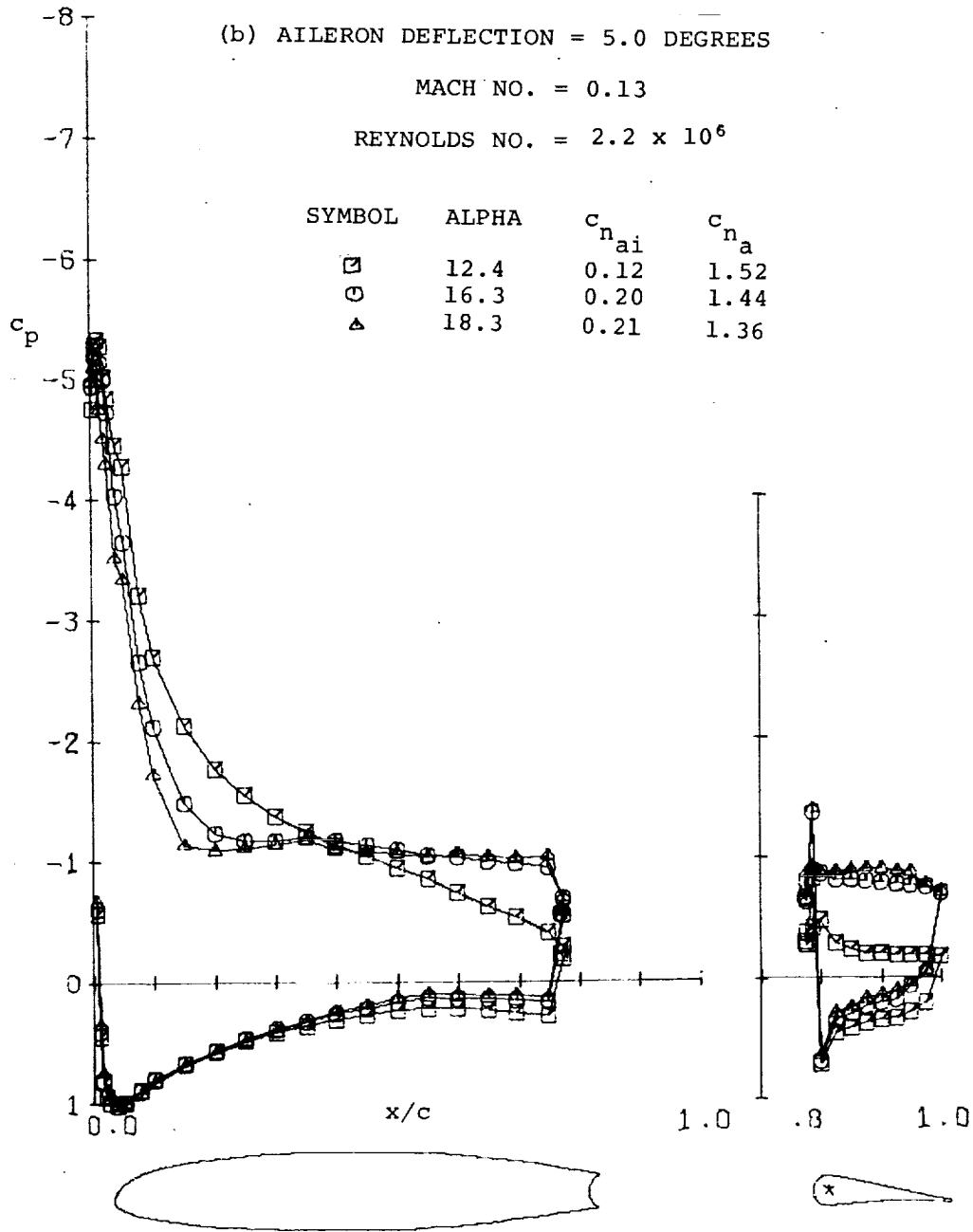


Figure 7 - Continued.

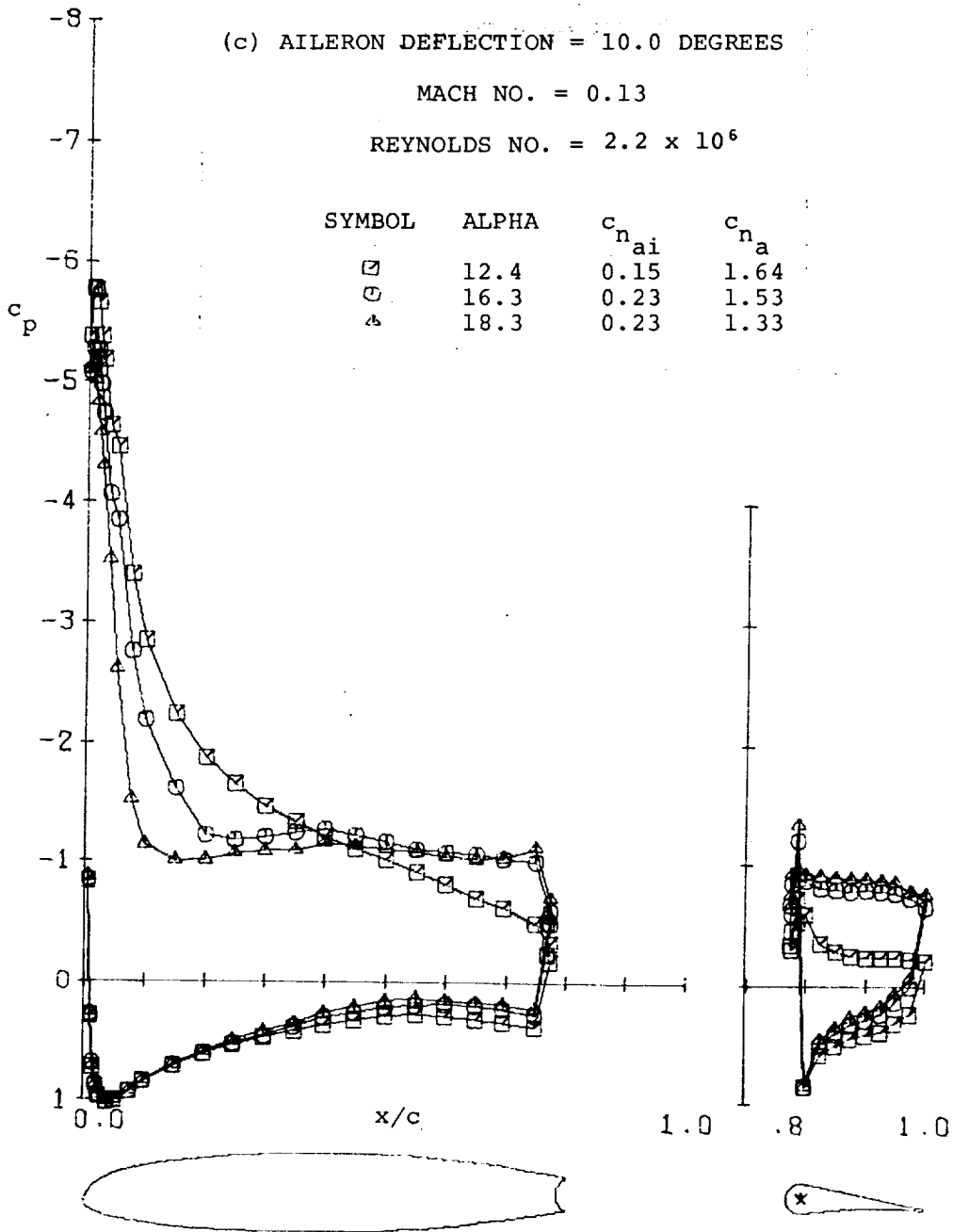


Figure 7 - Continued.

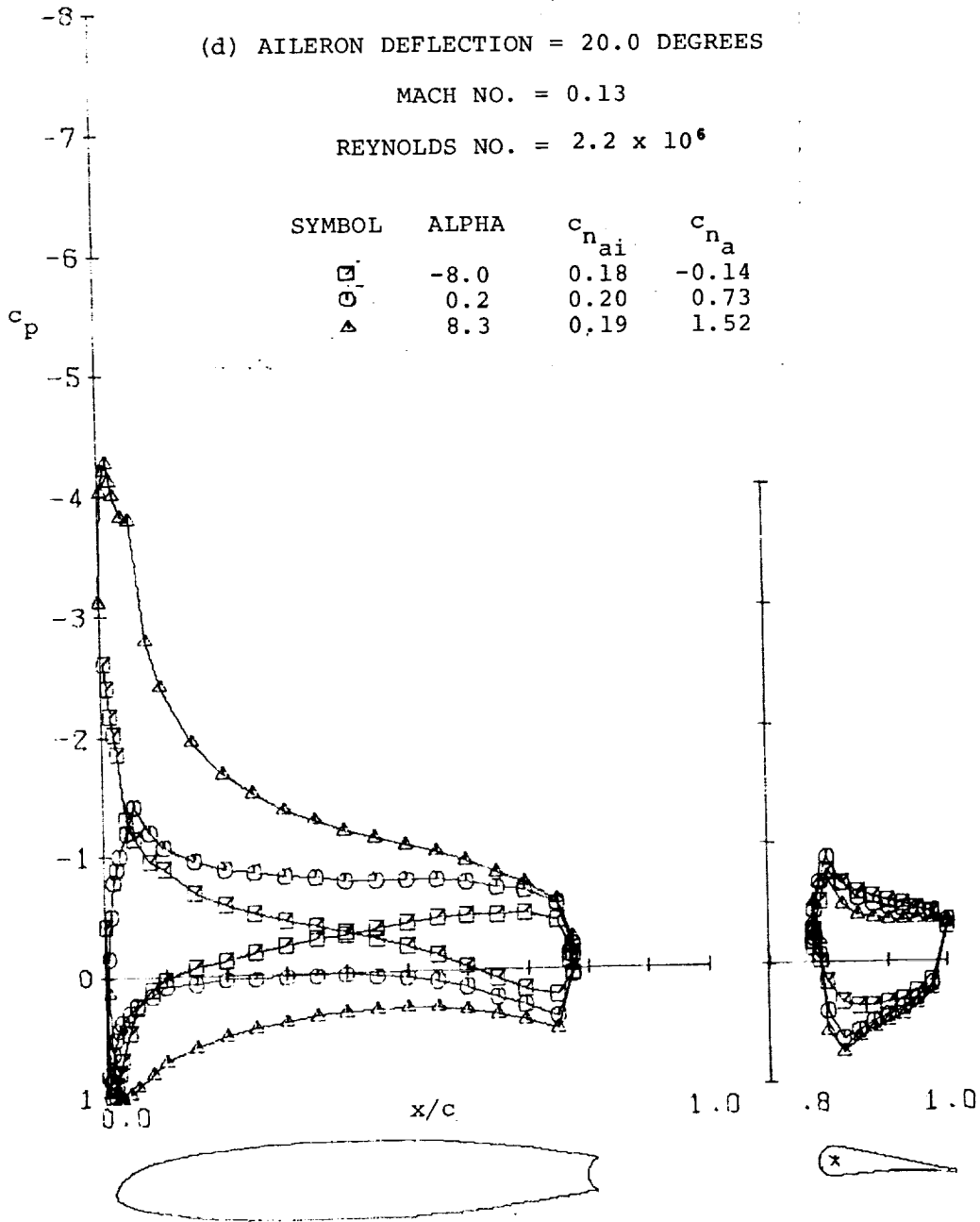


Figure 7 - Continued.

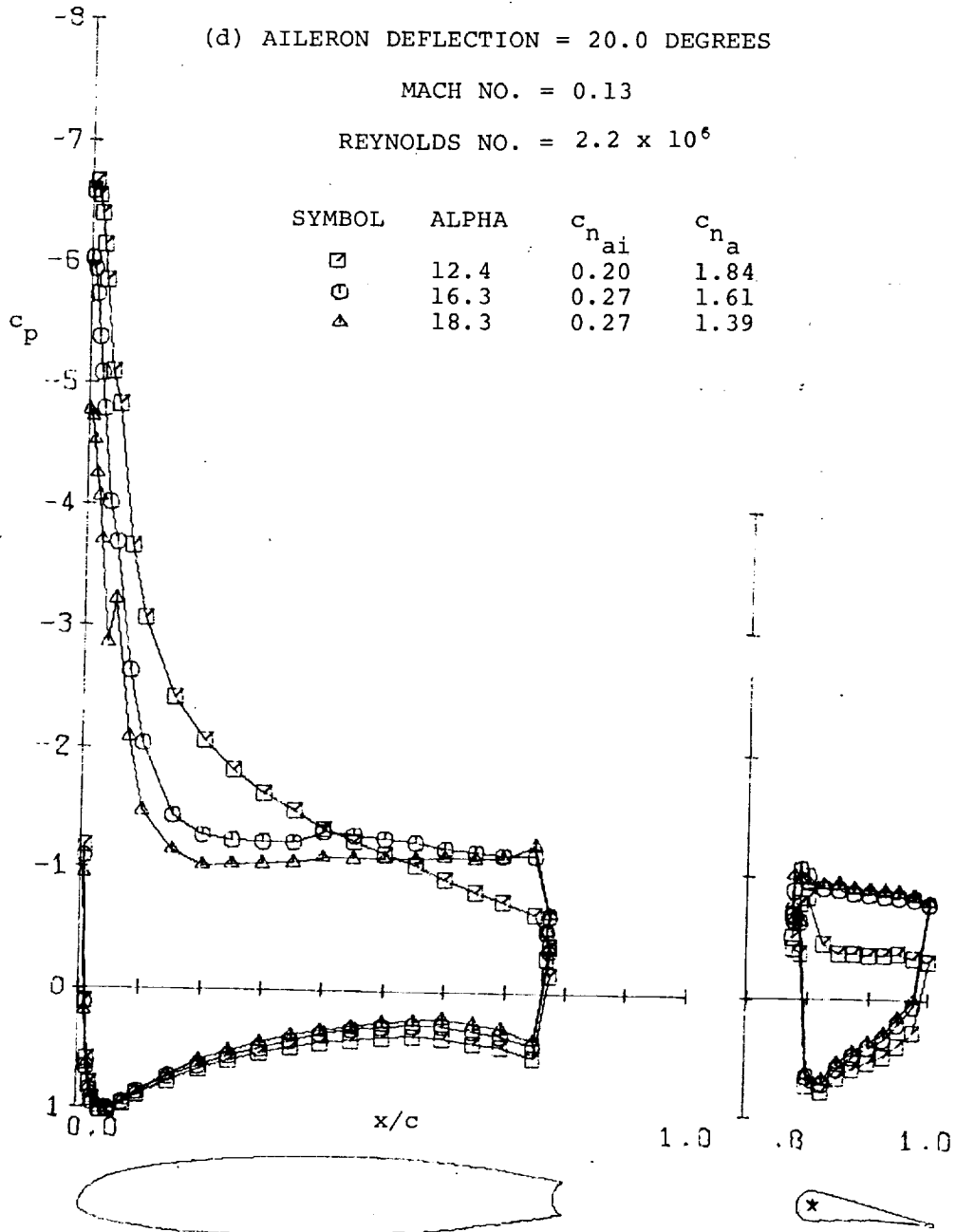


Figure 7 - Continued.

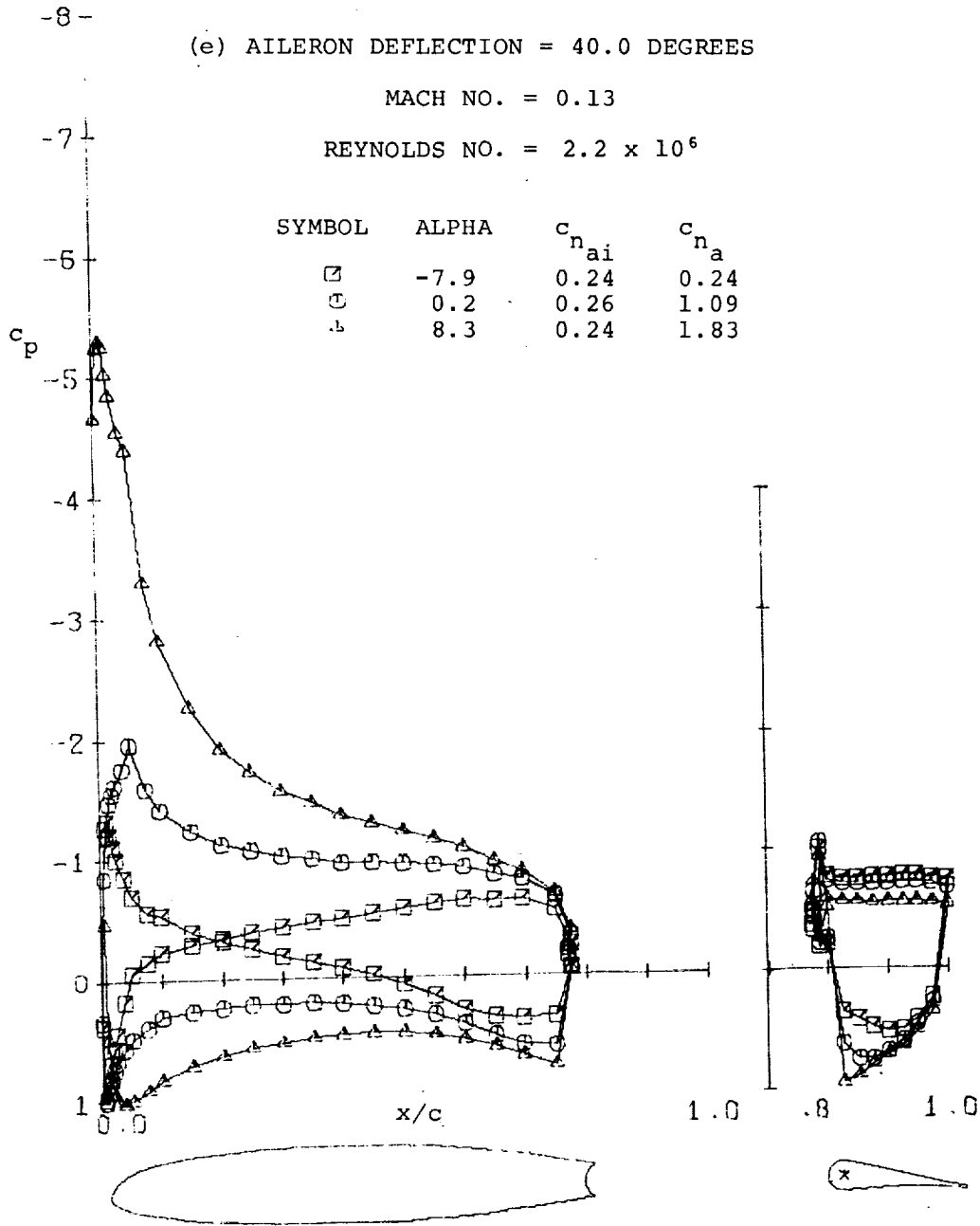


Figure 7 - Continued.

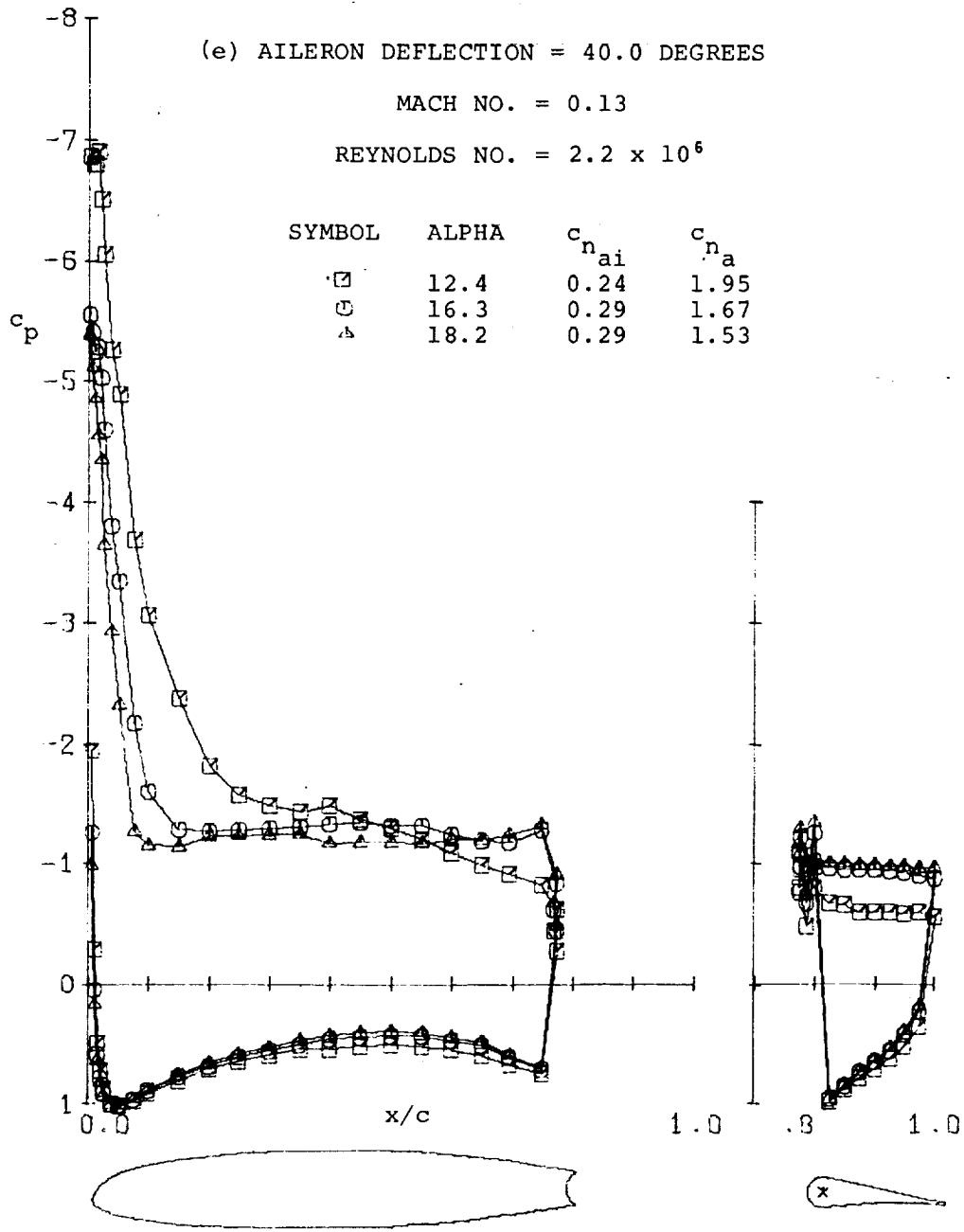


Figure 7 - Continued.

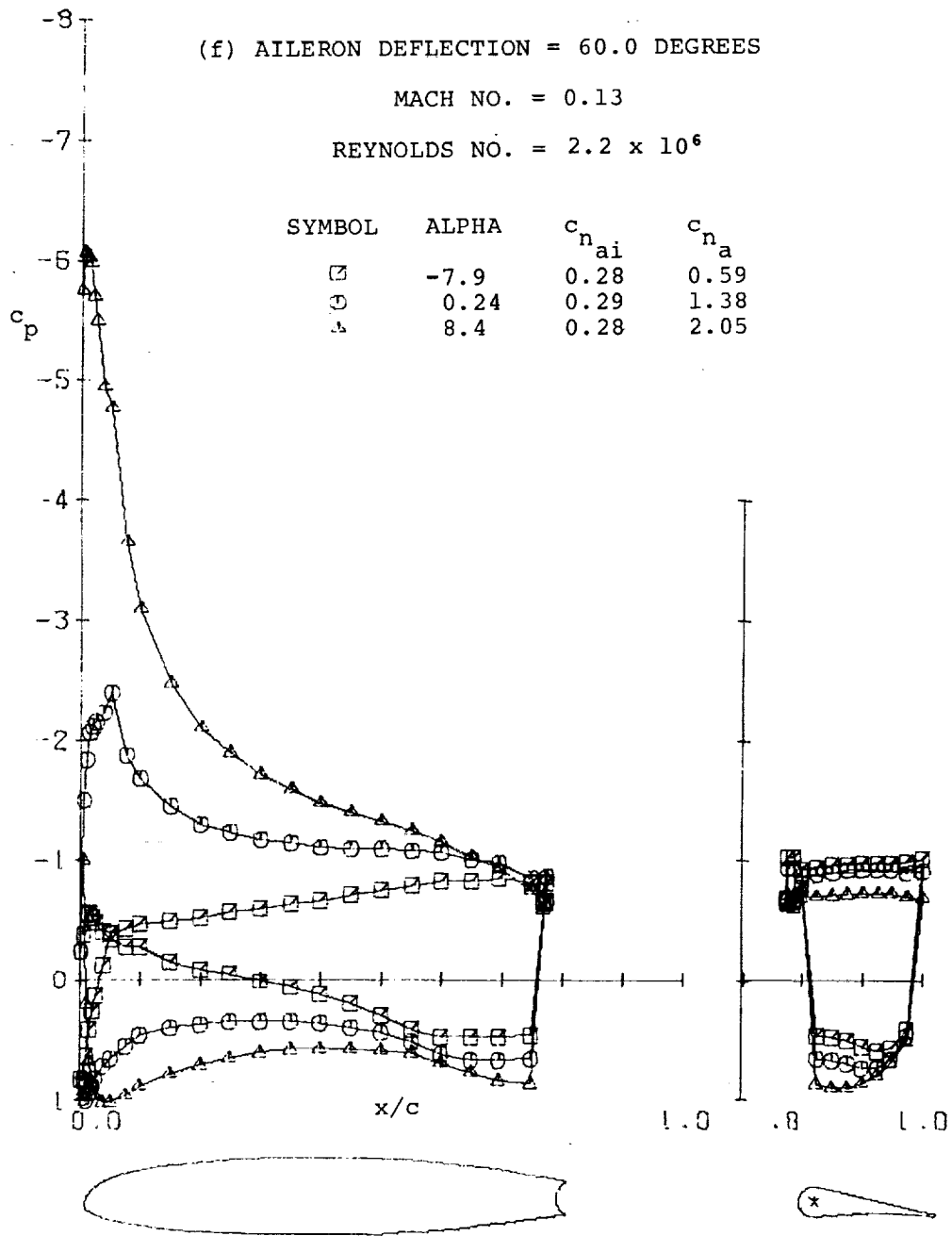


Figure 7 - Continued.

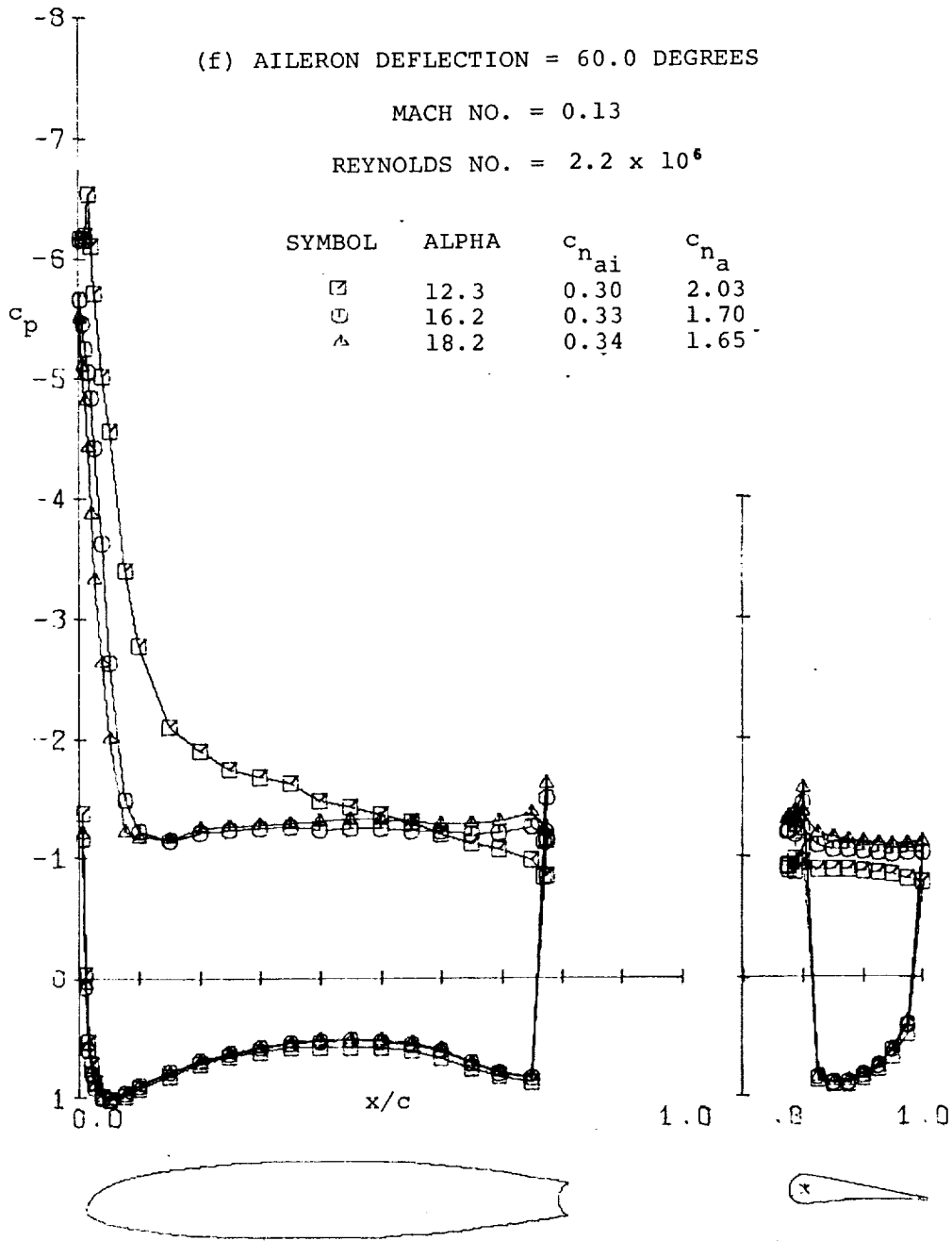


Figure 7 - Continued.

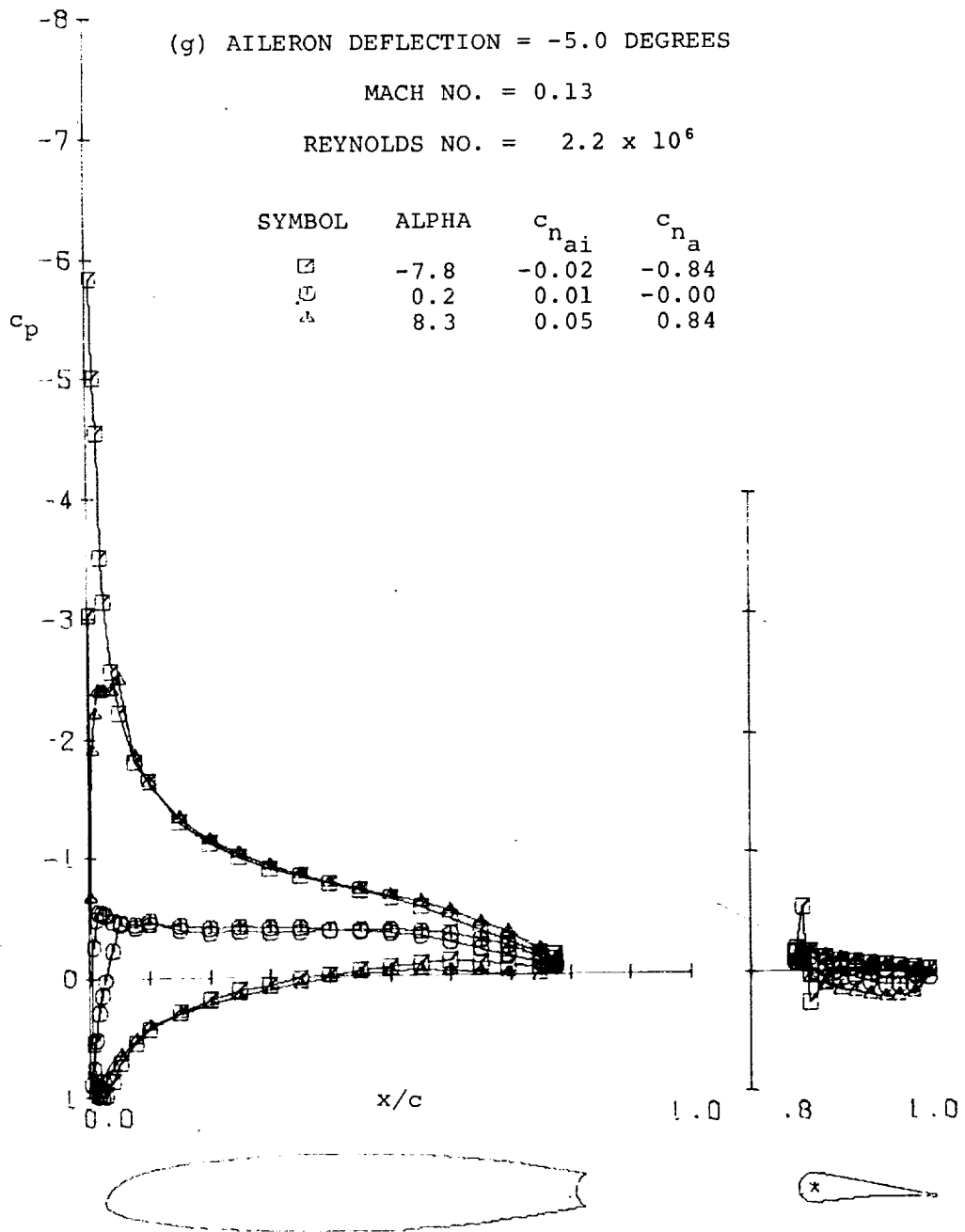


Figure 7 - Continued.

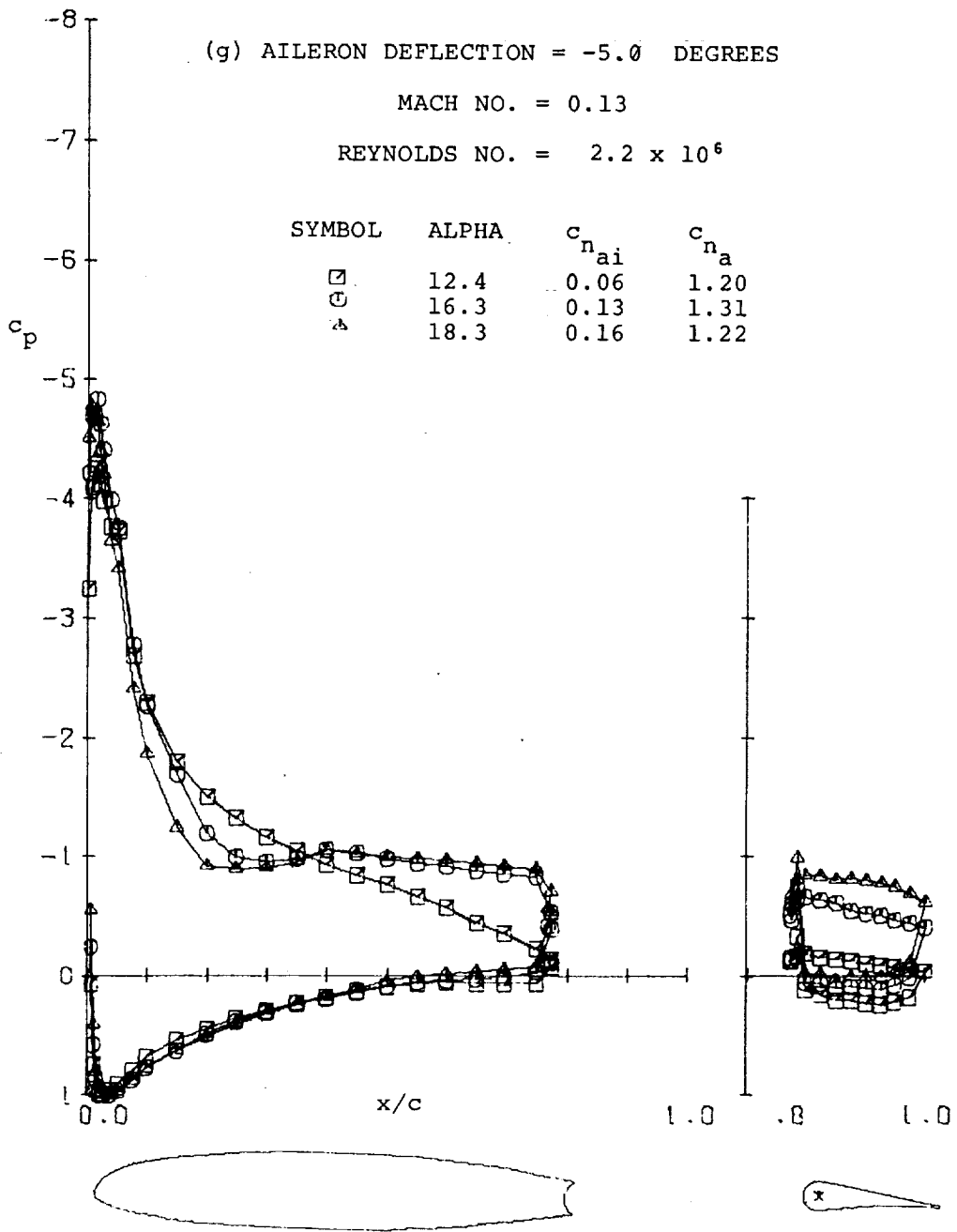


Figure 7 - Continued.

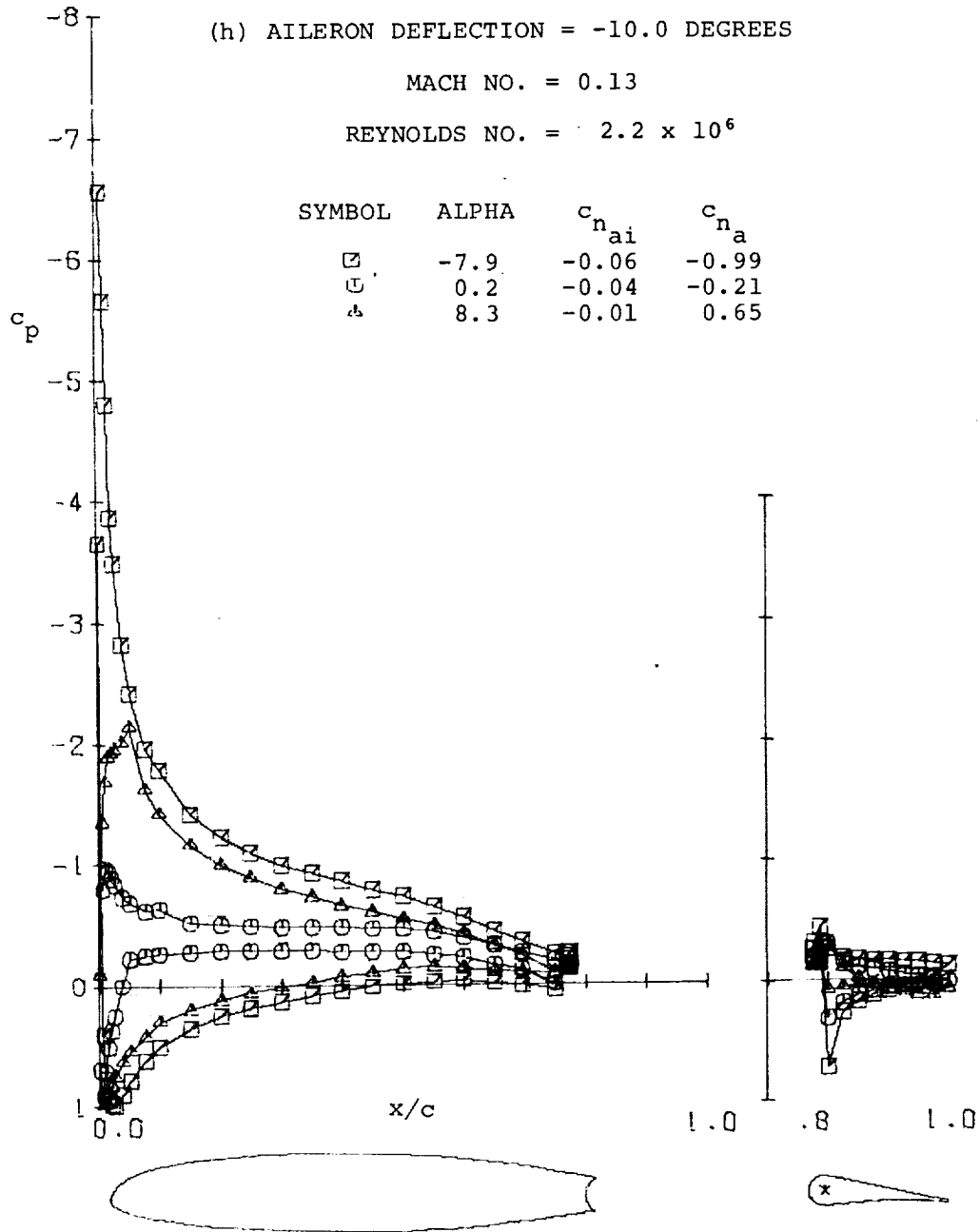


Figure 7 - Continued.

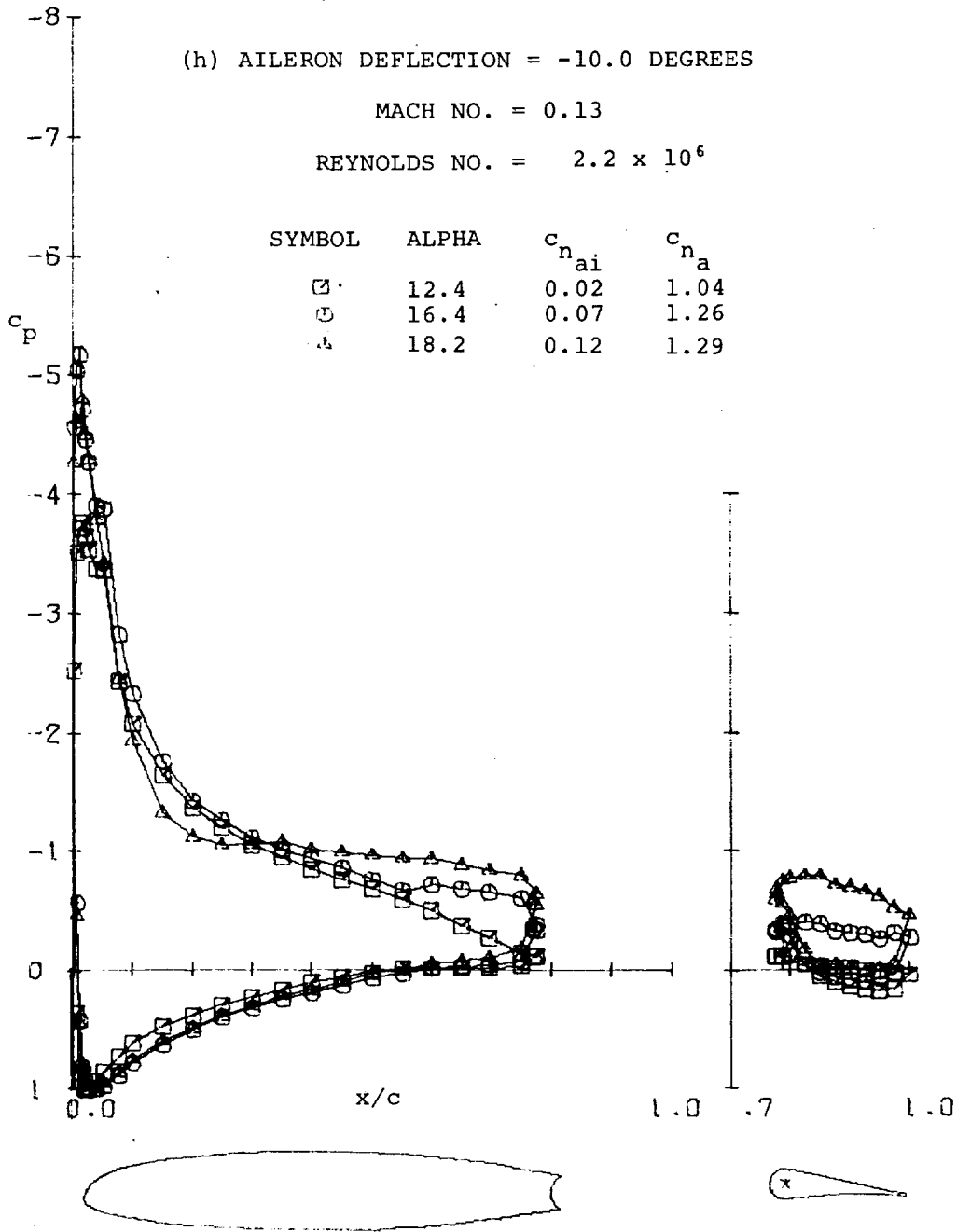


Figure 7 - Continued.

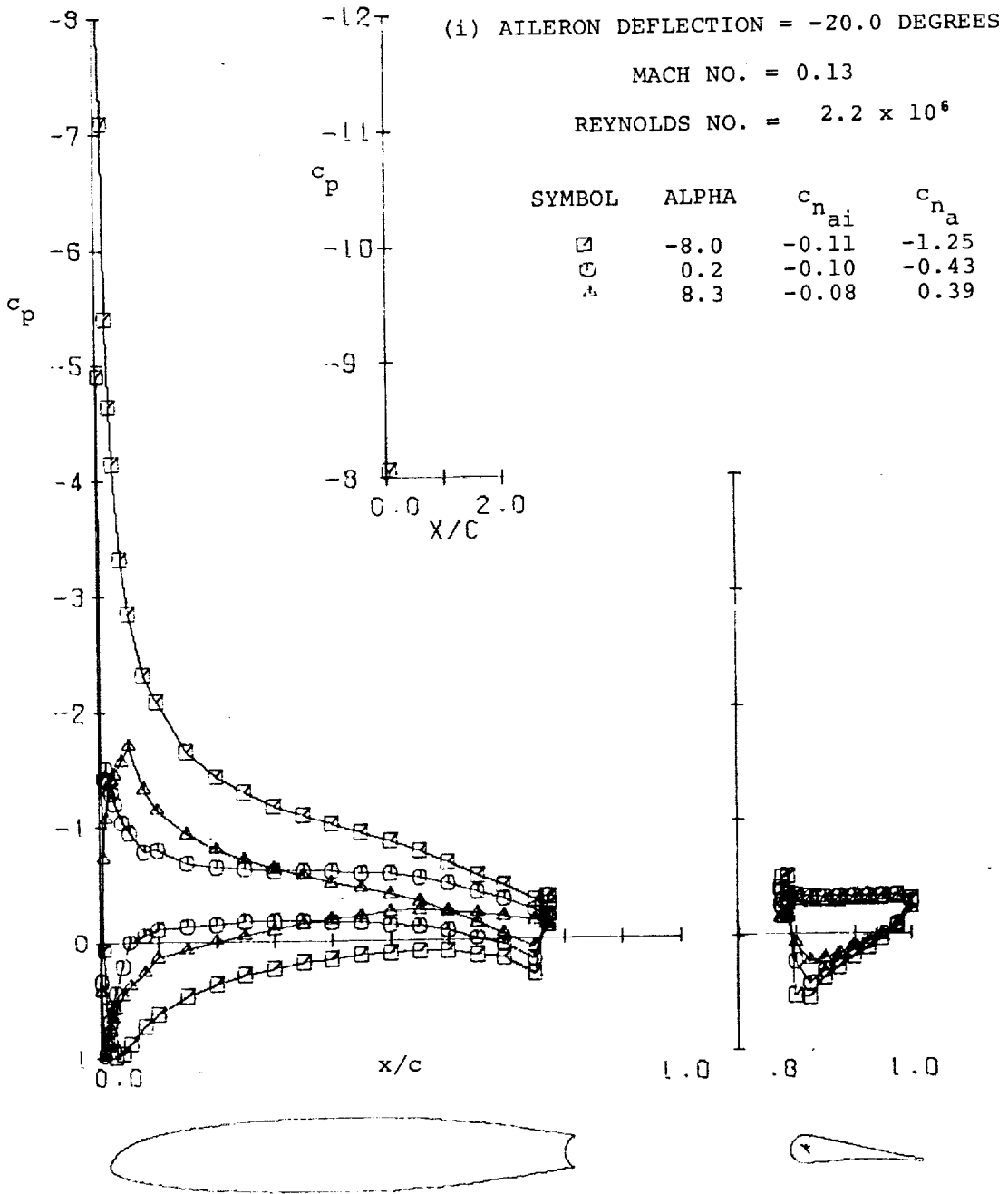


Figure 7 - Continued.

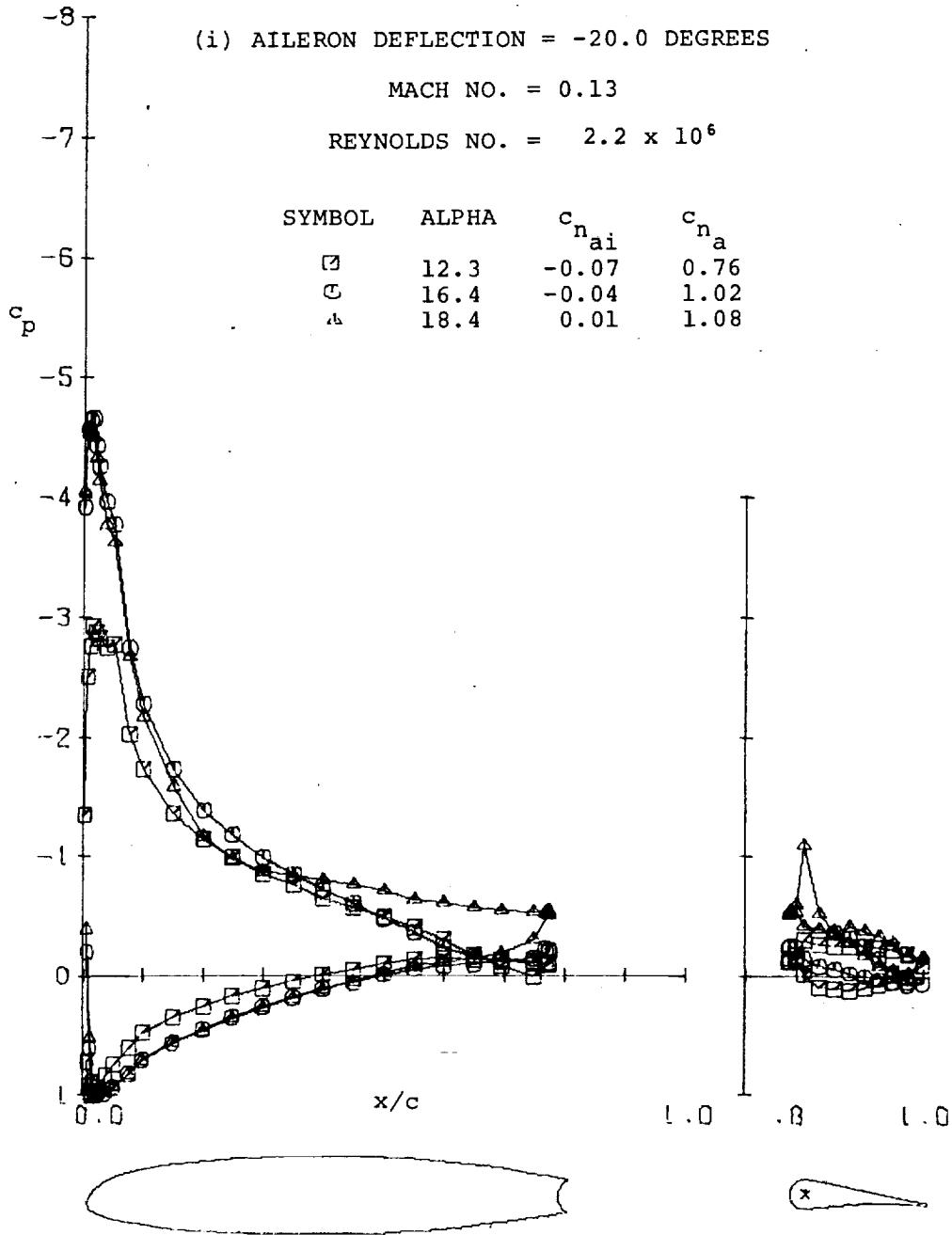


Figure 7 - Continued.

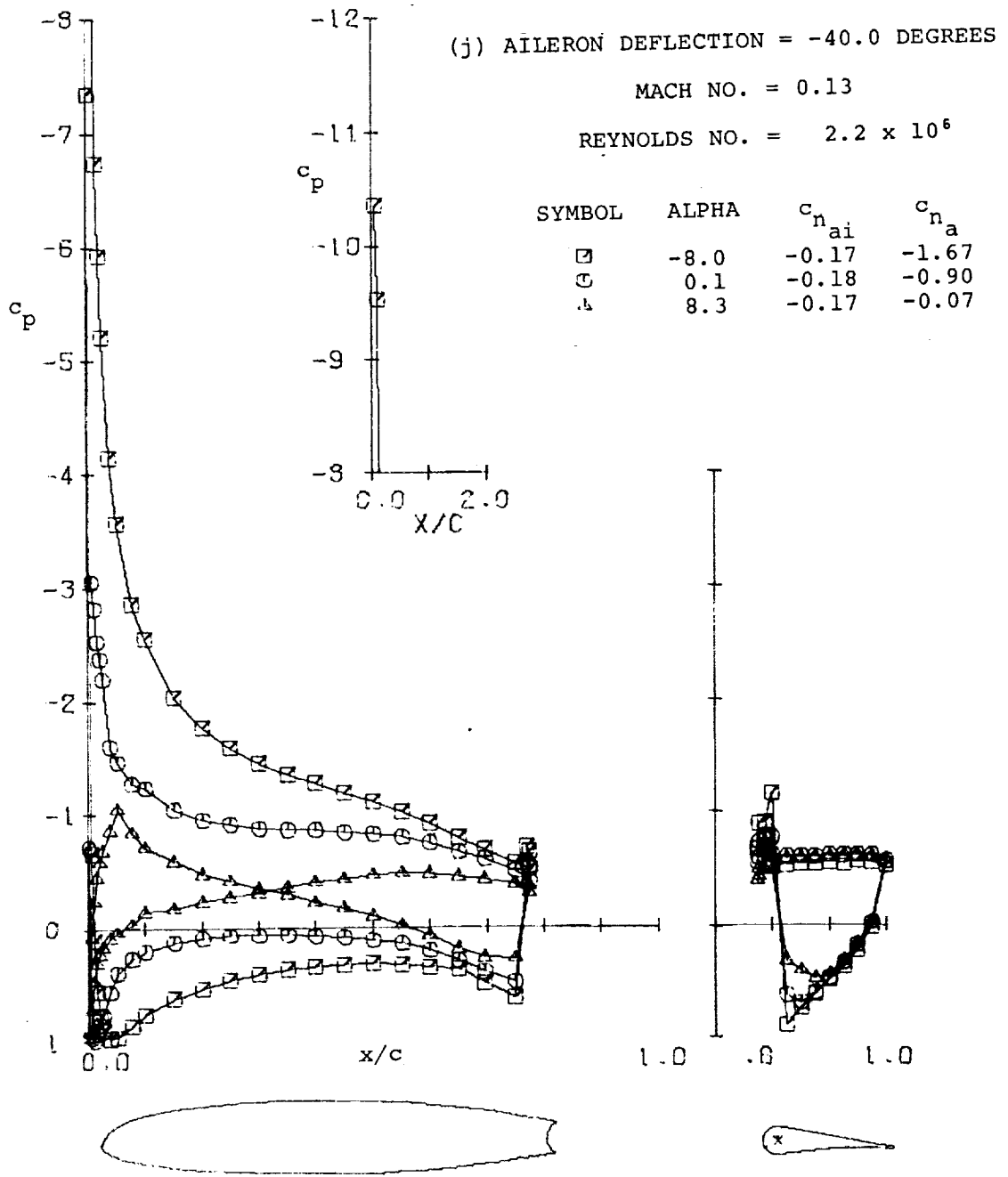


Figure 7 - Continued.

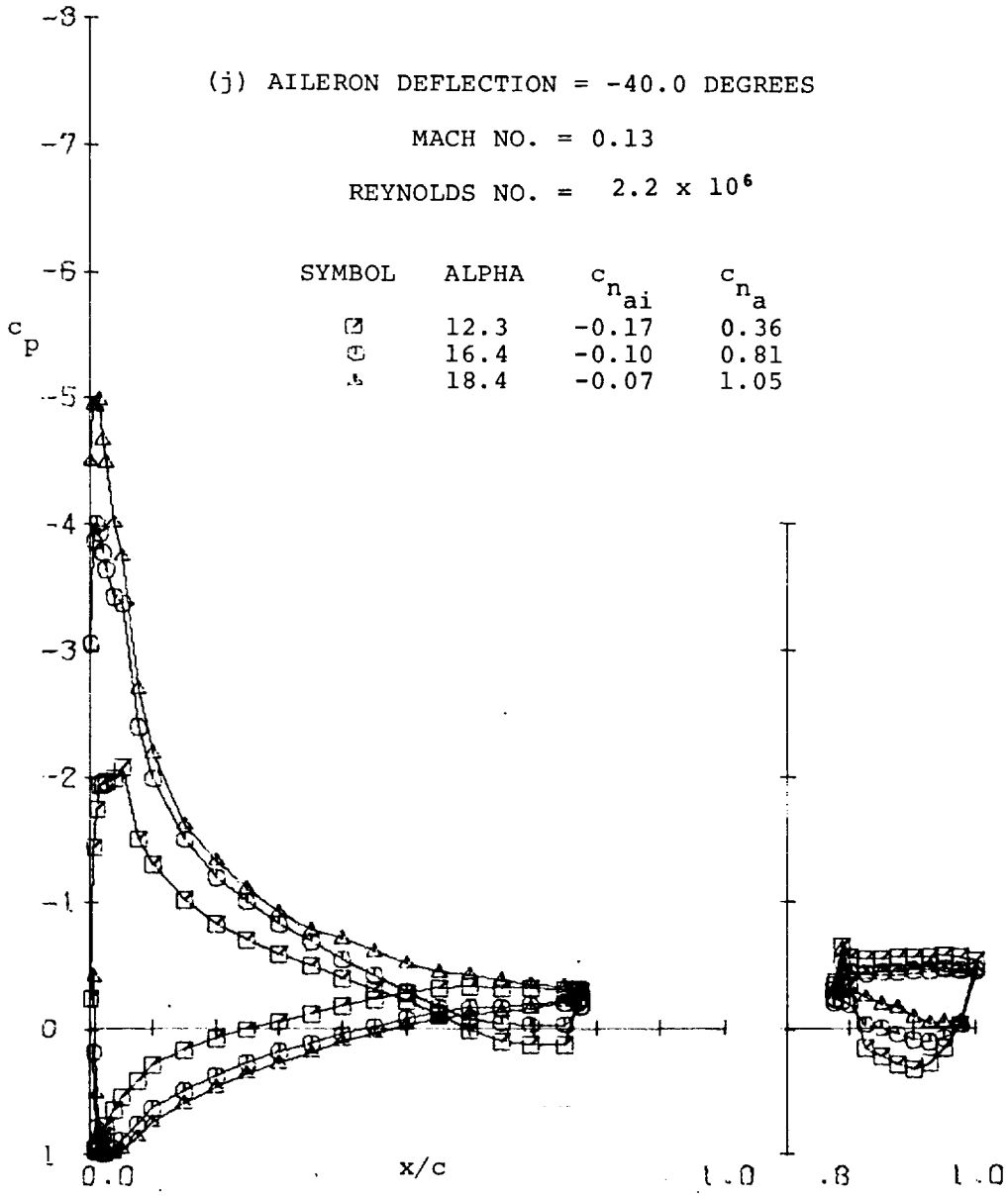


Figure 7 - Continued.

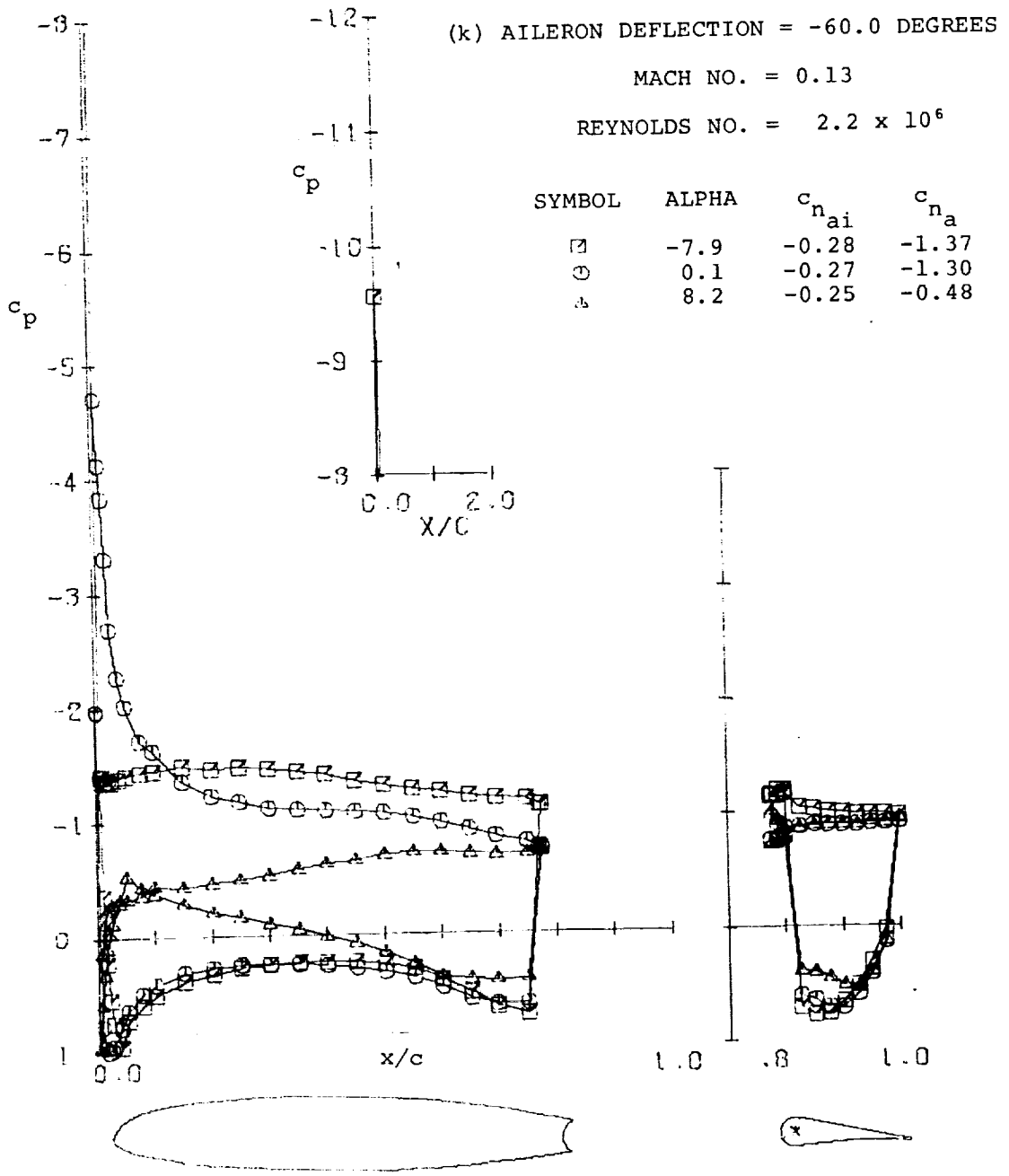


Figure 7 - Continued.

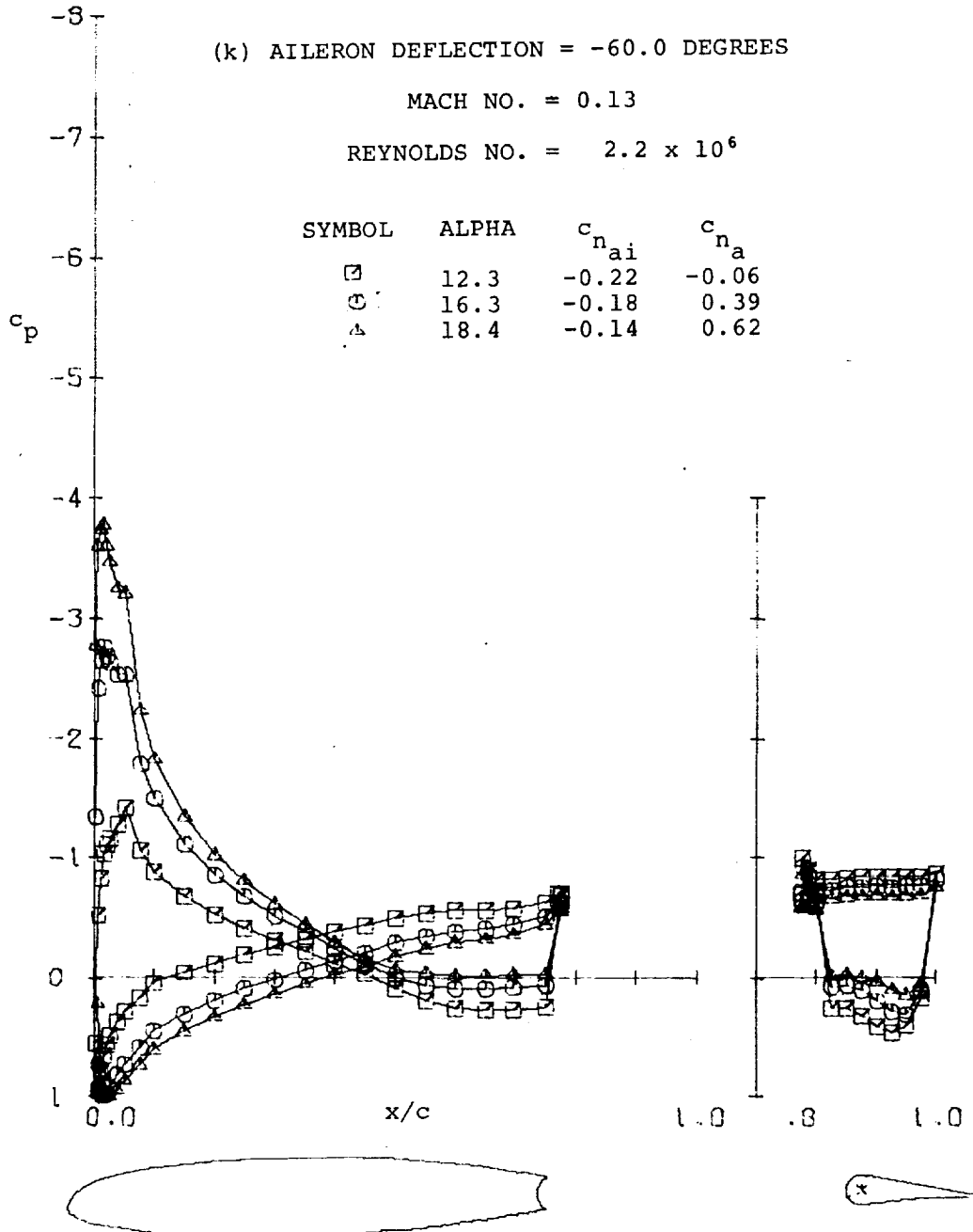


Figure 7 - Concluded.

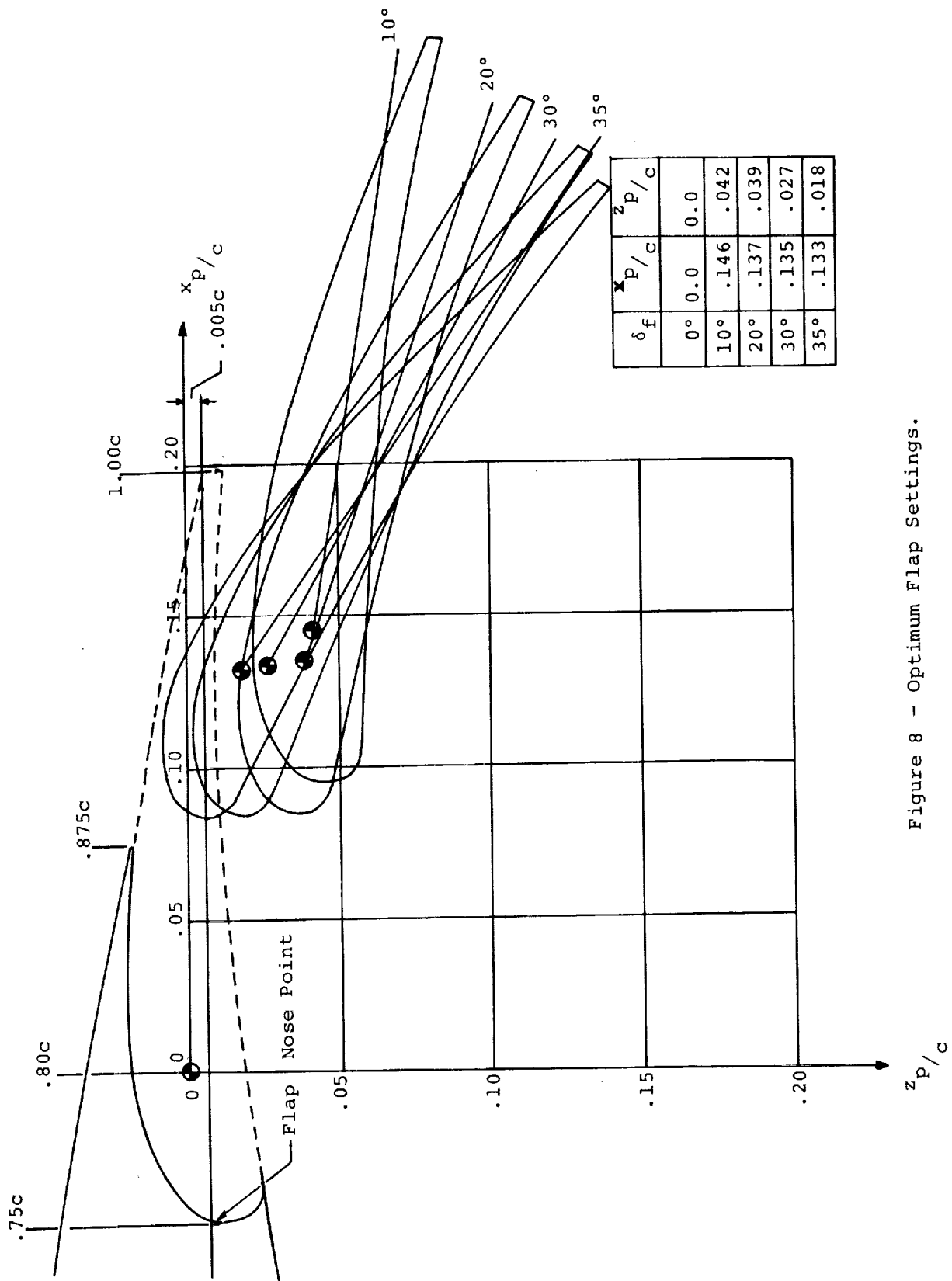
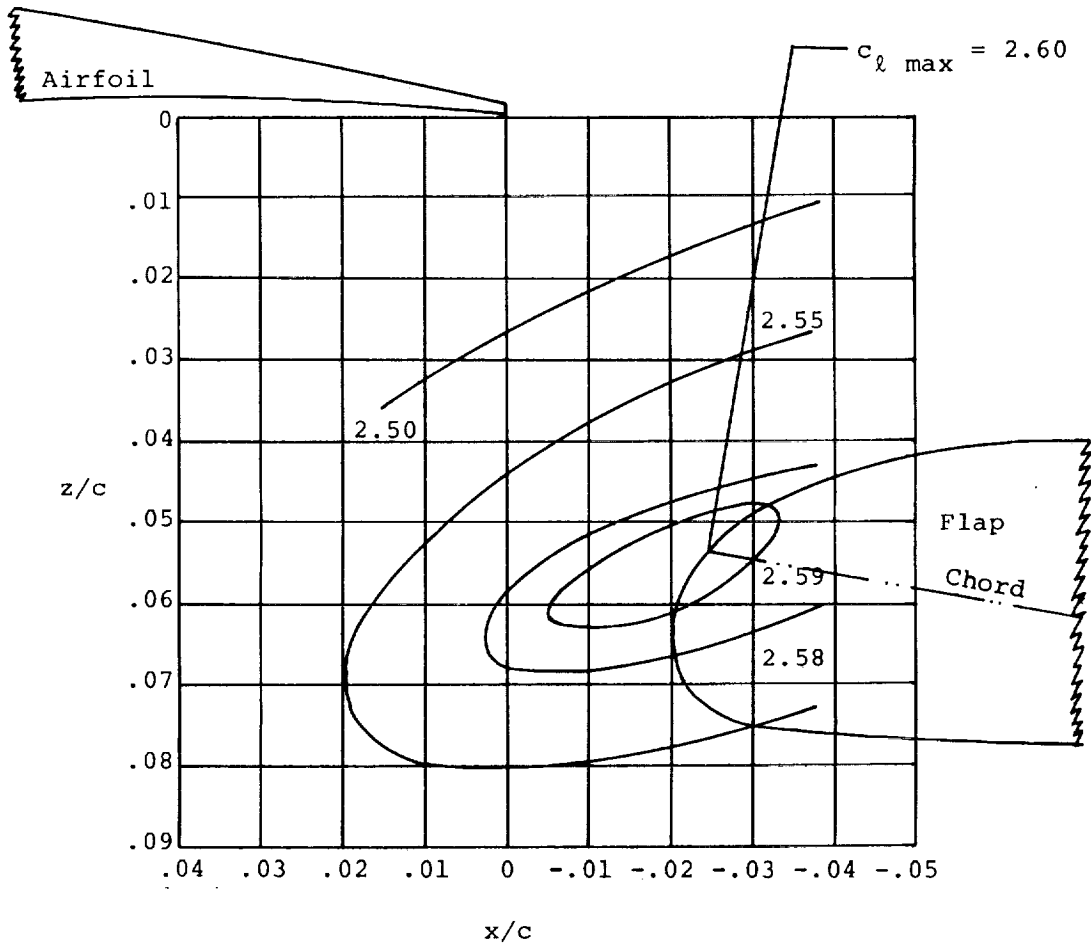


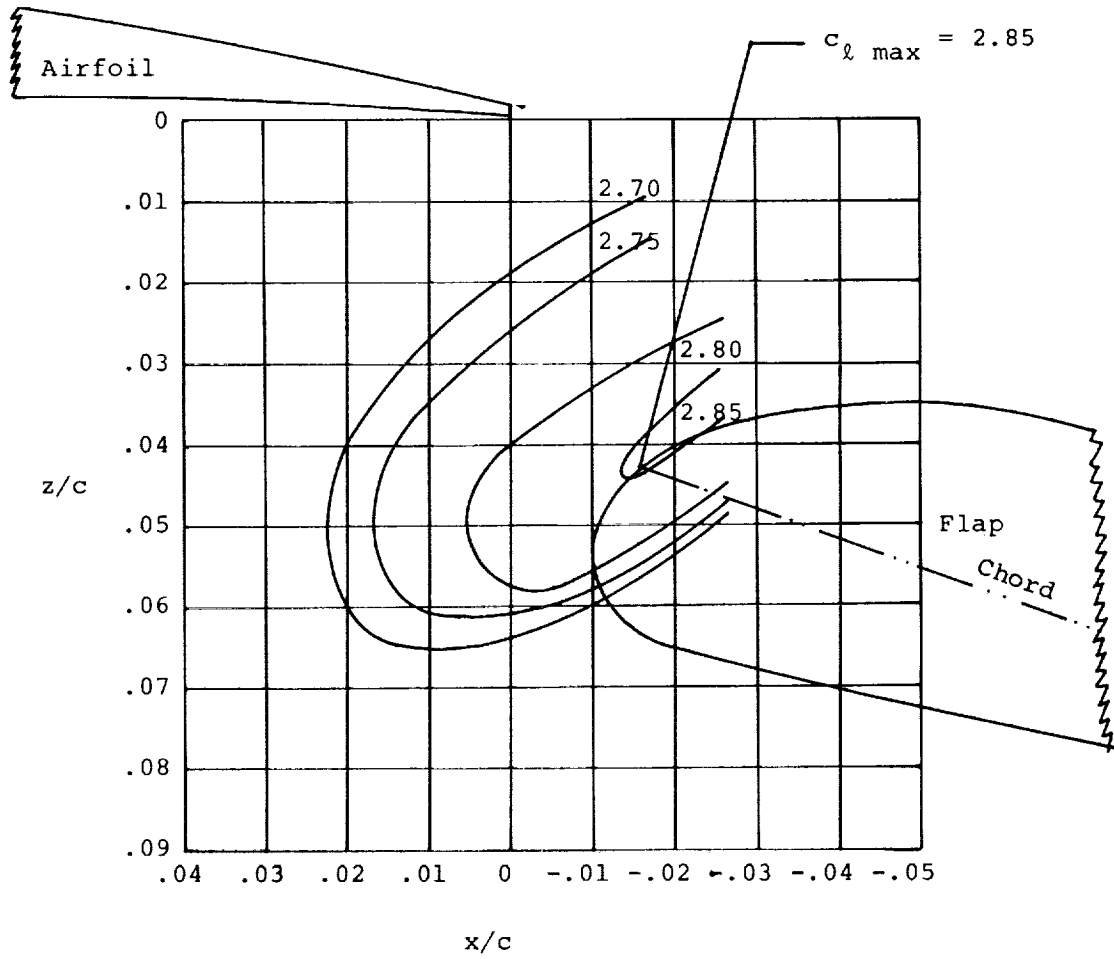
Figure 8 - Optimum Flap Settings.



Note: Contours are for locus of flap nose point, (see p.56).

(a) 10° Flap Deflection

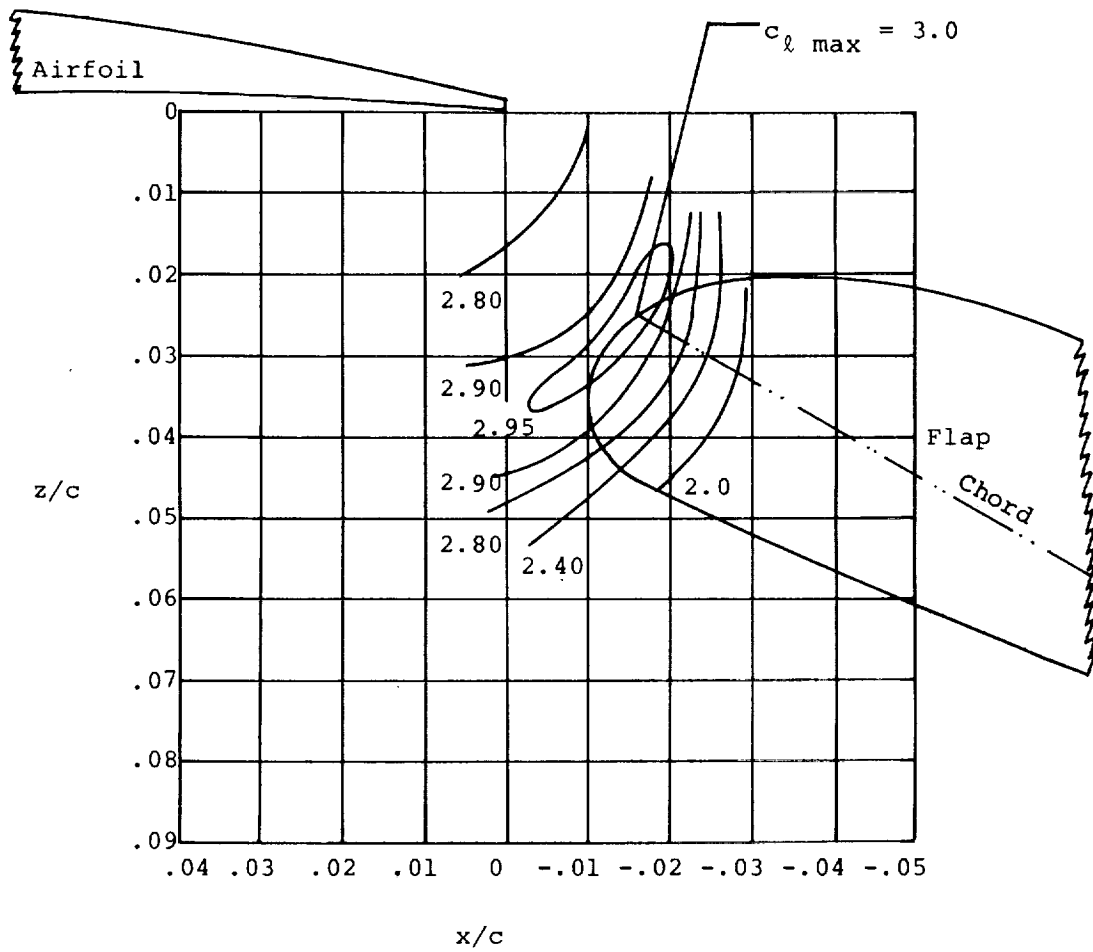
Figure 9 - $c_{l \max}$ Contours.



Note: Contours are for locus of flap nose point, (see p.56).

(b) 20° Flap Deflection

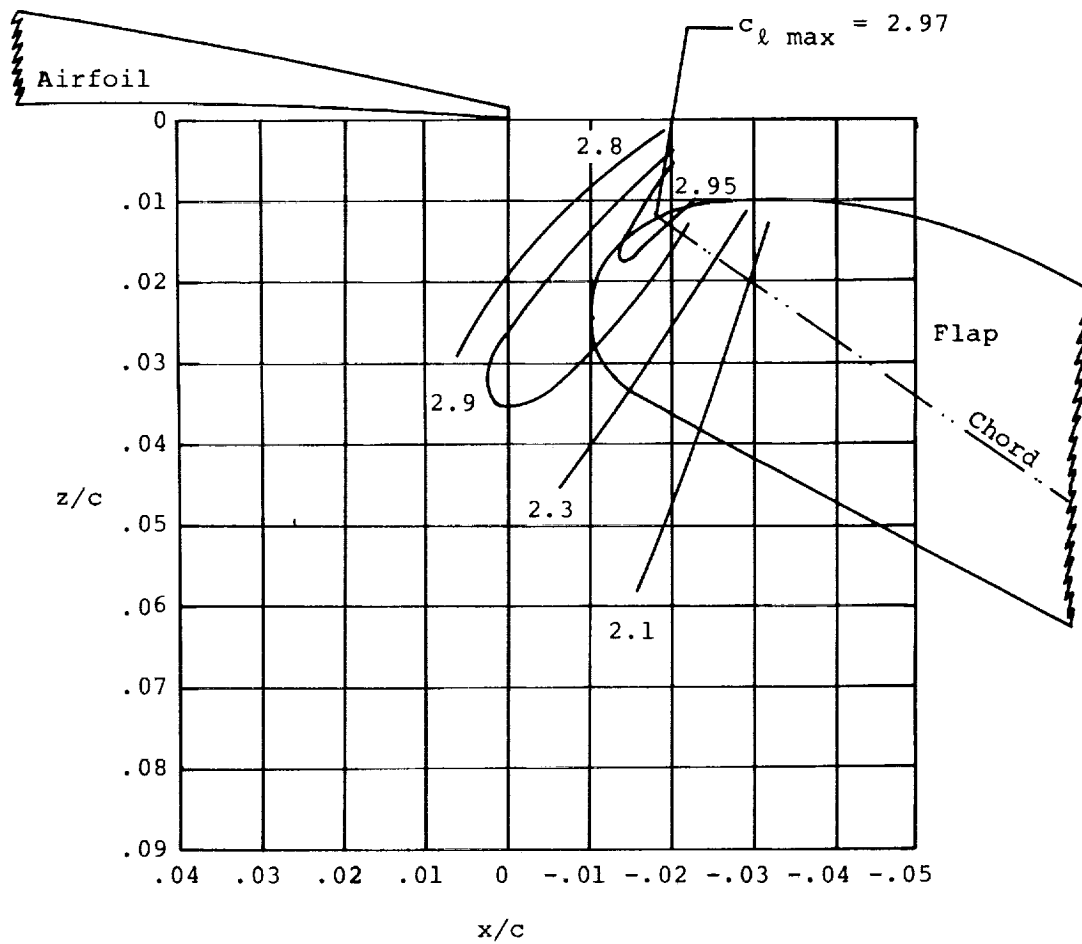
Figure '9 - $c_{l \max}$ Contours.



Note: Contours are for locus of flap nose point, (see p.56).

(c) 30° Flap Deflection

Figure 9 - $c_{l \max}$ Contours.

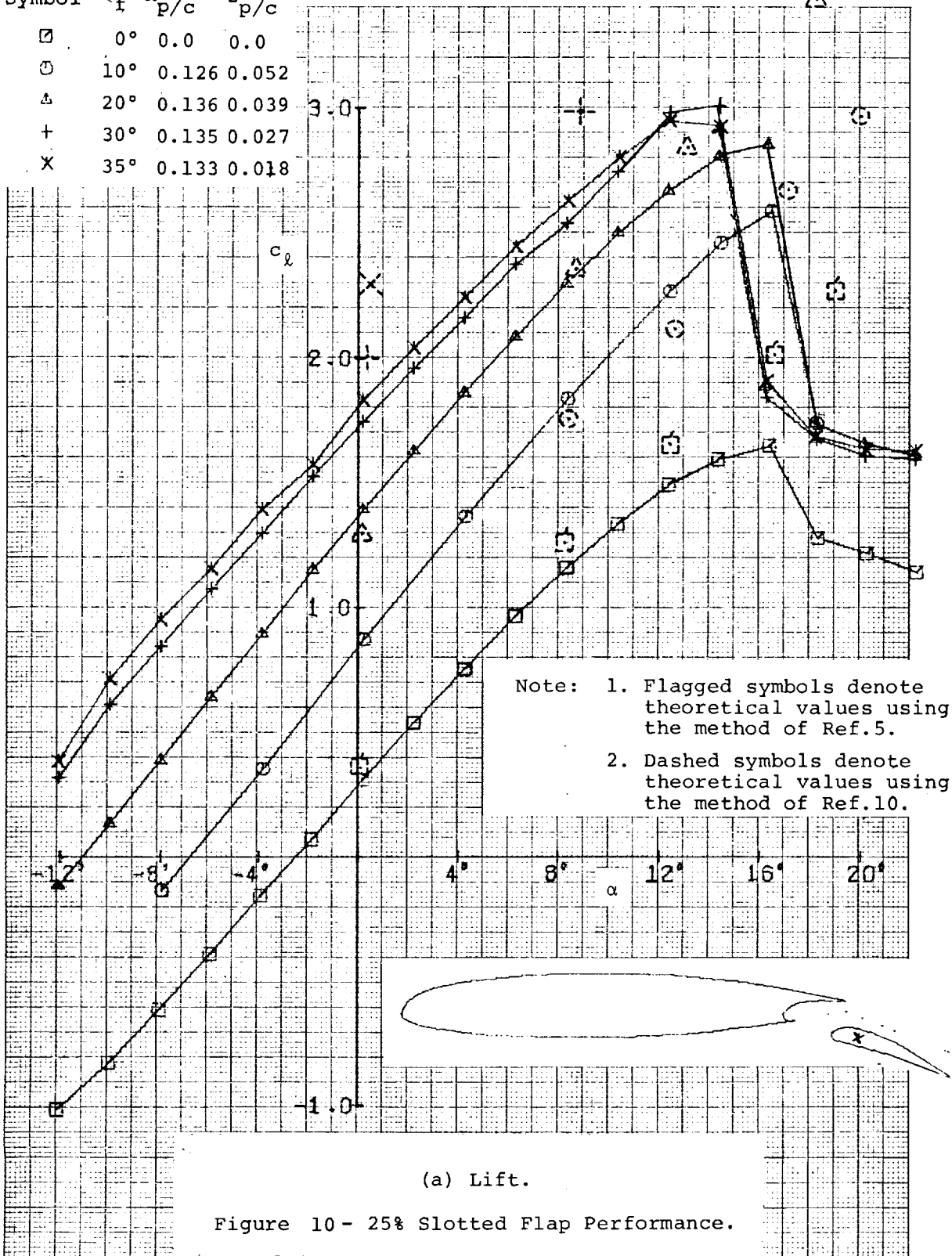


Note: Contours are for locus of flap nose point, (see p.56).

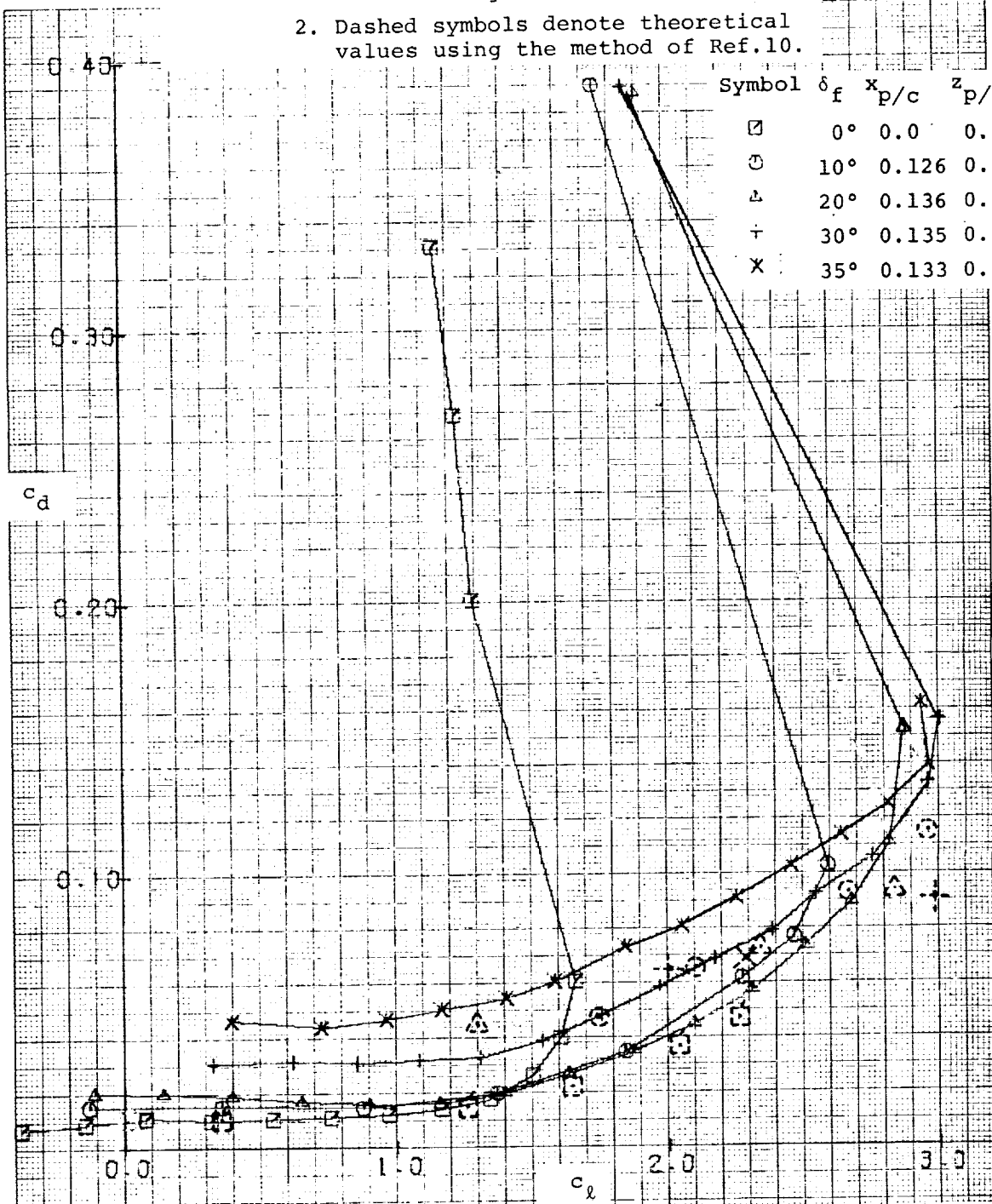
(d) 35° Flap Deflection

Figure 9 - $c_{l \max}$ Contours.

Symbol	δ_f	$x_{p/c}$	$z_{p/c}$
□	0°	0.0	0.0
○	10°	0.126	0.052
△	20°	0.136	0.039
+	30°	0.135	0.027
x	35°	0.133	0.018

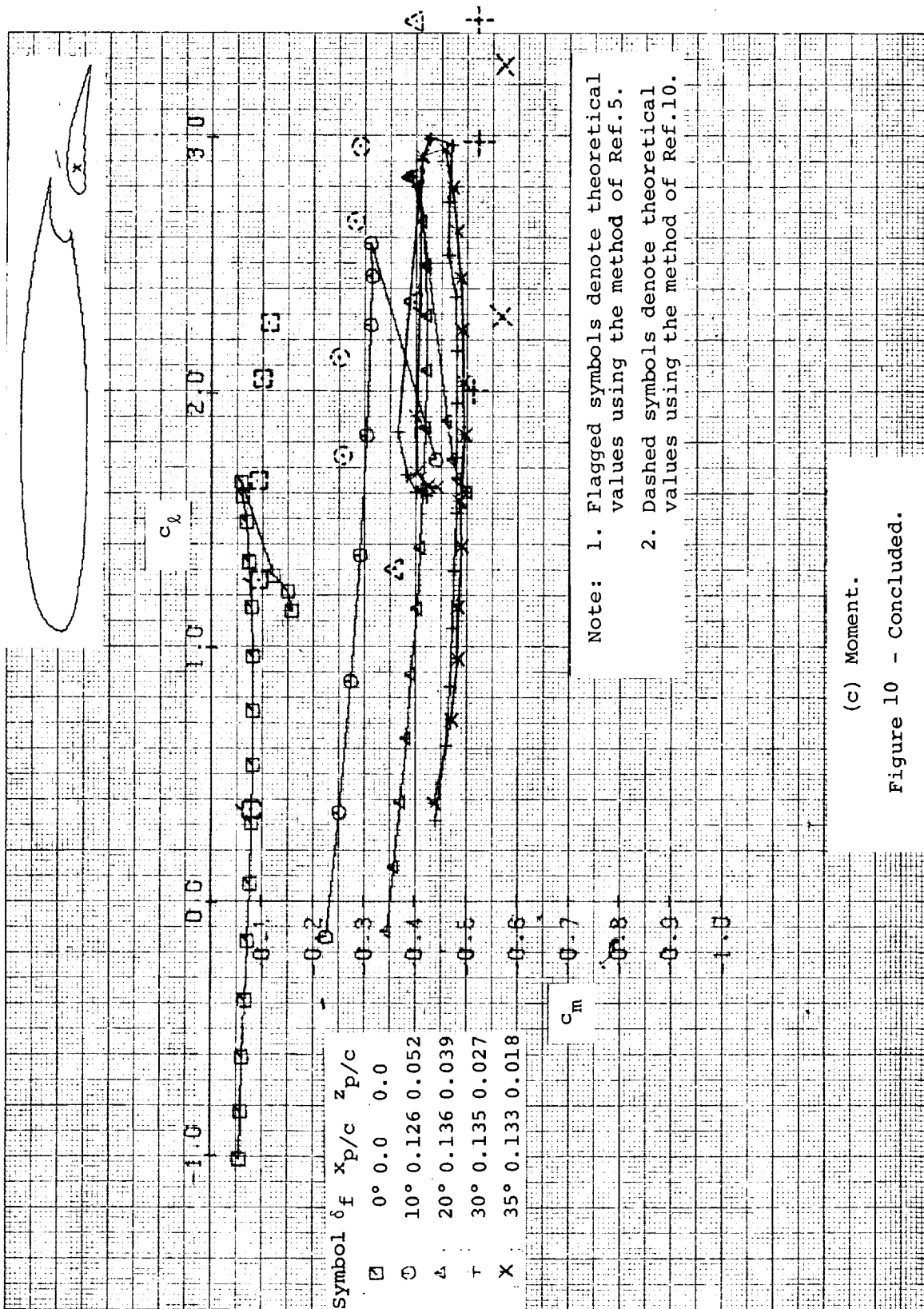


- Note: 1. Flagged symbols denote theoretical values using the method of Ref.5.
 2. Dashed symbols denote theoretical values using the method of Ref.10.



(b) Drag.

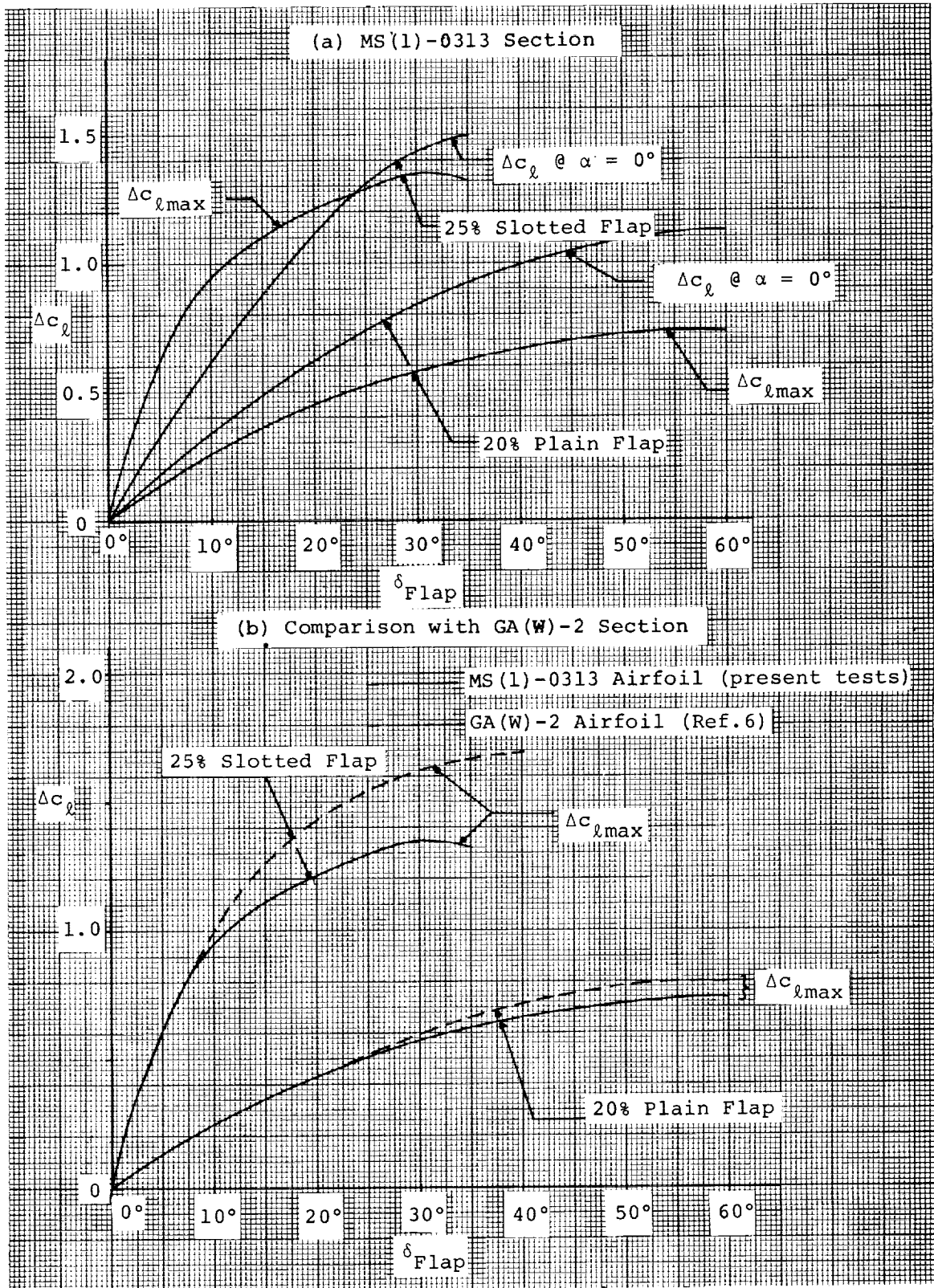
Figure 10 - Continued.



Note: 1. Flagged symbols denote theoretical values using the method of Ref.5.
 2. Dashed symbols denote theoretical values using the method of Ref.10.

(c) Moment.

Figure 10 - Concluded.



(a) FLAP DEFLECTION = 0.0 DEGREES

MACH NO. = 0.13

REYNOLDS NO. = 2.2×10^6

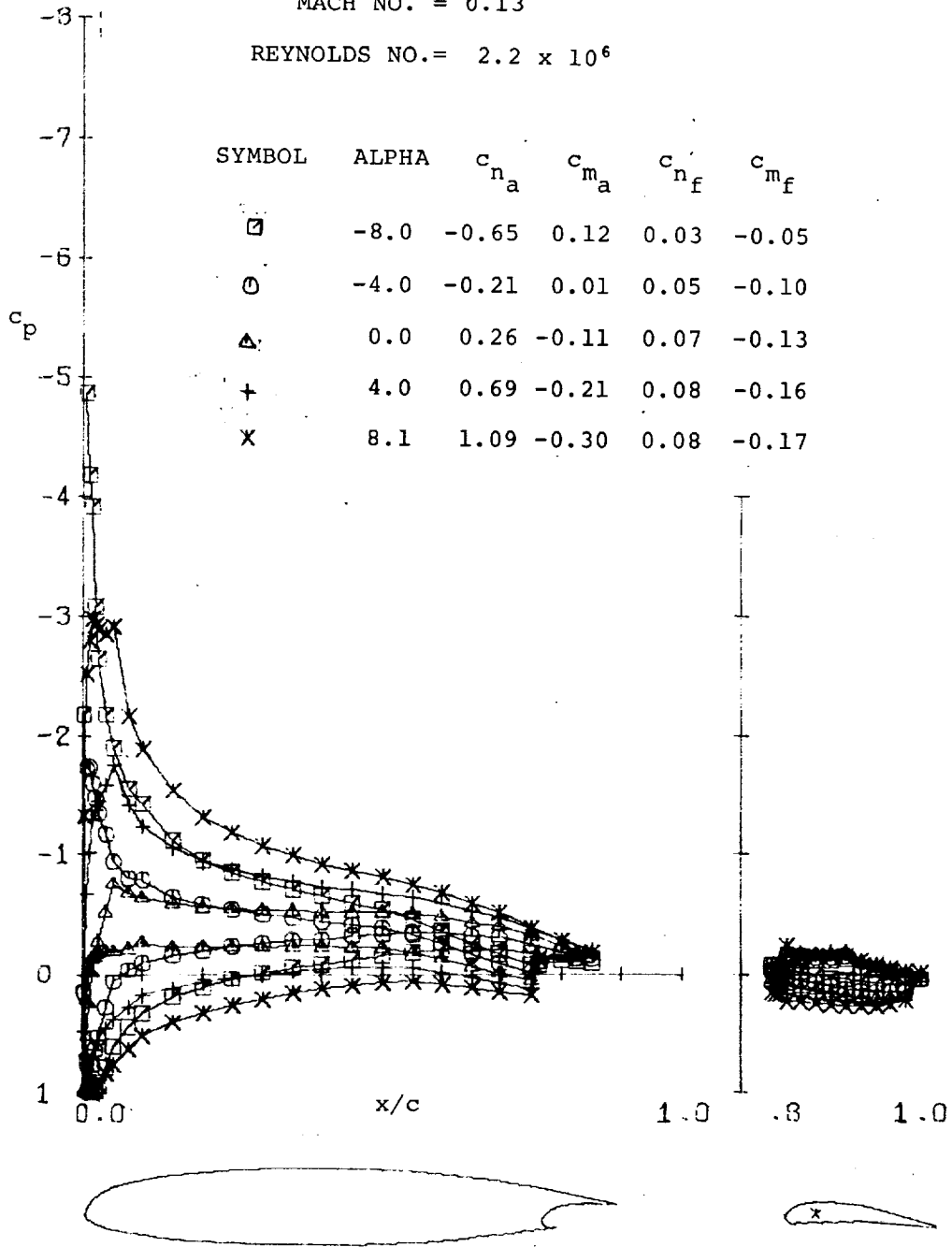


Figure 12 - Pressure Distribution with 25% Slotted Flap.

(a) FLAP DEFLECTION = 0.0 DEGREES

MACH NO. = 0.13

REYNOLDS NO. = 2.2×10^6

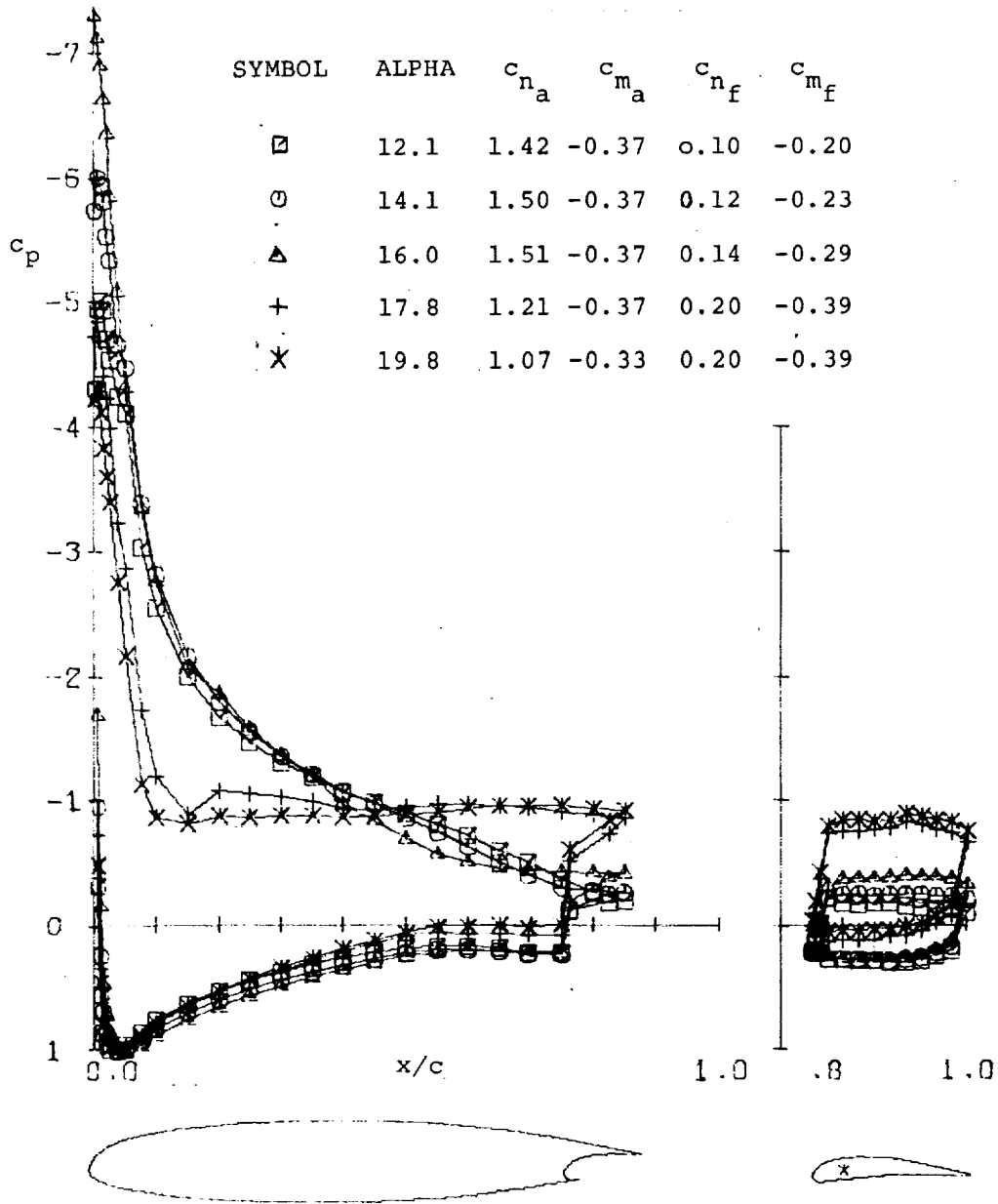


Figure 12 - Continued.

(b) FLAP DEFLECTION = 10.0 DEGREES

MACH NO. = 0.13

REYNOLDS NO. = 2.2×10^6

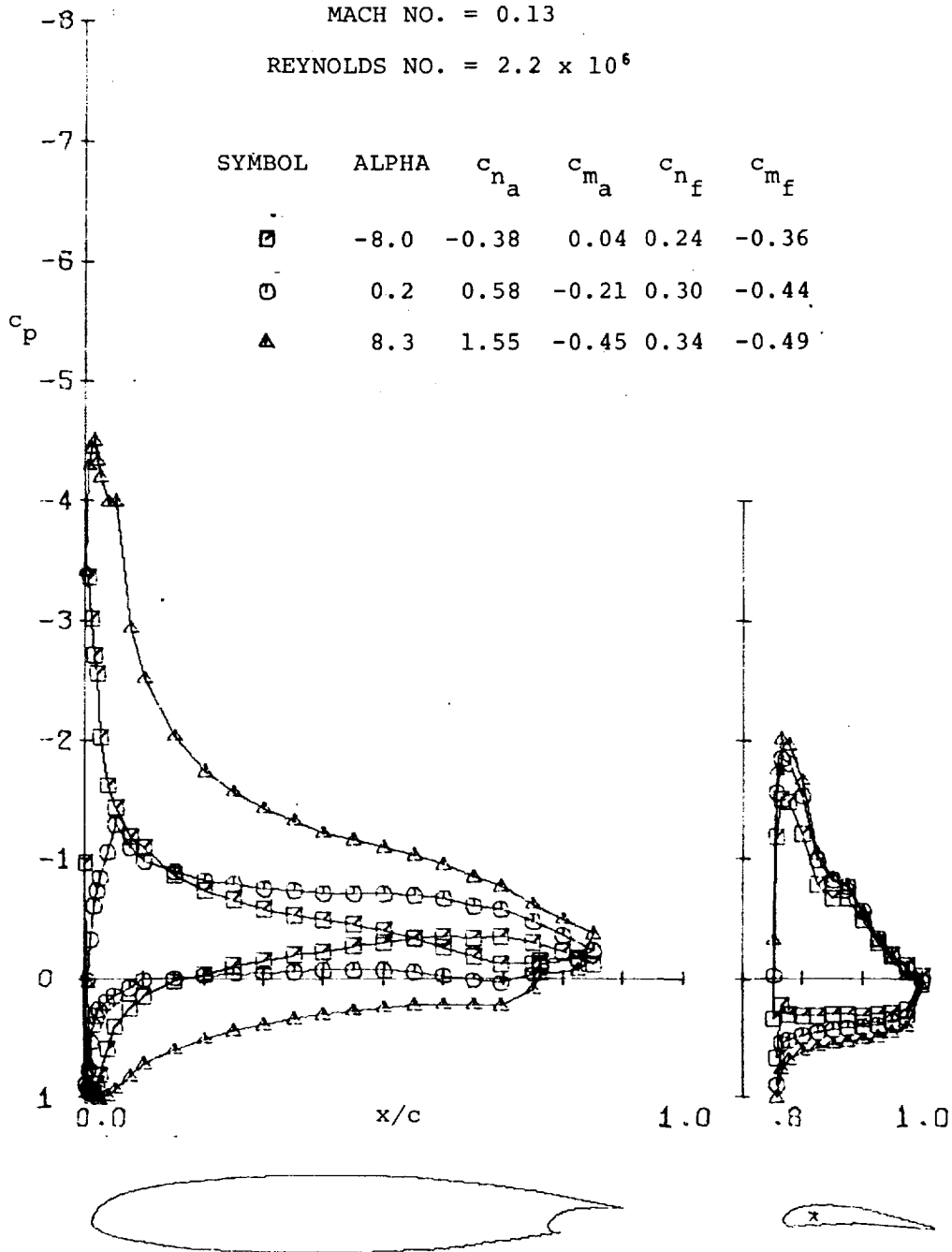


Figure 12 - Continued.

(b) FLAP DEFLECTION = 10.0 DEGREES

MACH NO. = 0.13

REYNOLDS NO. = 2.2×10^6

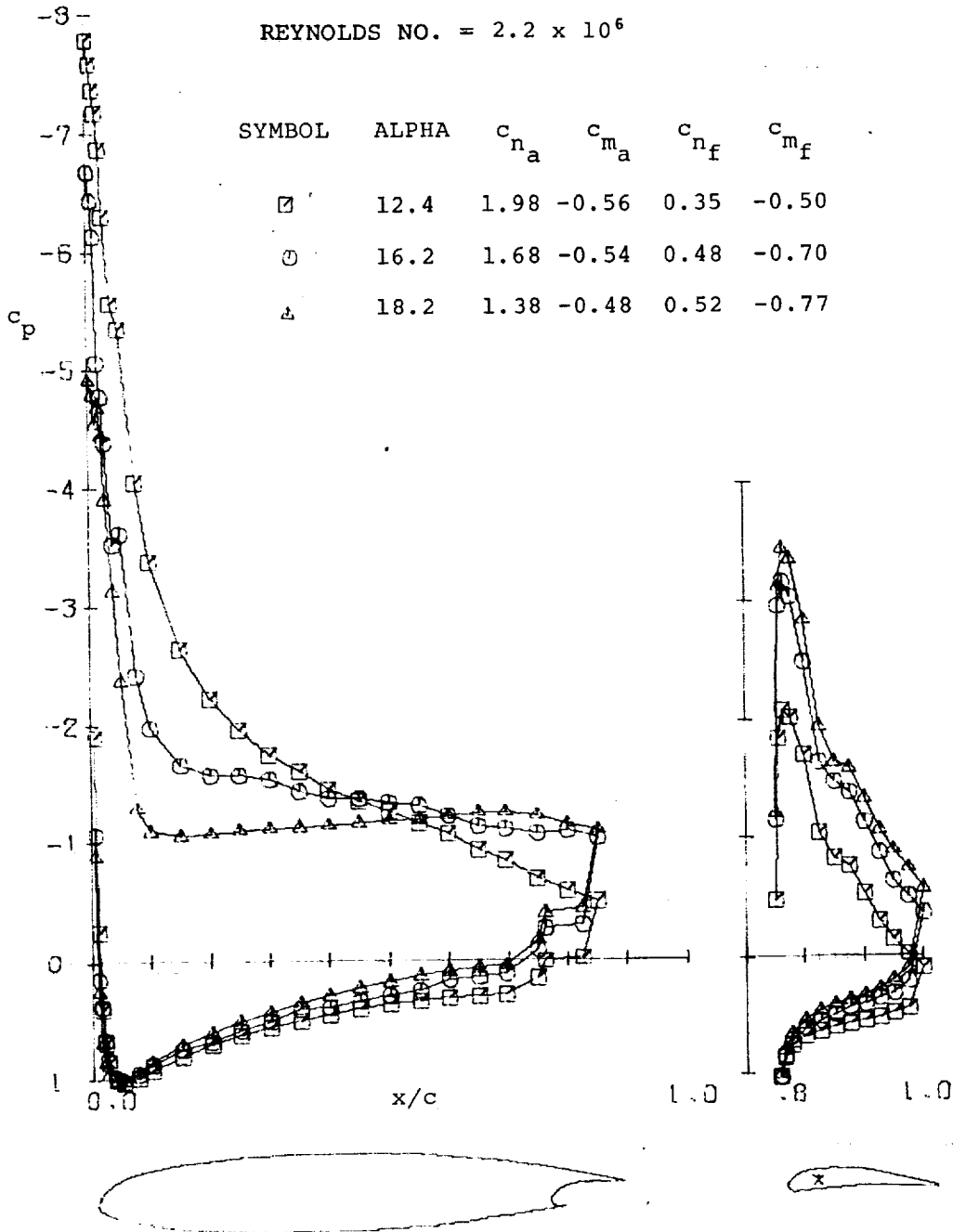


Figure 12 - Continued.

(c) FLAP DEFLECTION = 20.0 DEGREES

MACH NO. = 0.13

REYNOLDS NO. = 2.2×10^6

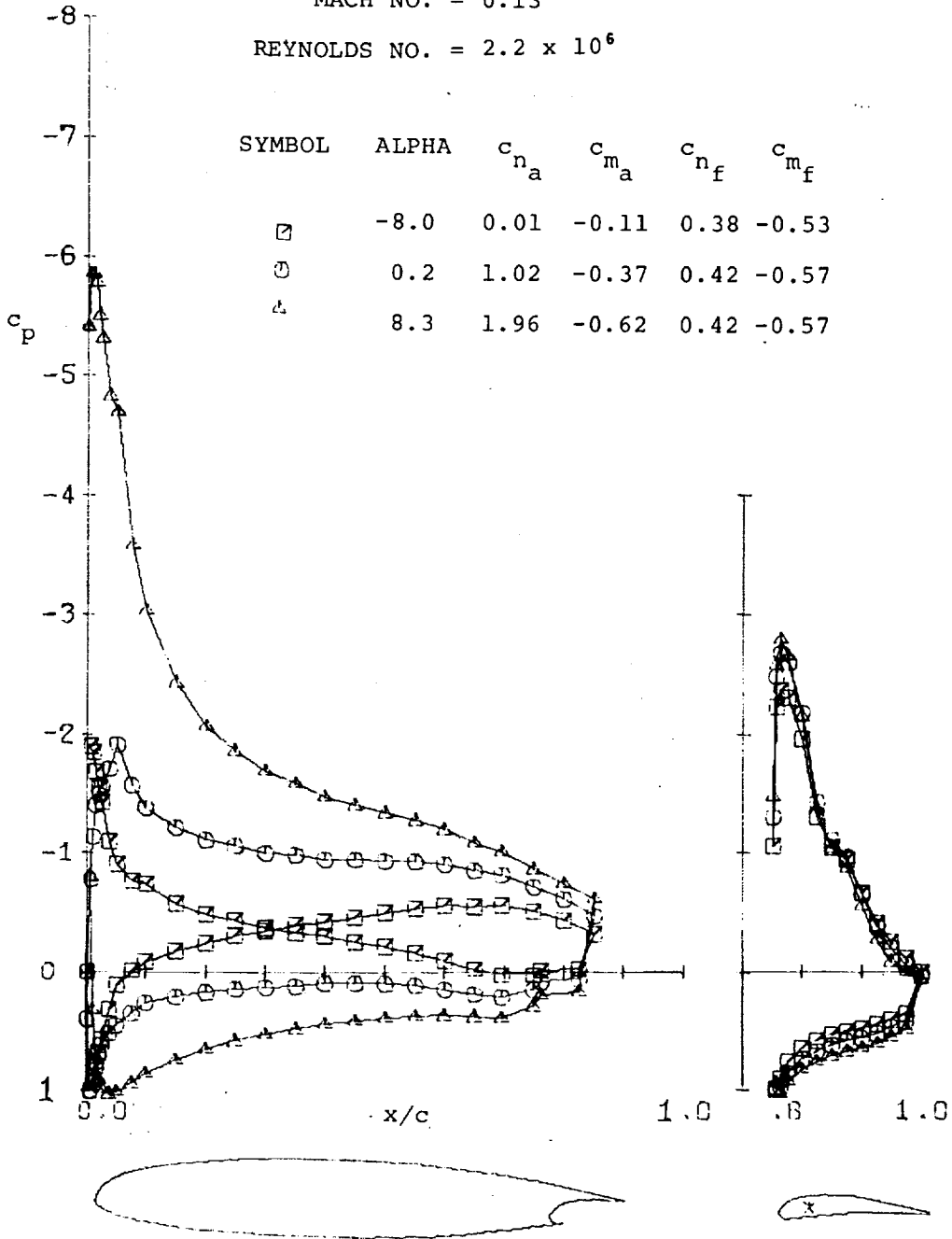


Figure 12 - Continued.

(c) FLAP DEFLECTION = 20.0 DEGREES

MACH NO. = 0.13

REYNOLDS NO. = 2.2×10^6

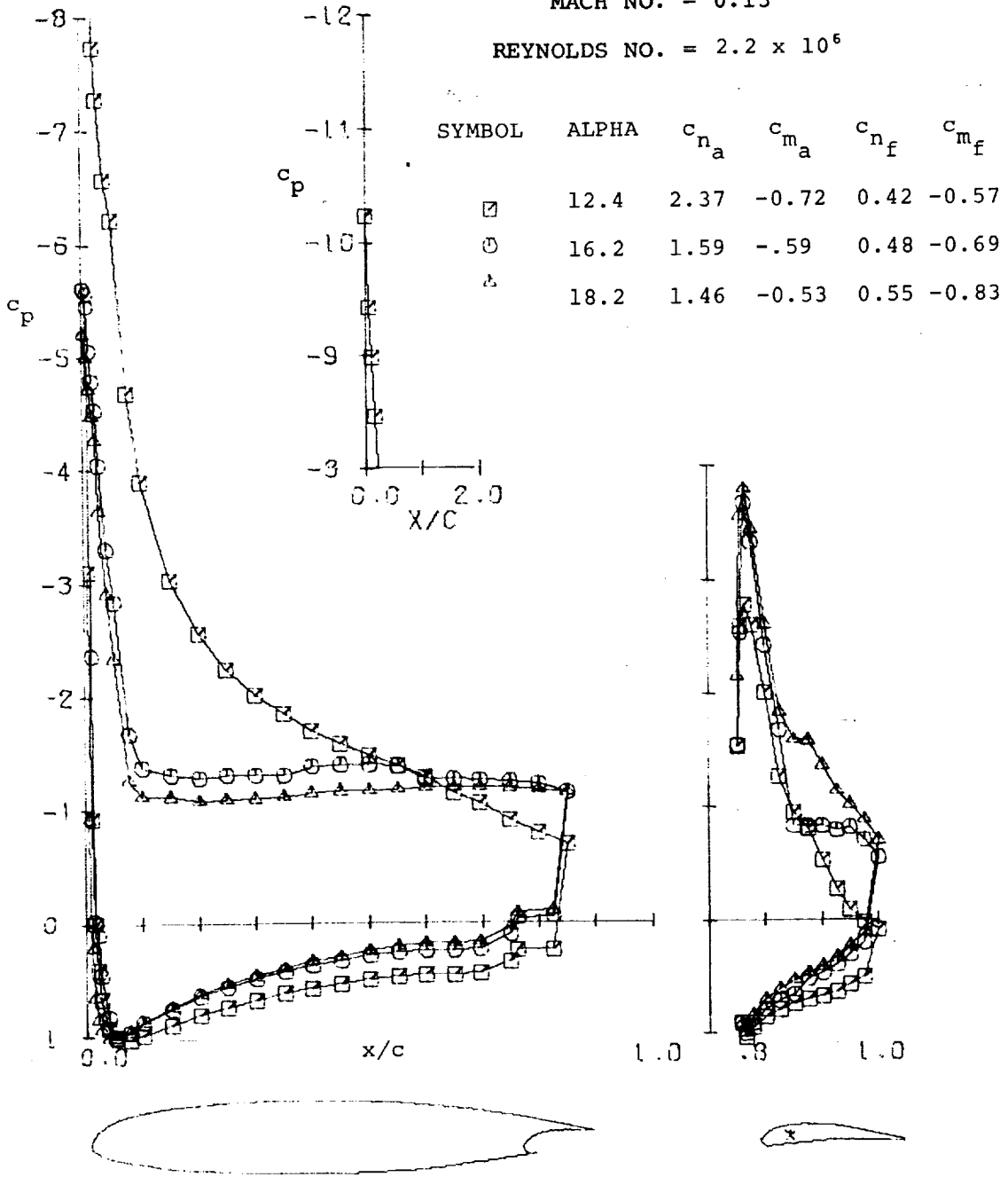


Figure 12 - Continued.

(d) FLAP DEFLECTION = 30.0 DEGREES

MACH NO. = 0.13

REYNOLDS NO. = 2.2×10^6

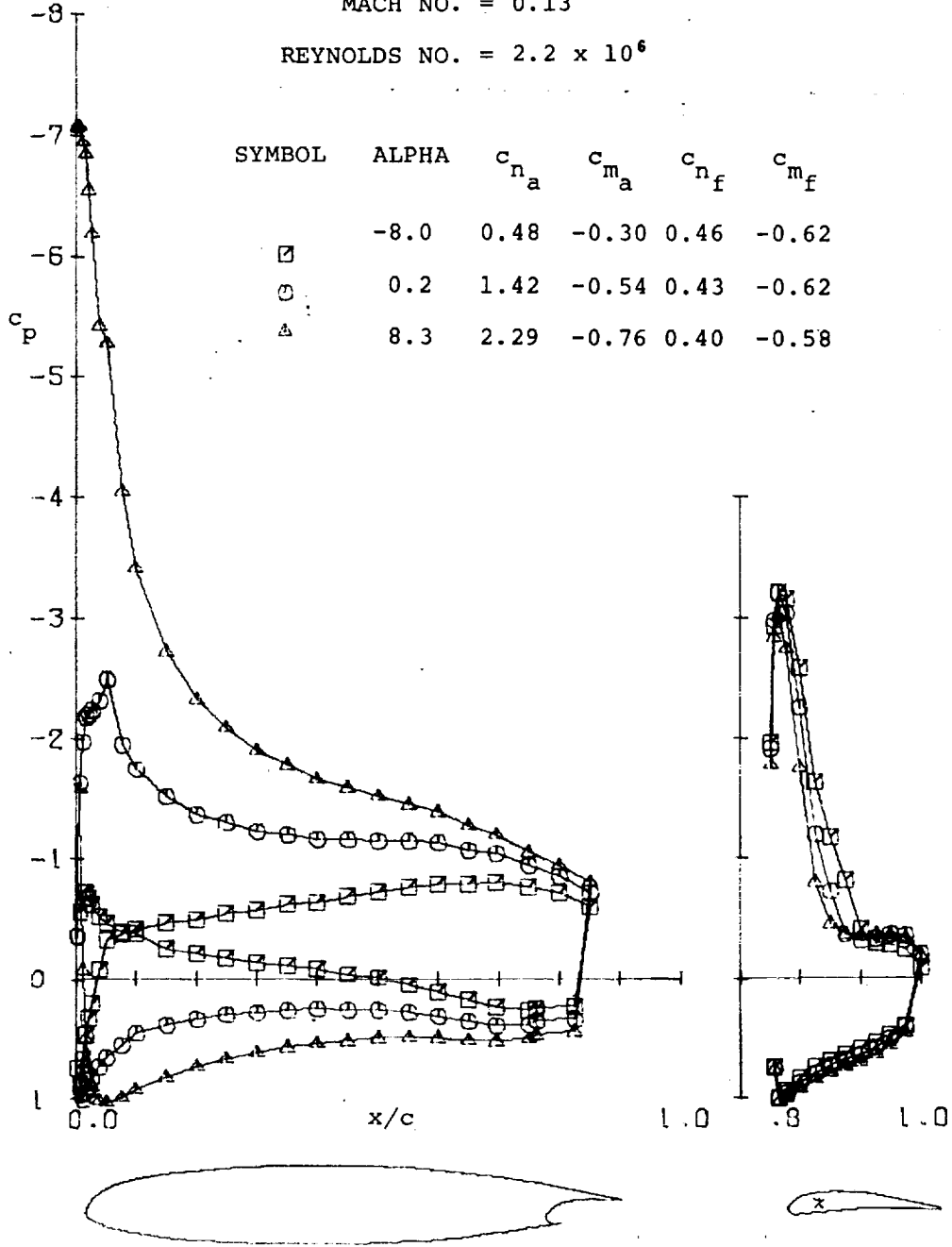


Figure 12 - Continued.

(d) FLAP DEFLECTION = 30.0 DEGREES

MACH NO. = 0.13

REYNOLDS NO. = 2.2×10^6

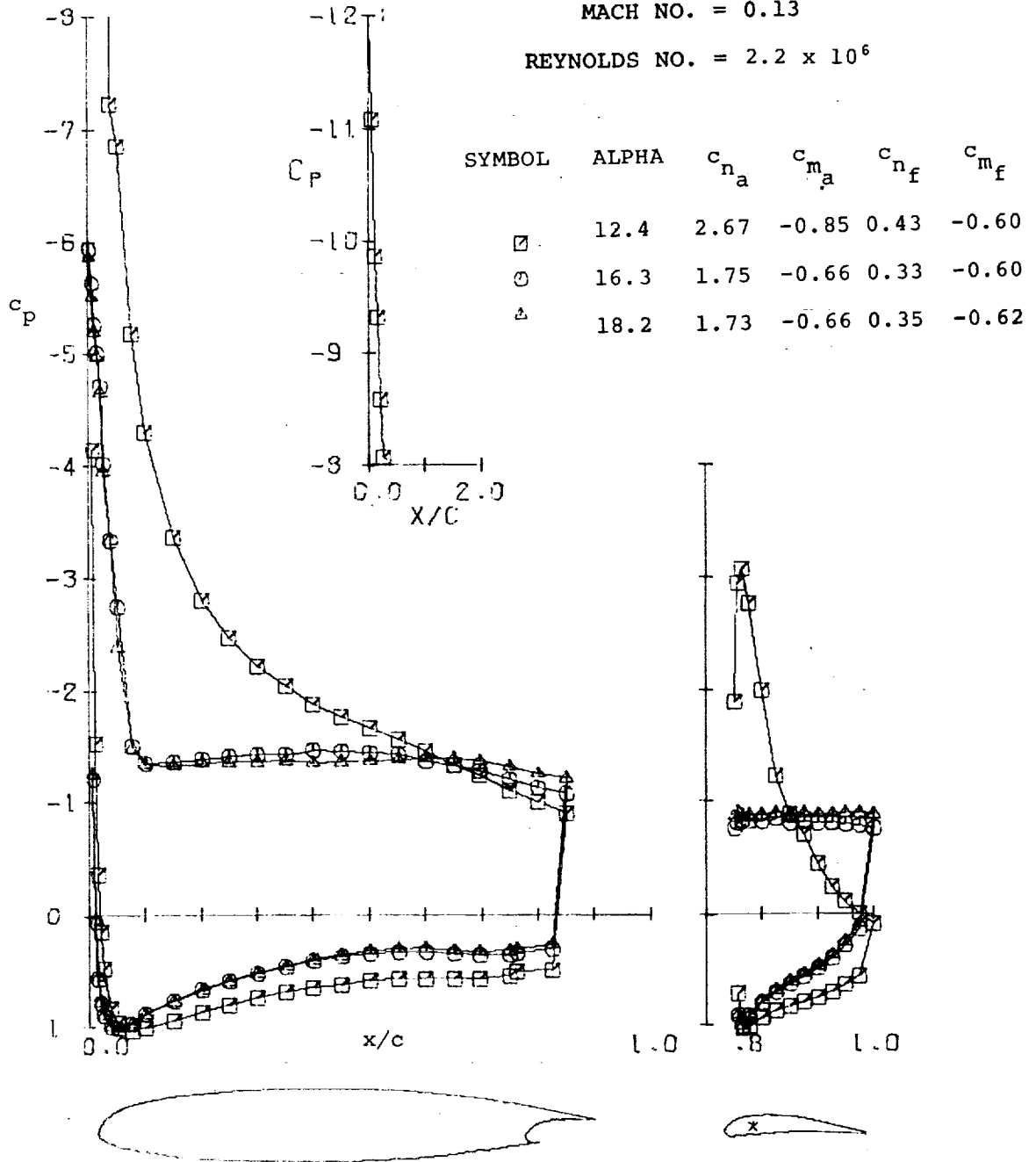


Figure 12 - Continued.

(e) FLAP DEFLECTION = 35.0 DEGREES

MACH NO. = 0.13

REYNOLDS NO. = 2.2×10^6

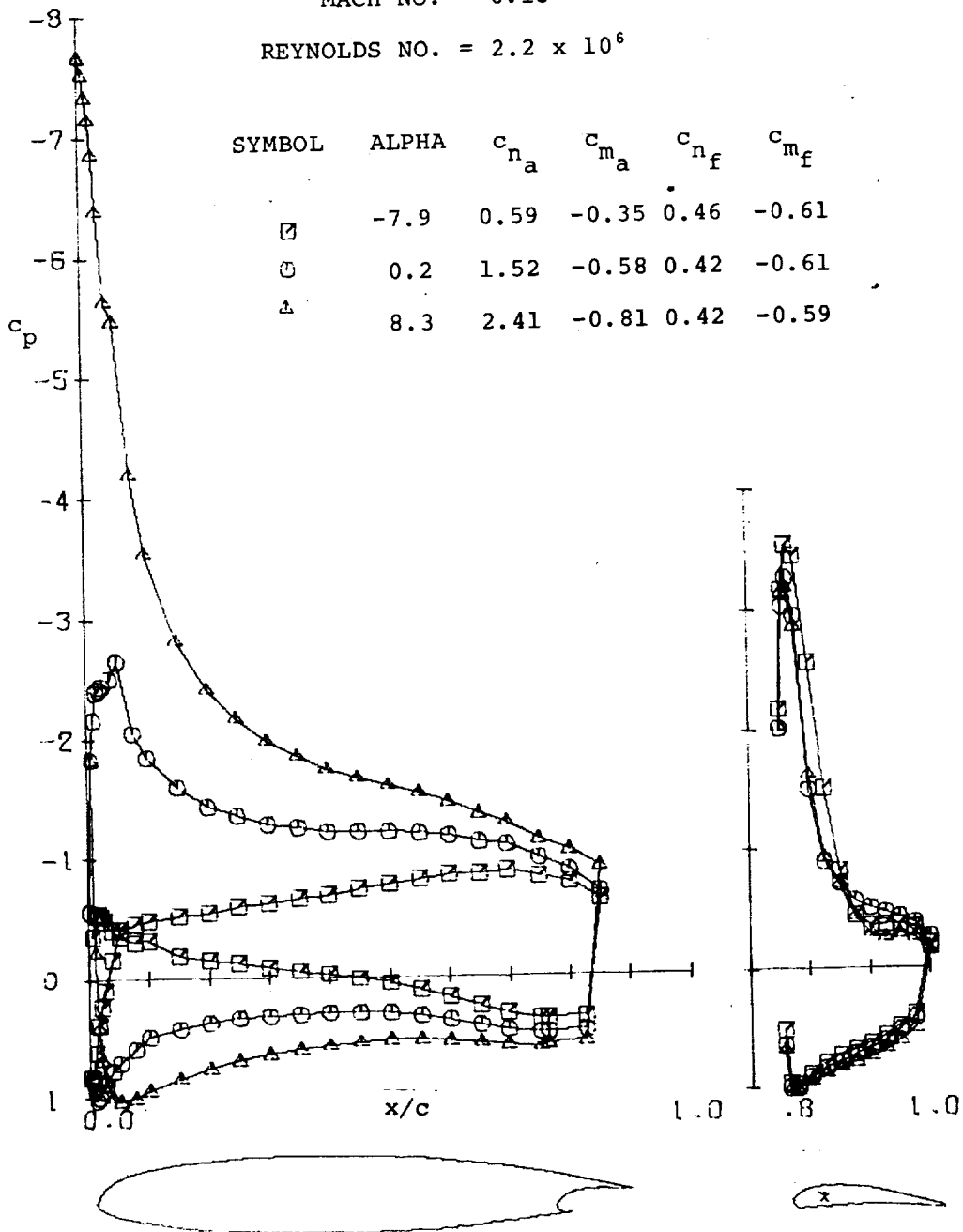


Figure 12 - Continued.

(e) FLAP DEFLECTION = 35.0 DEGREES

MACH NO. = 0.13

REYNOLDS NO. = 2.2×10^6

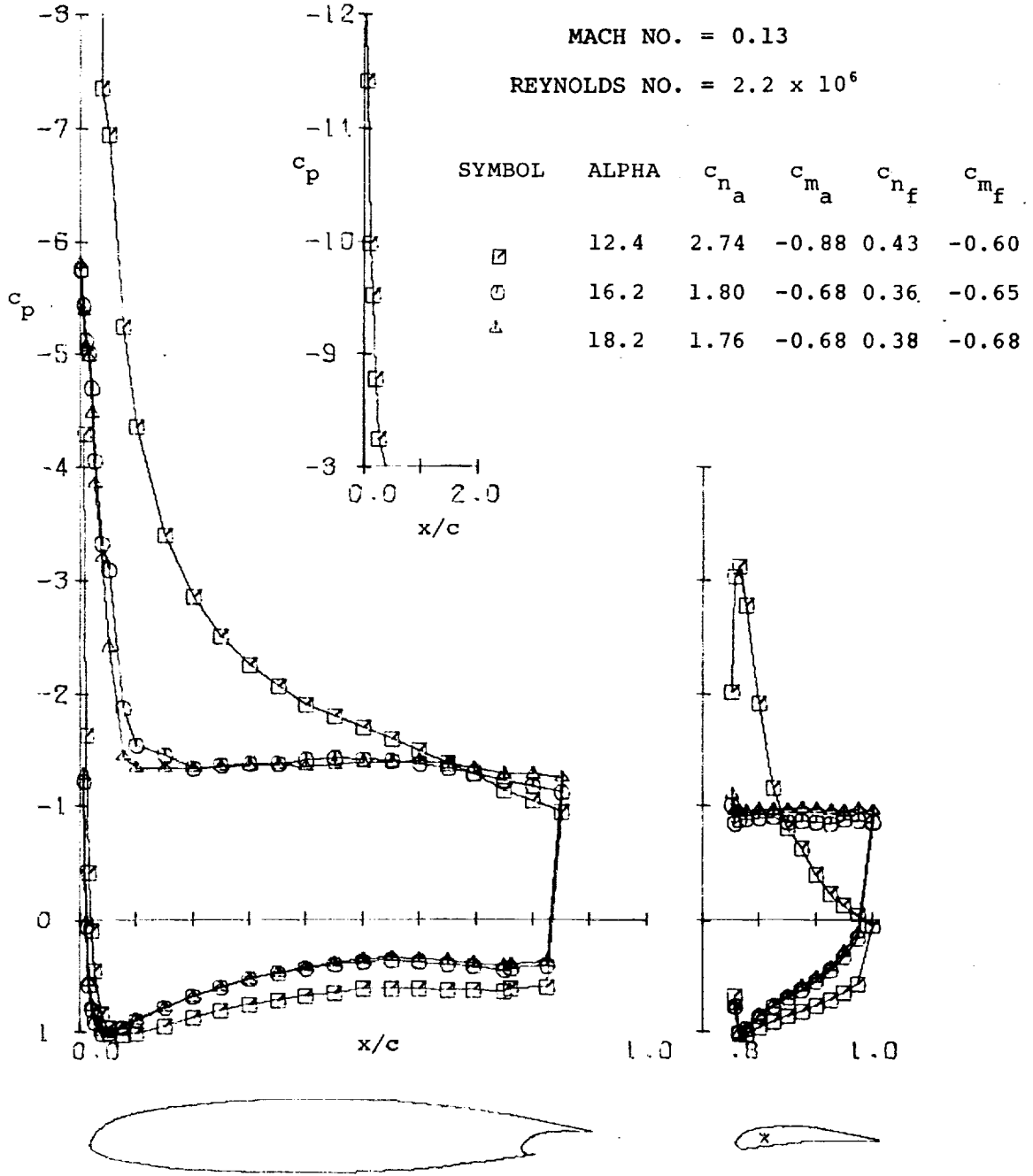


Figure 12 - Concluded.

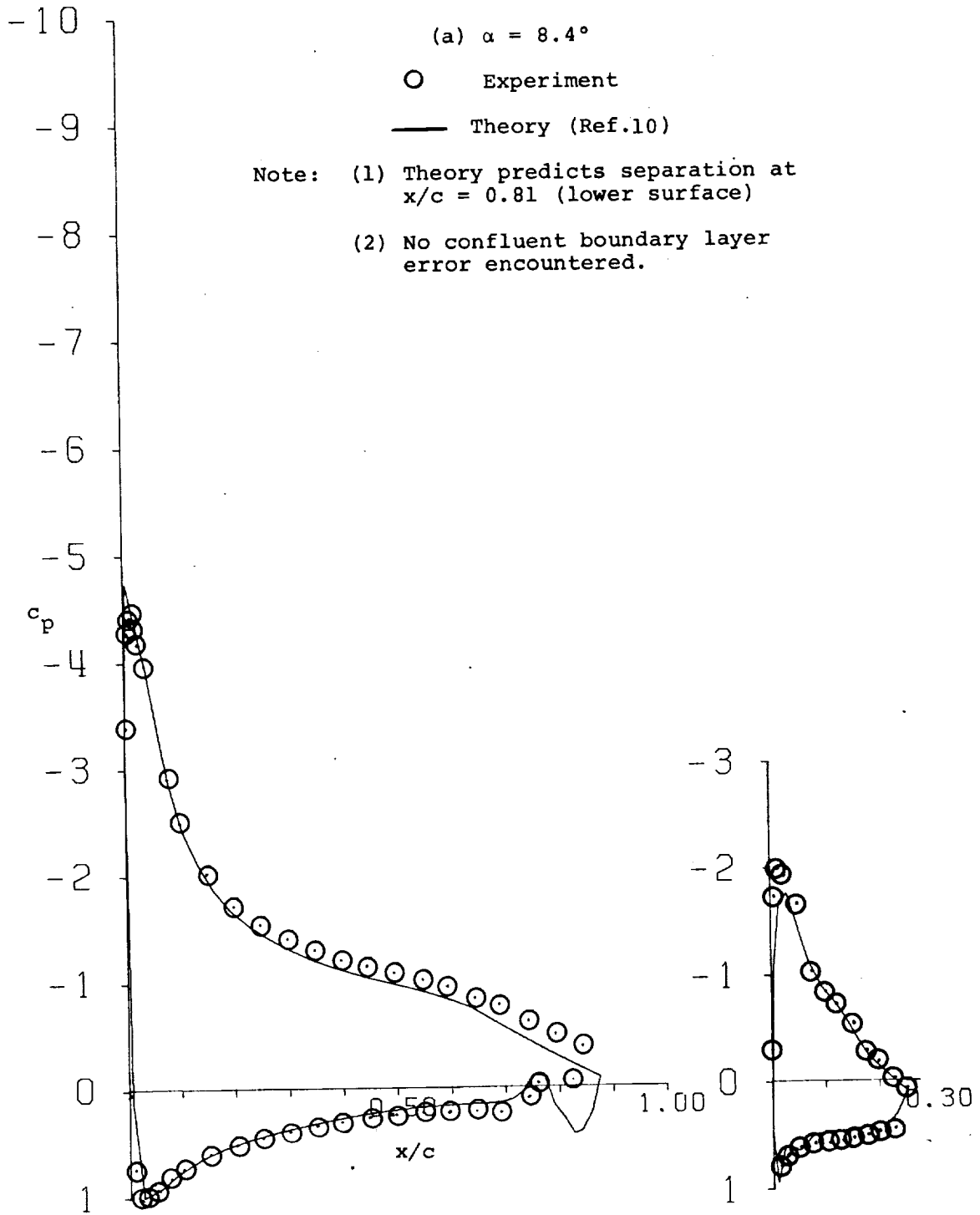


Figure 13 - Pressure Distributions with 25% Slotted Flap, 10° Flap Deflection.

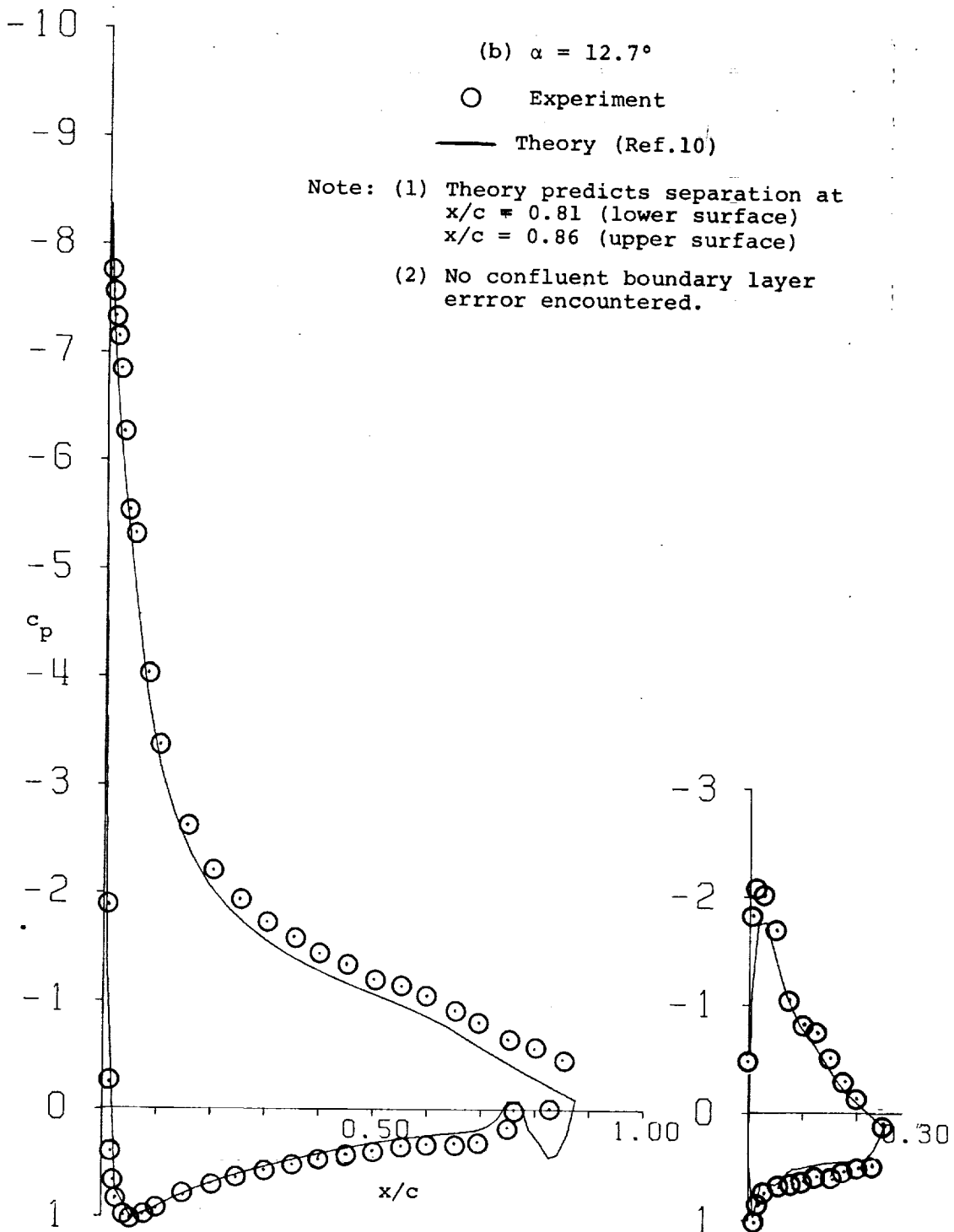


Figure 13 - Continued.

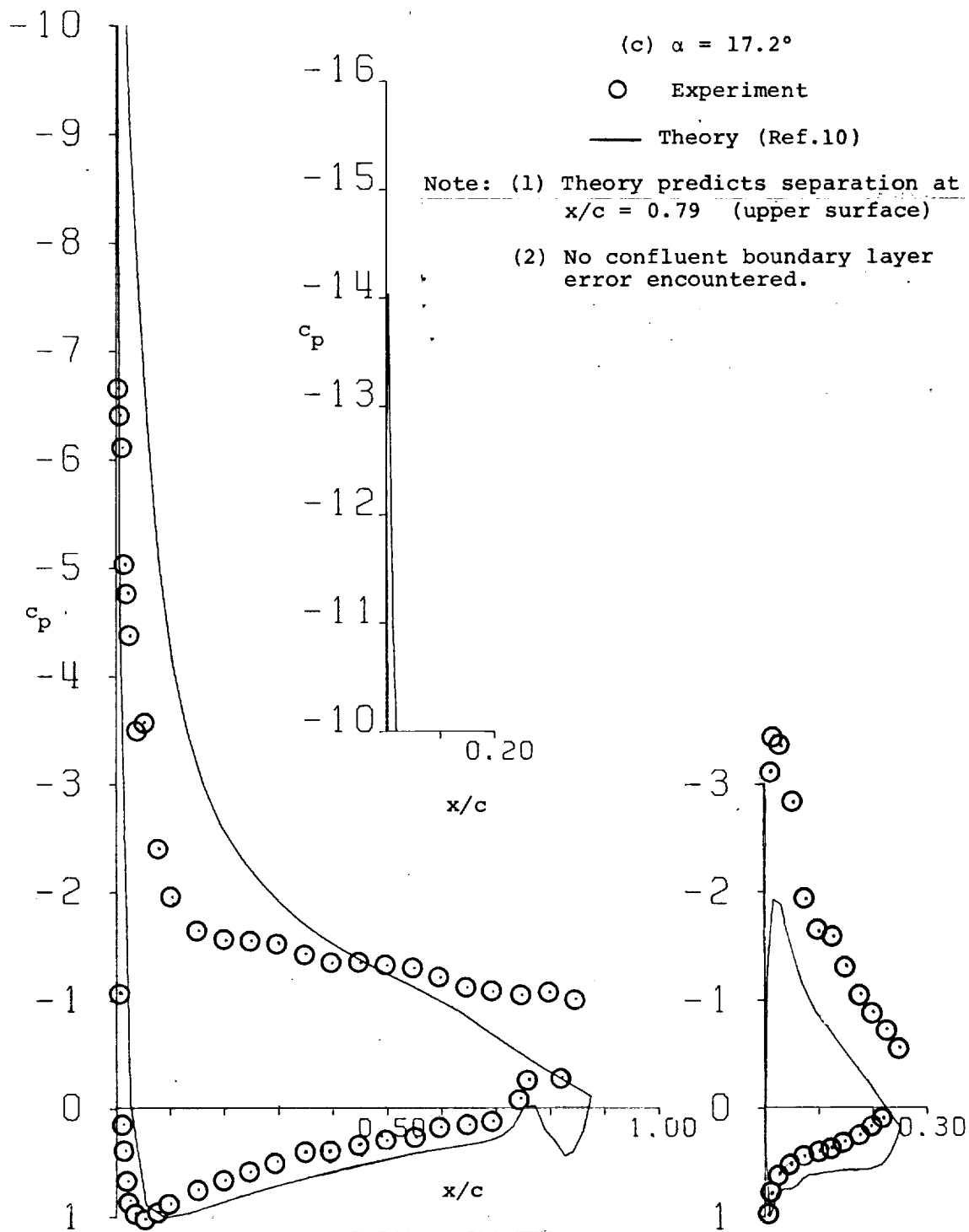


Figure 13 - Continued.

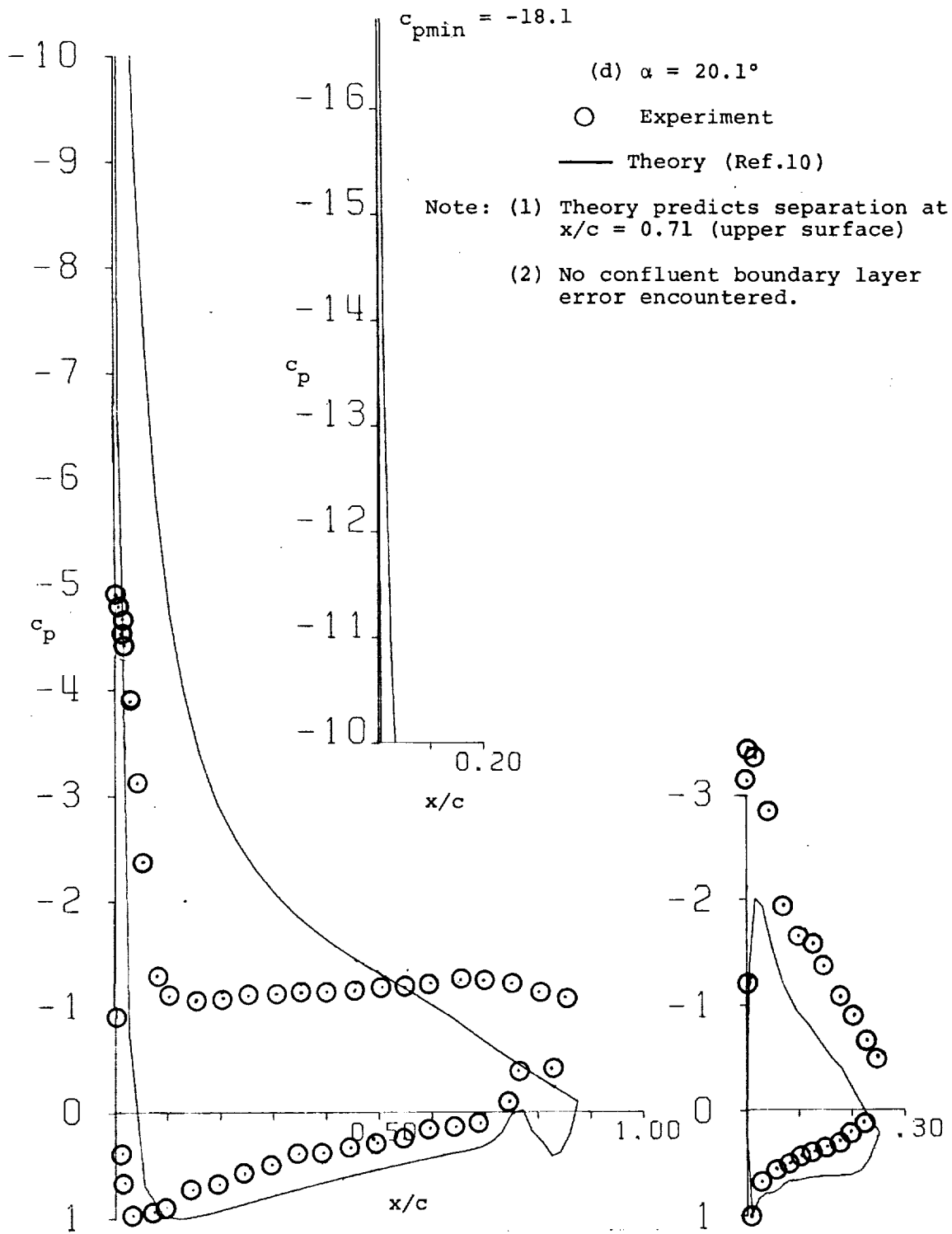


Figure 13 - Concluded.

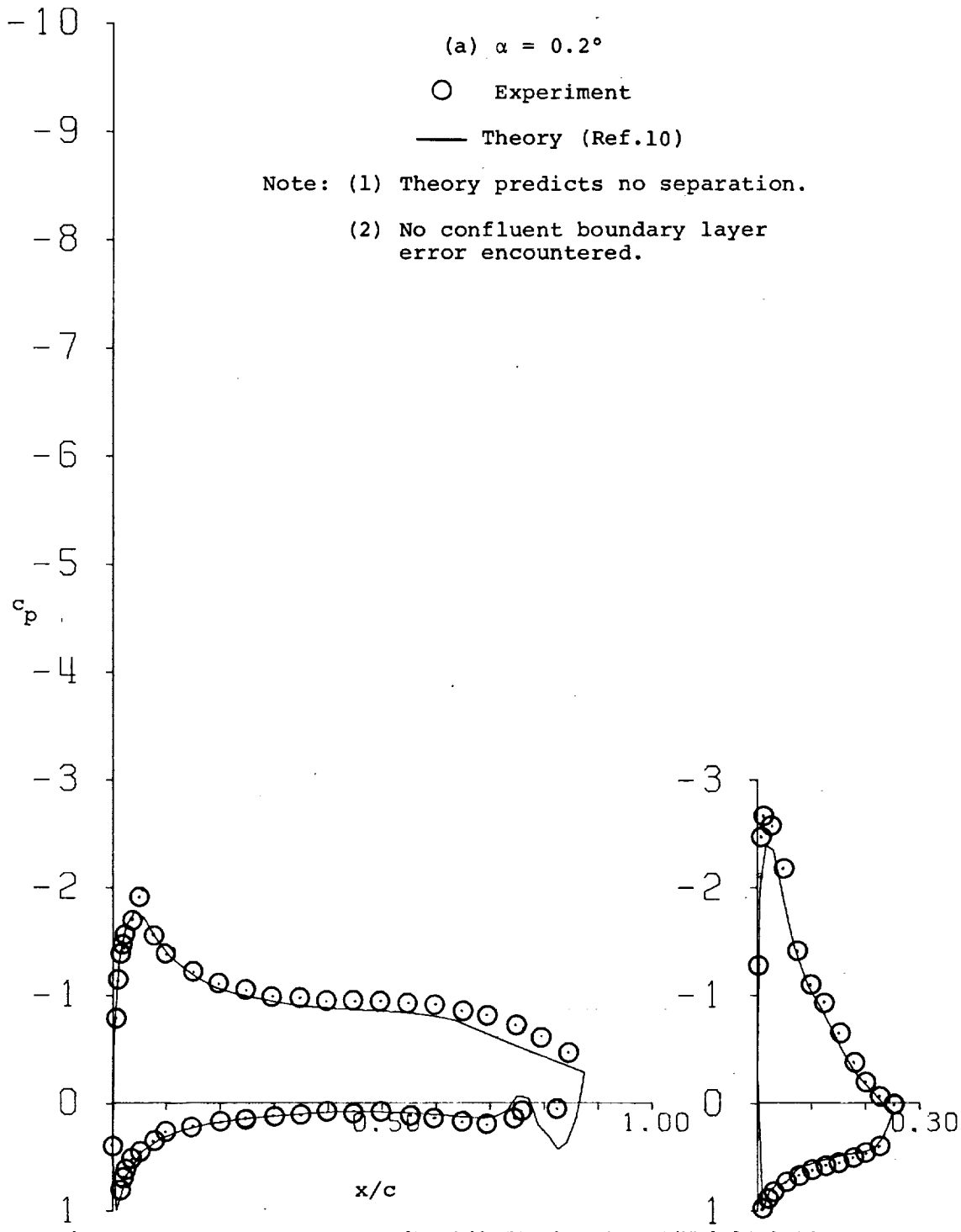


Figure 14 - Pressure Distributions with 25% Slotted Flap, 20° Flap Deflection.

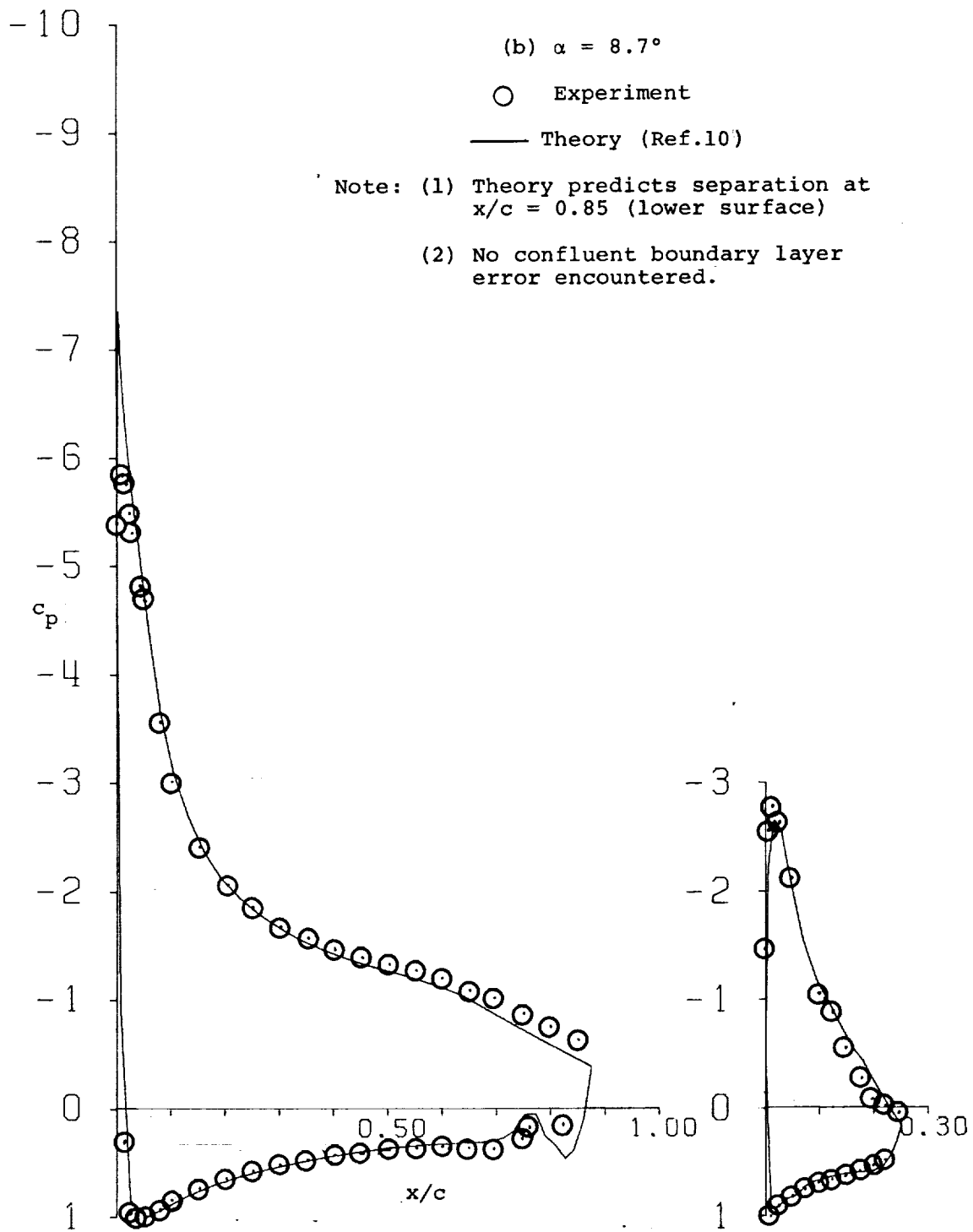


Figure 14 - Continued.

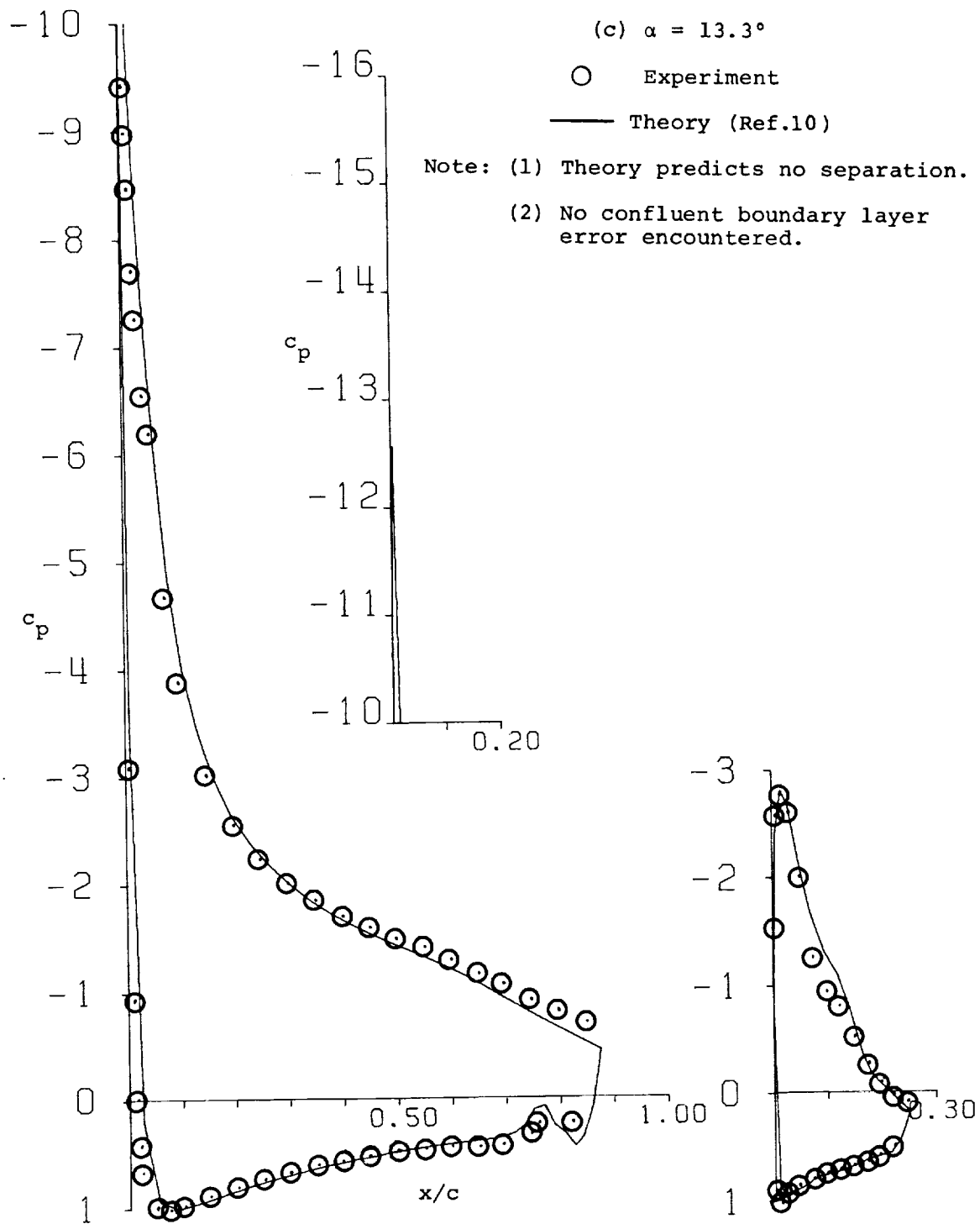


Figure 14 - Continued.

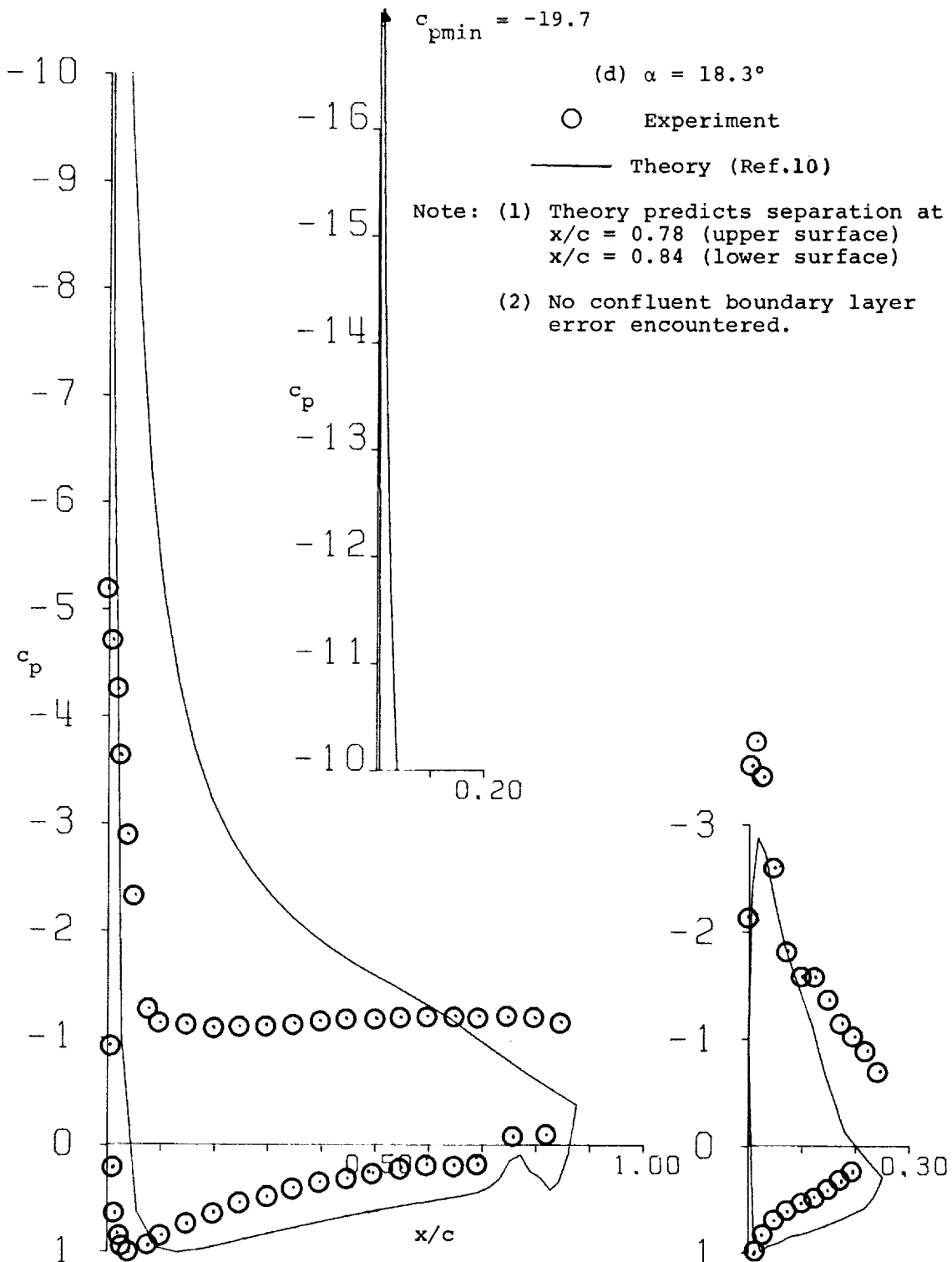


Figure 14 - Concluded.

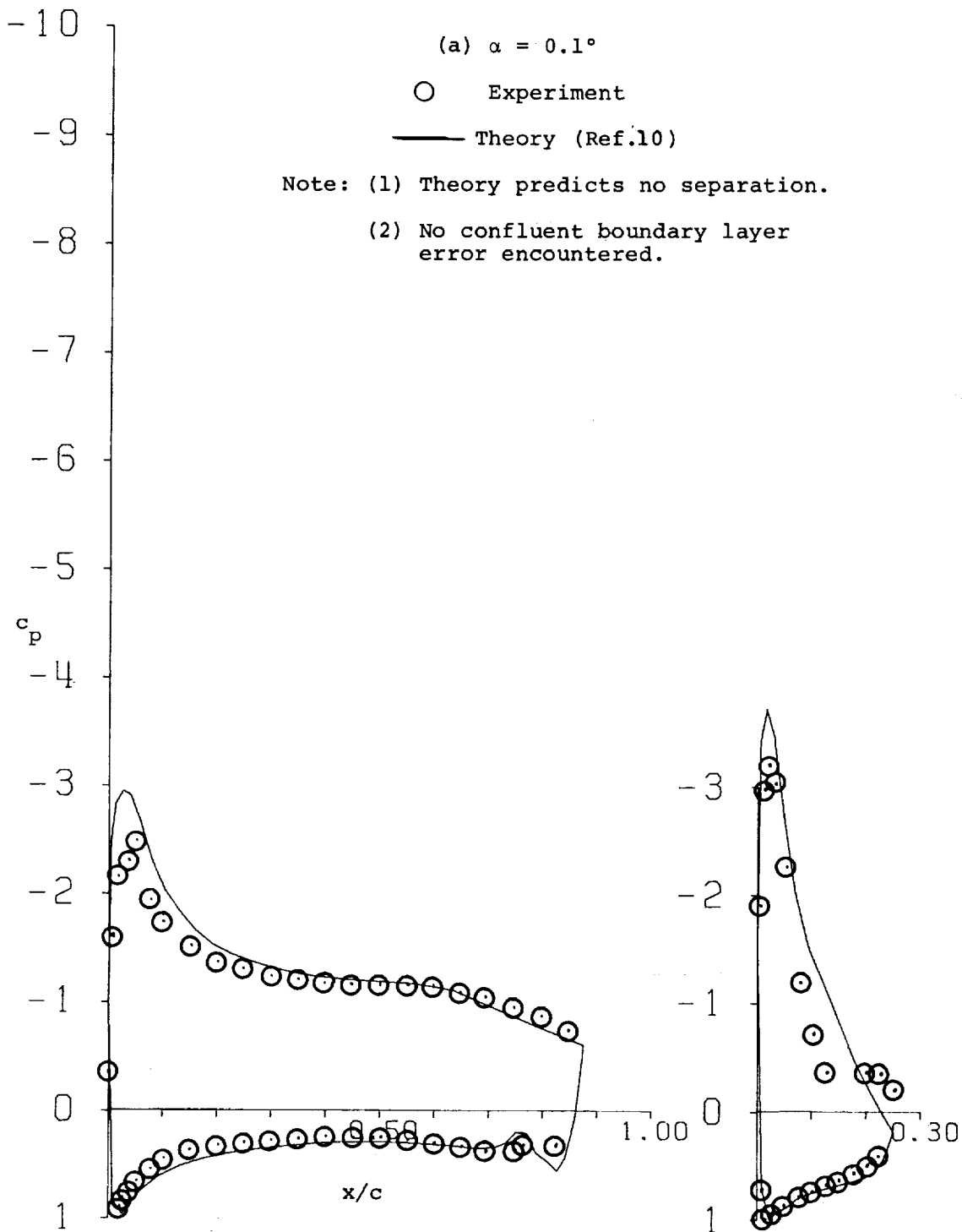


Figure 15 - Pressure Distributions with 25% Slotted Flap,
 30° Flap Deflection.

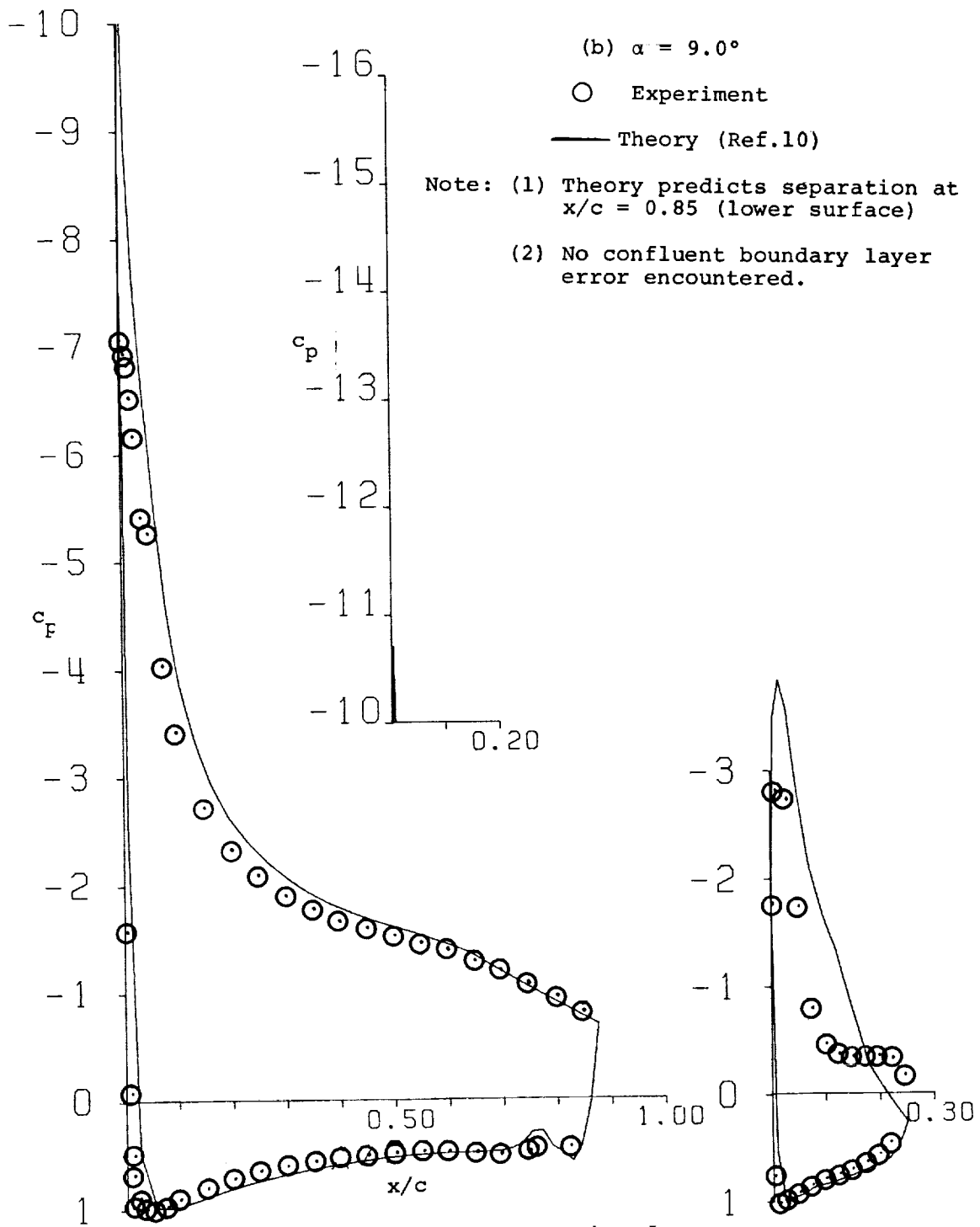


Figure 15 - Continued.

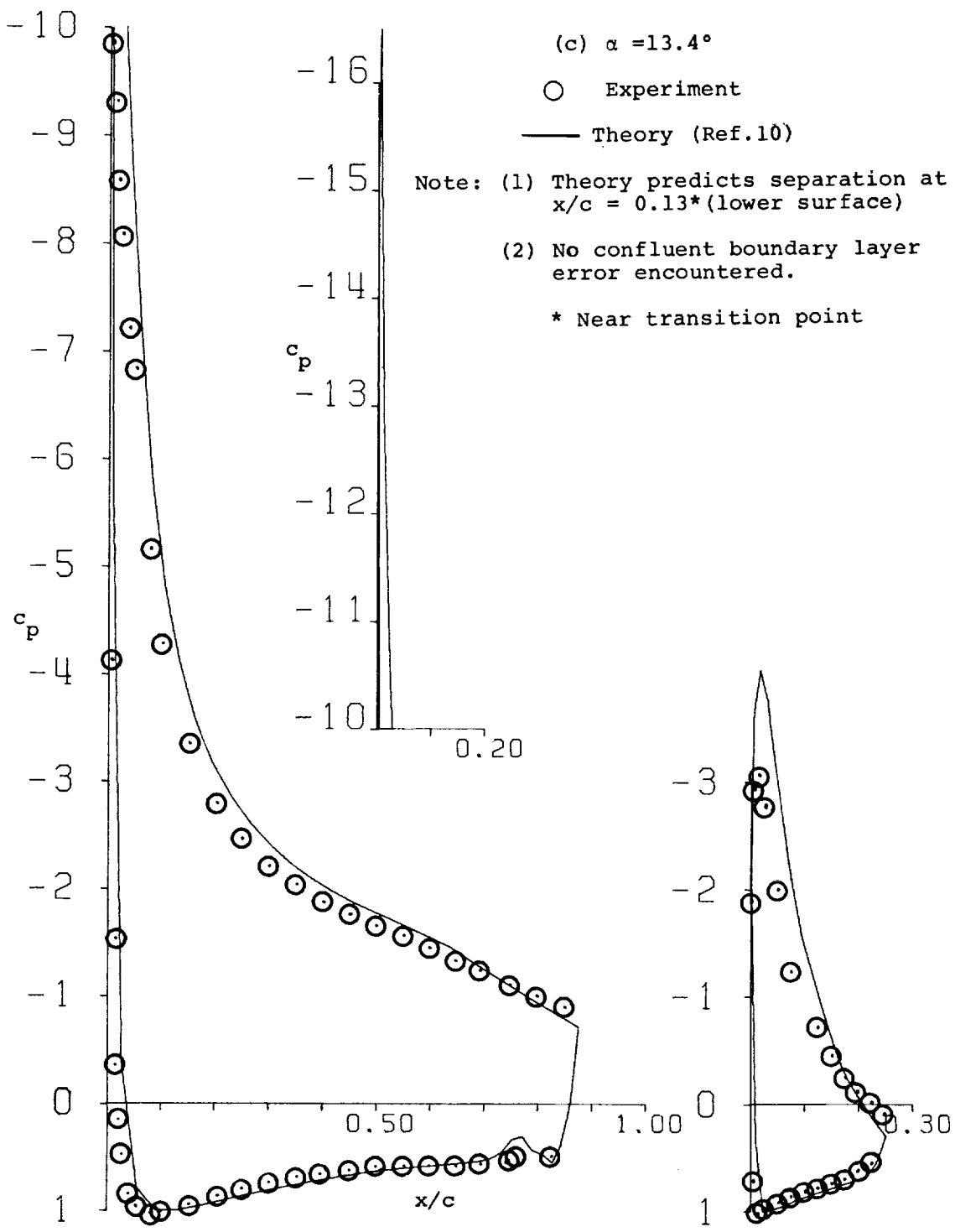
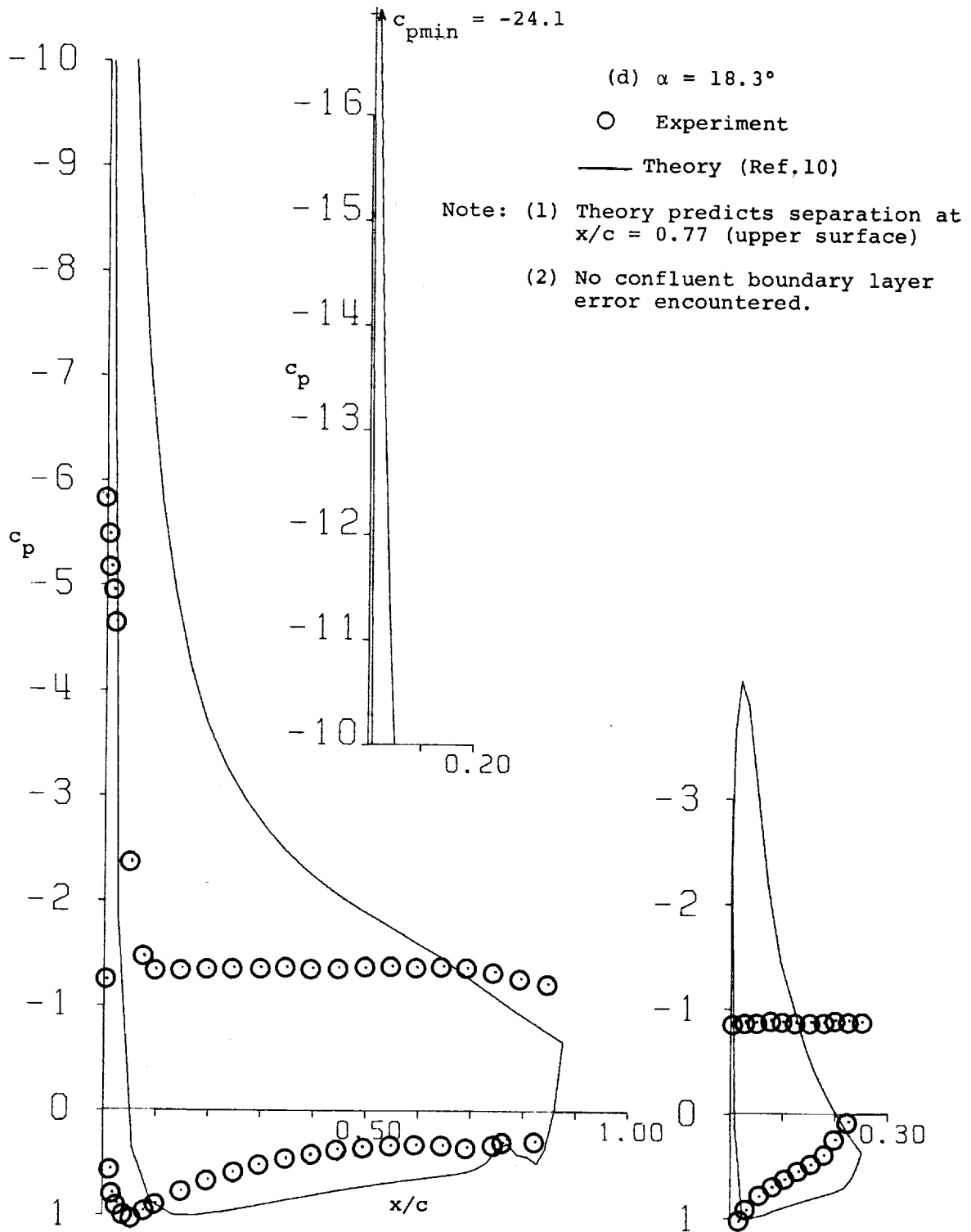


Figure 15 - Continued.



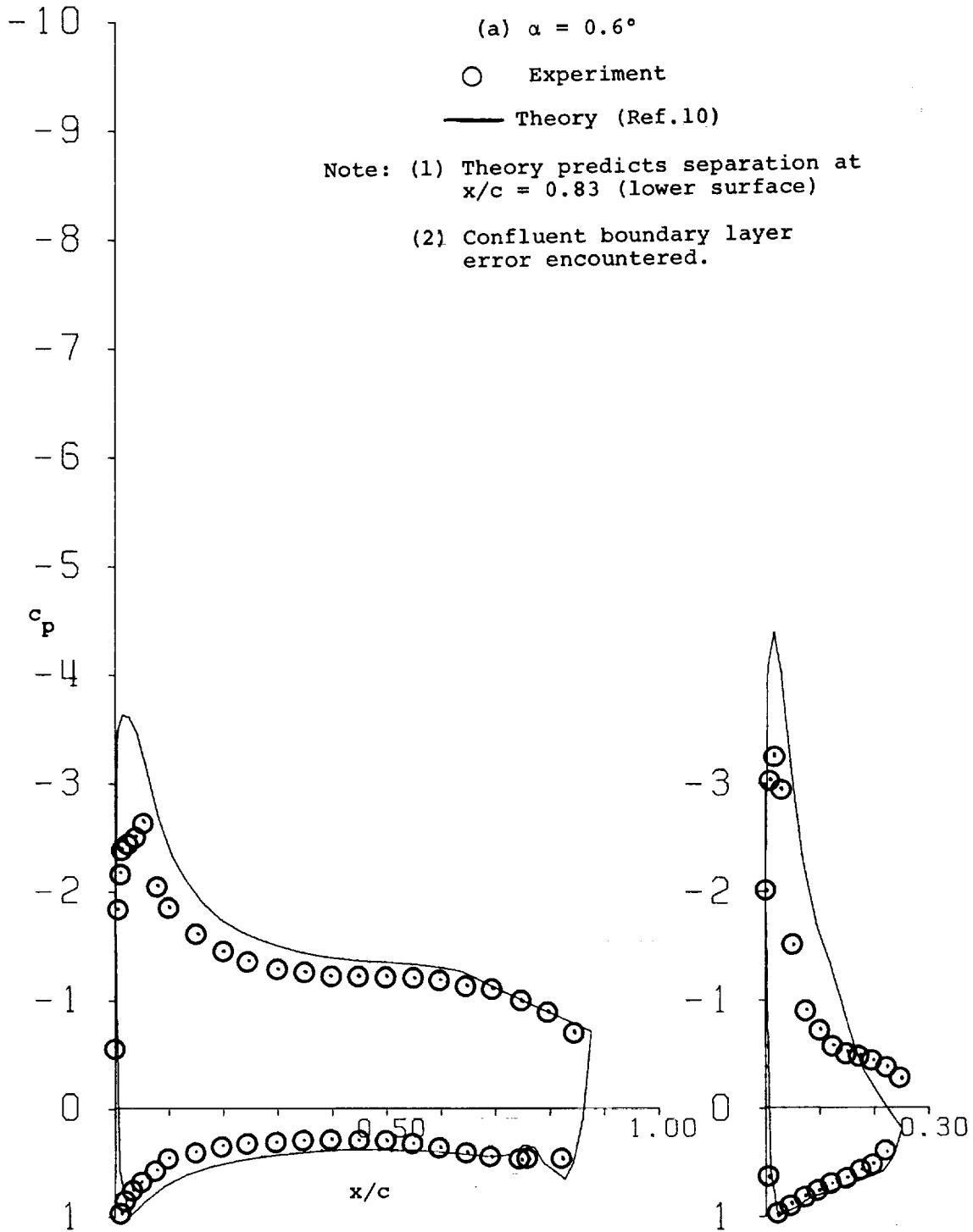


Figure 16 - Pressure Distributions with 25% Slotted Flap, 35° Flap Deflection.

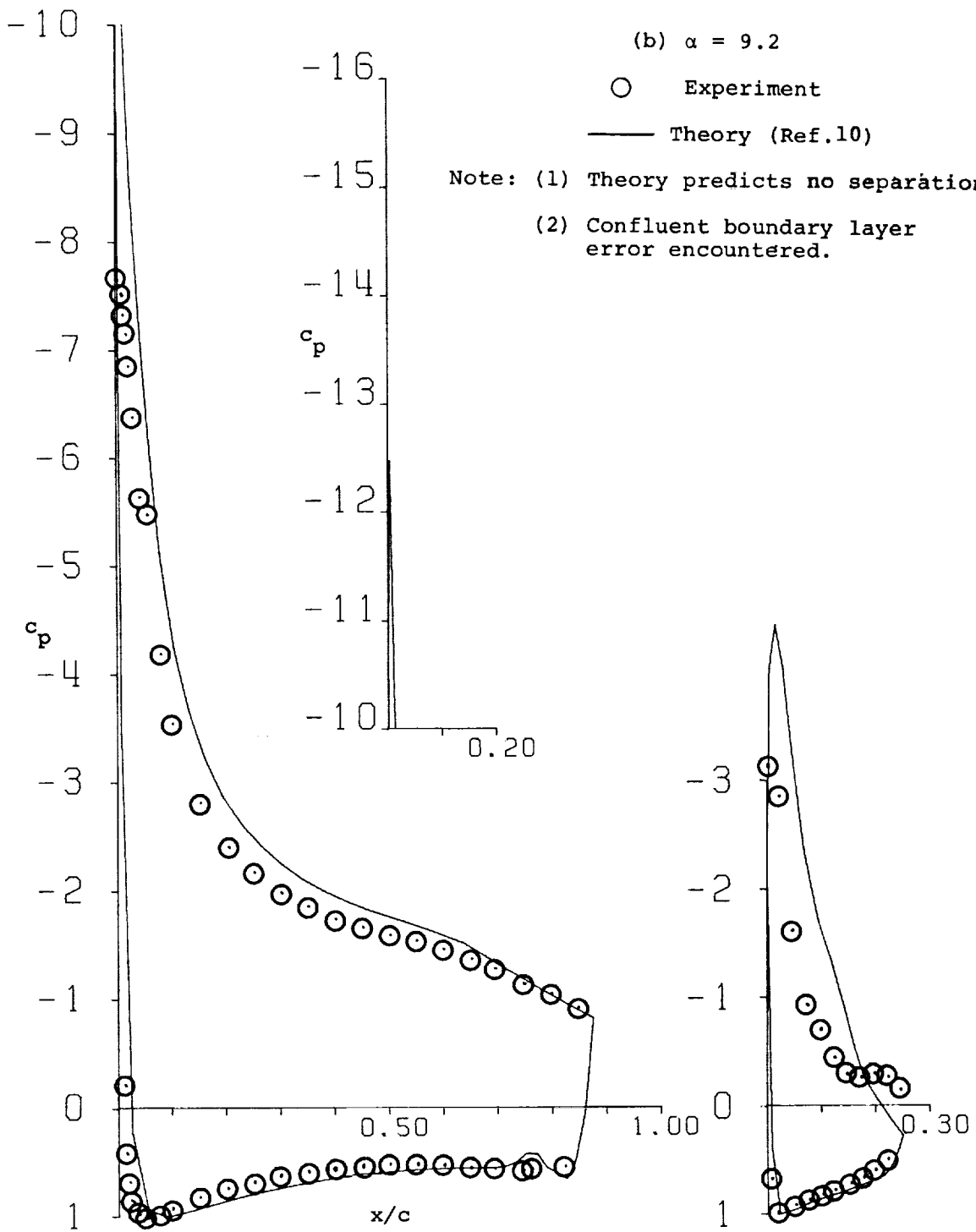


Figure 16 - Continued.

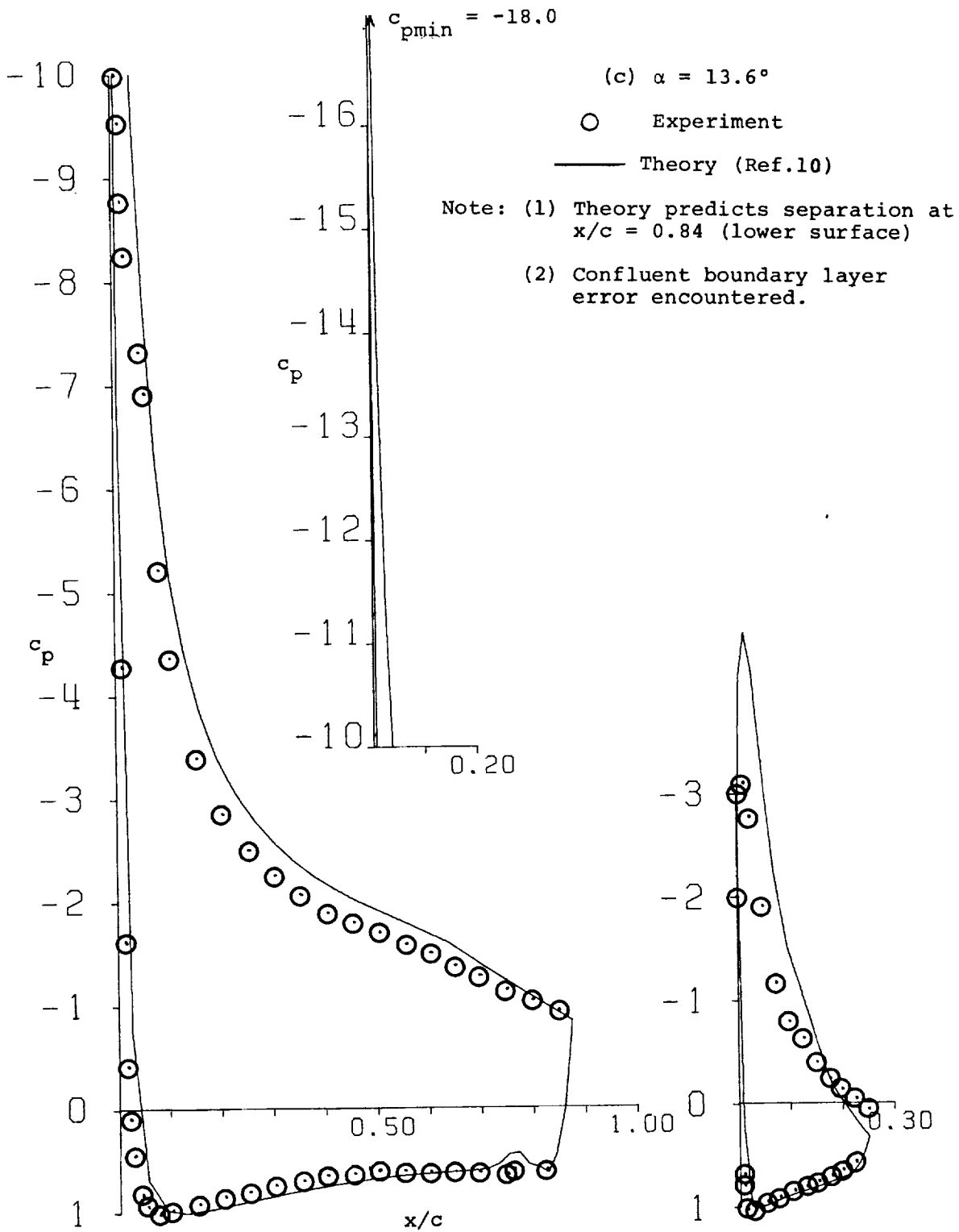


Figure 16 - Continued.

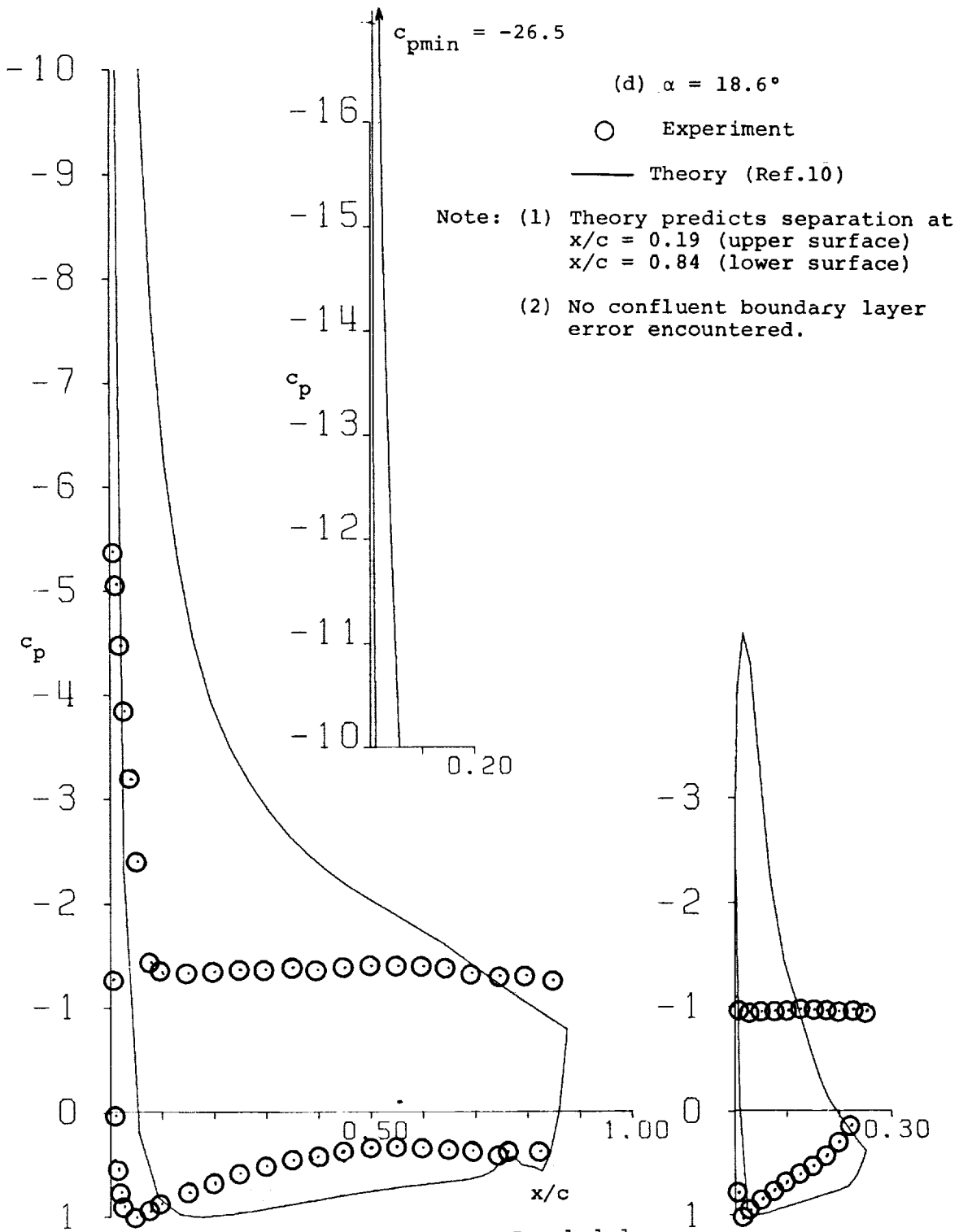
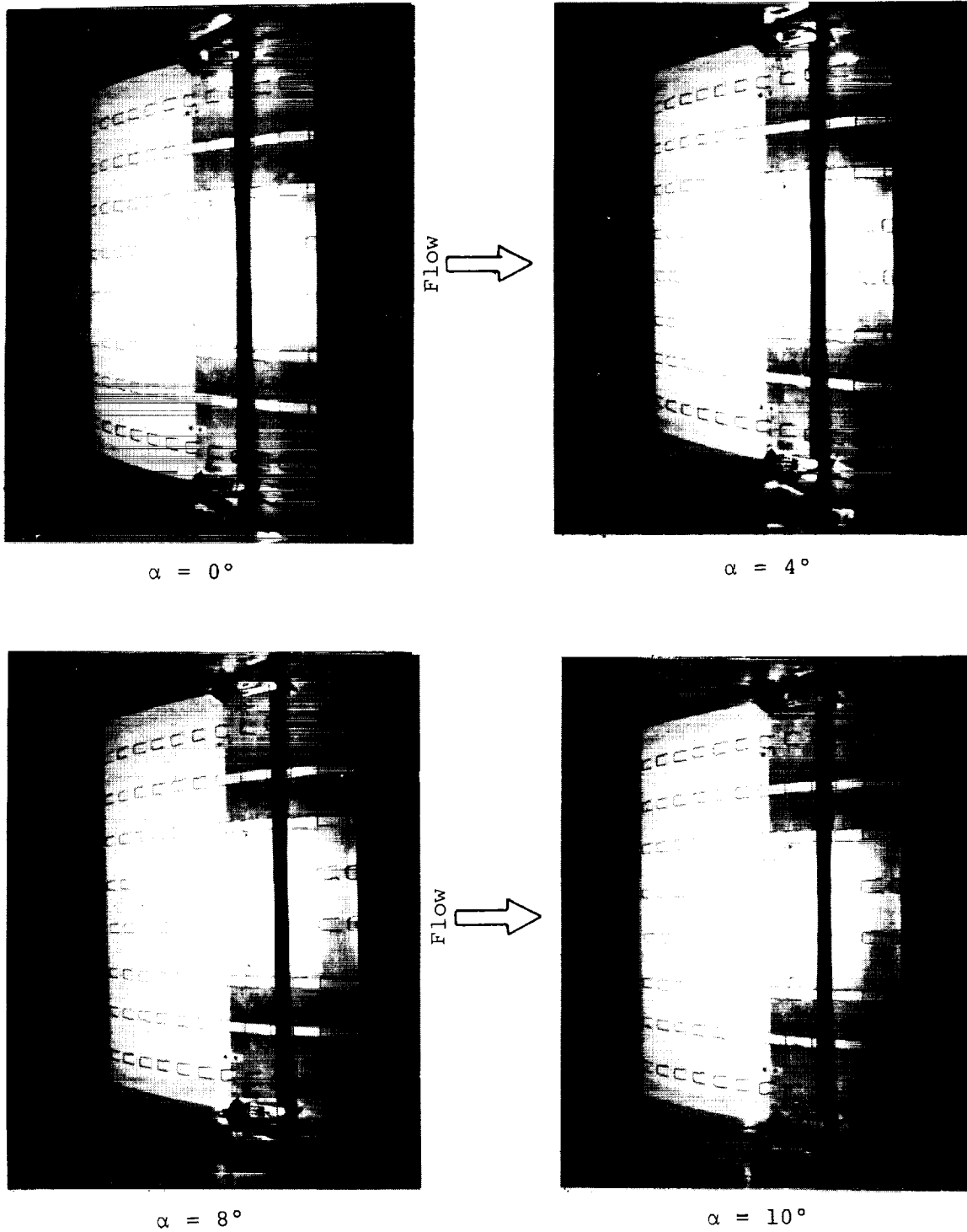
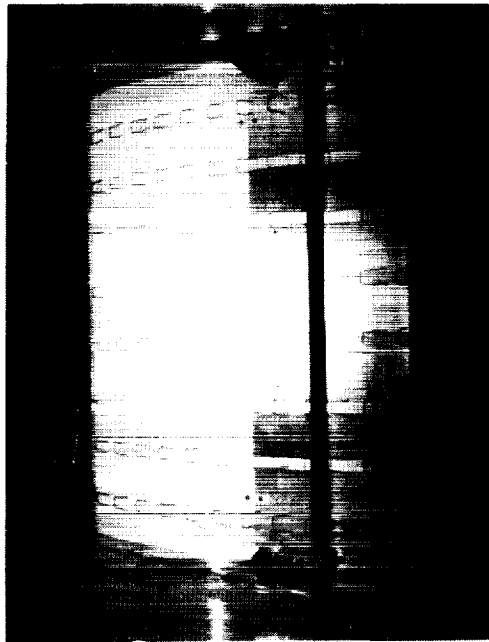


Figure 16 - Concluded.

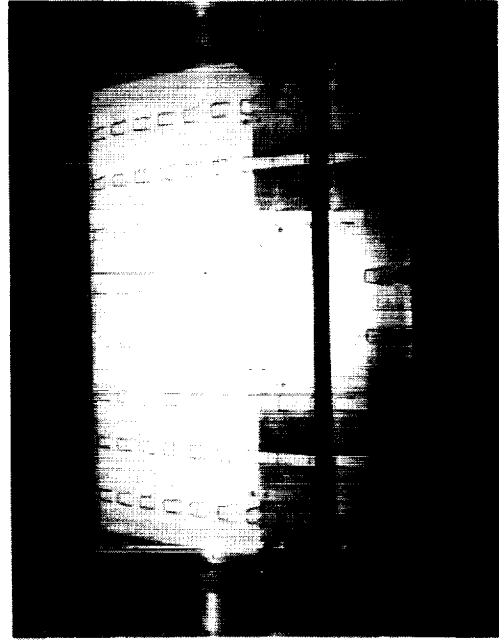


(a) Low angles of attack

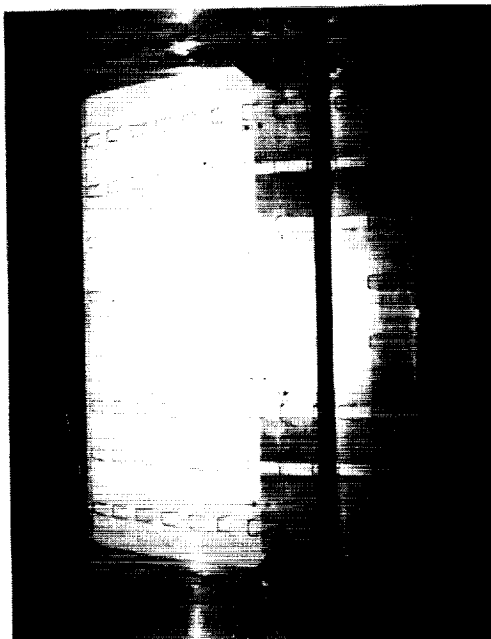
Figure 17 - Tuft Patterns with 25% Slotted Flap, 10° Flap Deflection.



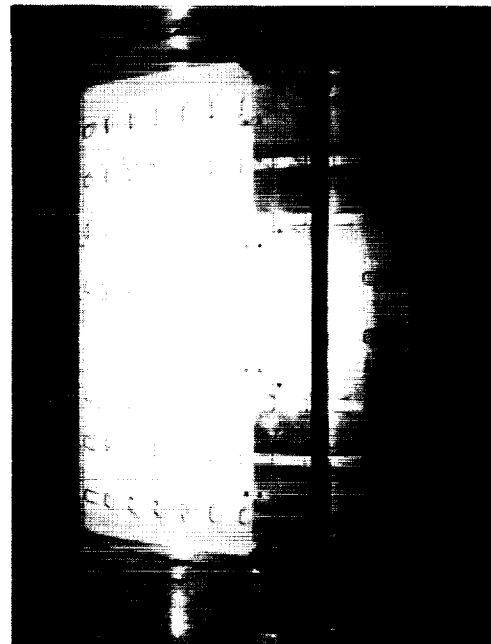
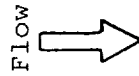
$\alpha = 12^\circ$



$\alpha = 14^\circ$



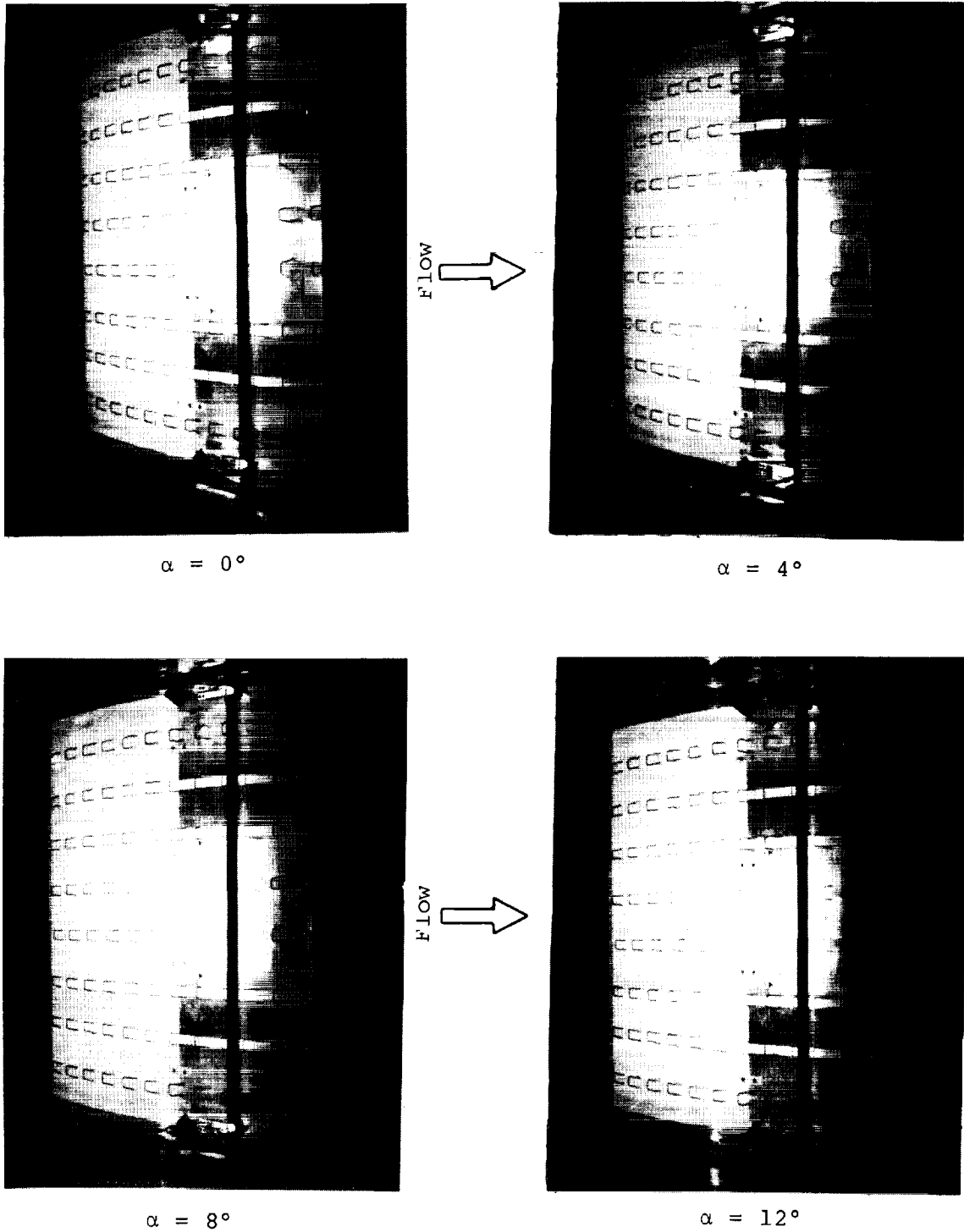
$\alpha = 16^\circ$



$\alpha = 18^\circ$

(b) High angles of attack

Figure 17 - Concluded.

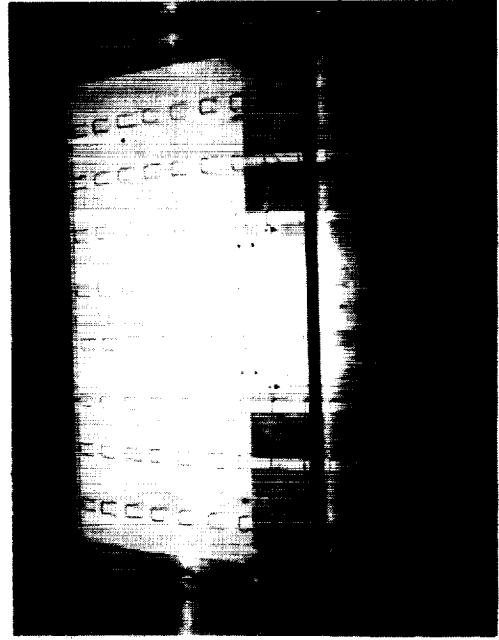


(a) Low angles of attack

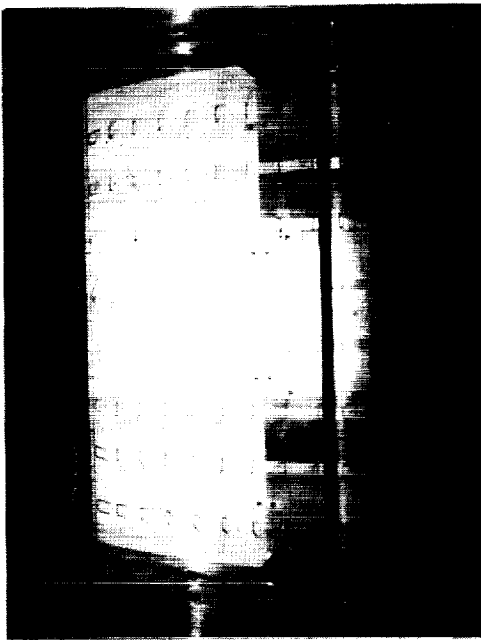
Figure 18 - Tuft Patterns with 25% Slotted Flap, 20° Flap Deflection.



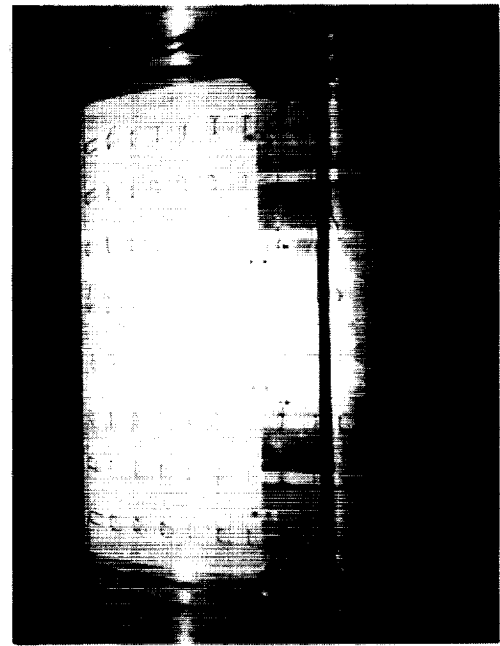
$\alpha = 14^\circ$



$\alpha = 16^\circ$



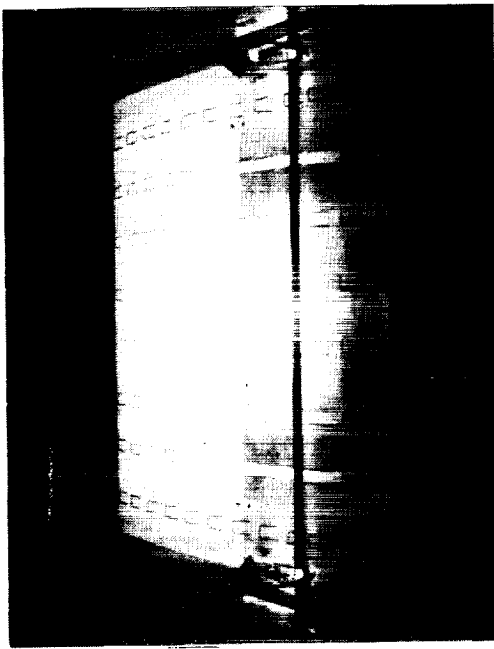
$\alpha = 17^\circ$



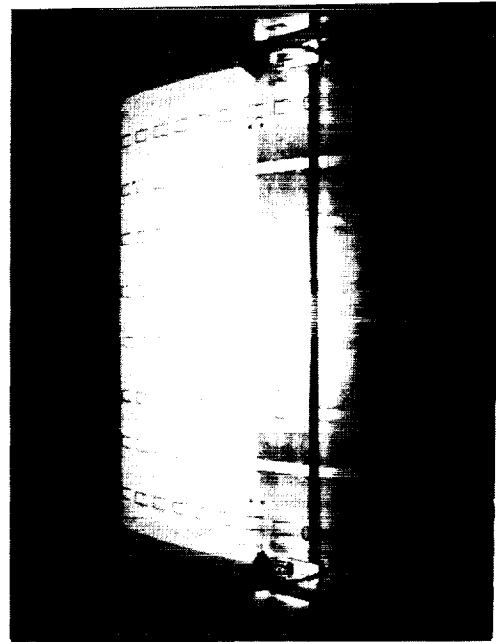
$\alpha = 18^\circ$

(b) High angles of attack

Figure 18 - Concluded.

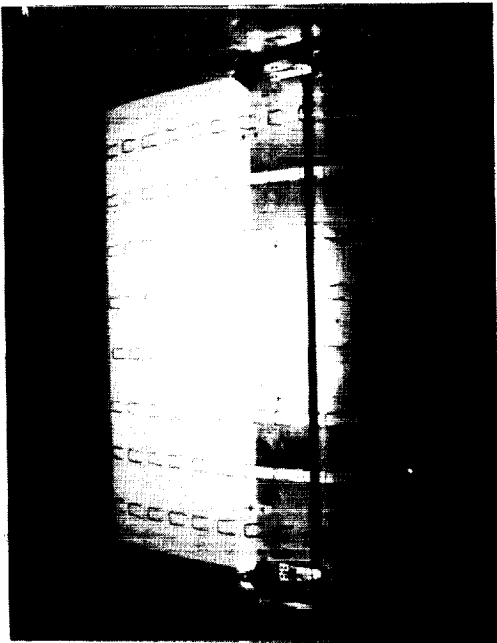


$\alpha = 0^\circ$

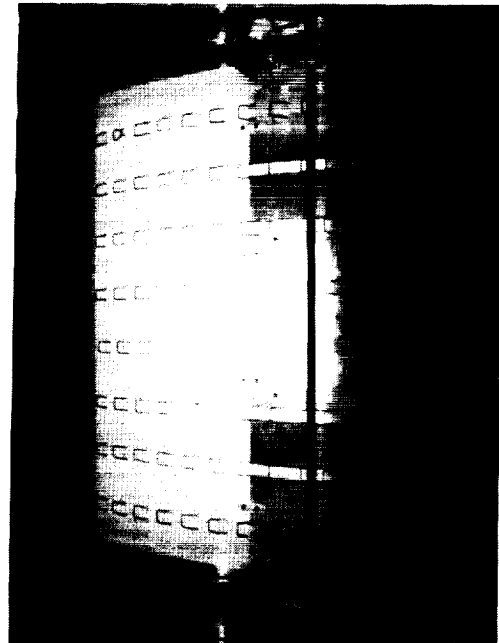


$\alpha = 4^\circ$

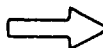
Flow 



$\alpha = 8^\circ$

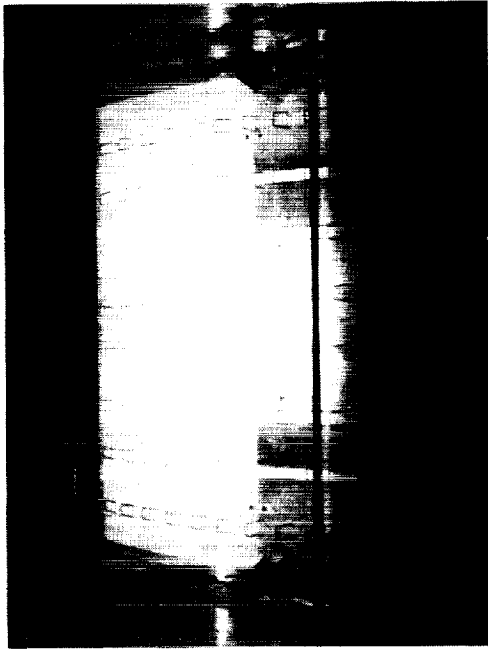


$\alpha = 10^\circ$

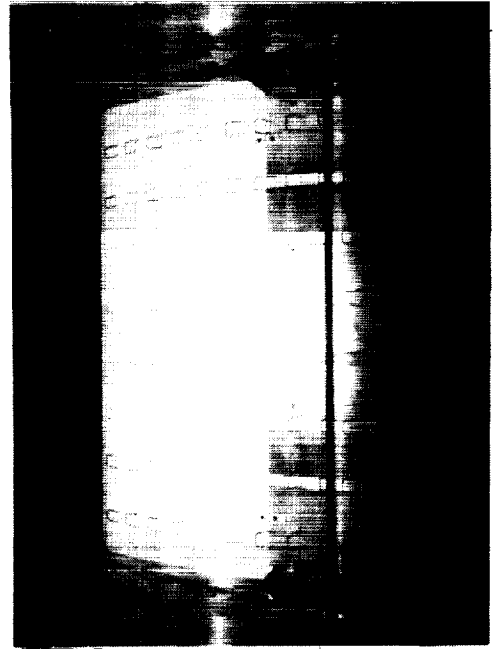
Flow 

(a) Low angles of attack

Figure 19 - Tuft Patterns with 25% Slotted Flap, 30° Flap Deflection.

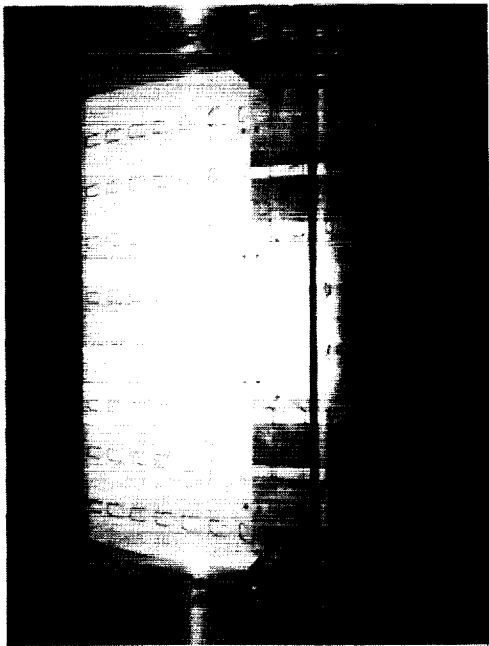


$\alpha = 12^\circ$

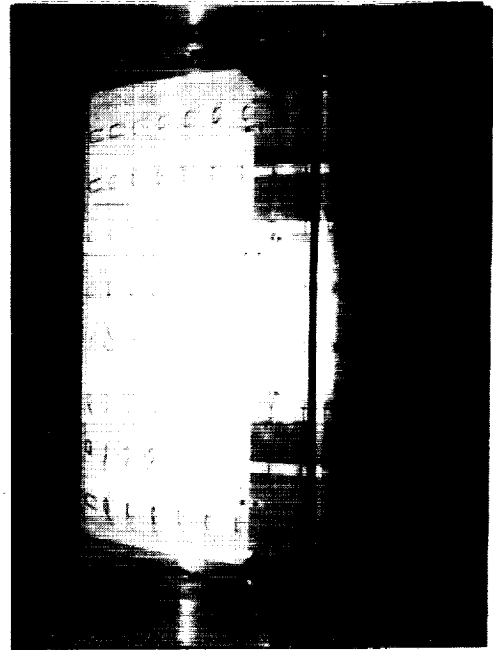


$\alpha = 14^\circ$

FLOW
→



$\alpha = 15^\circ$

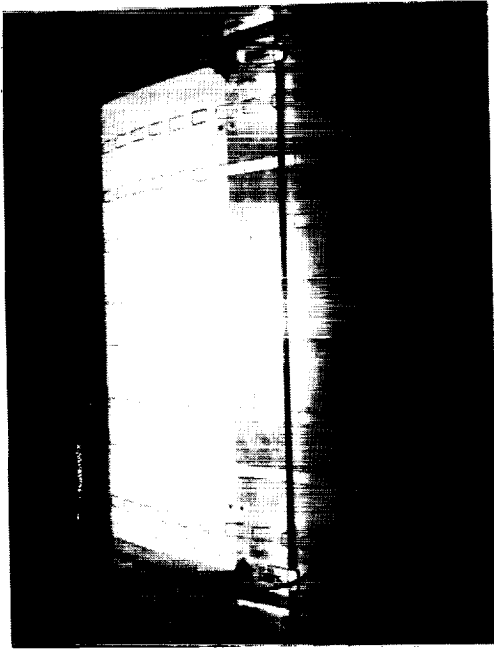


$\alpha = 16^\circ$

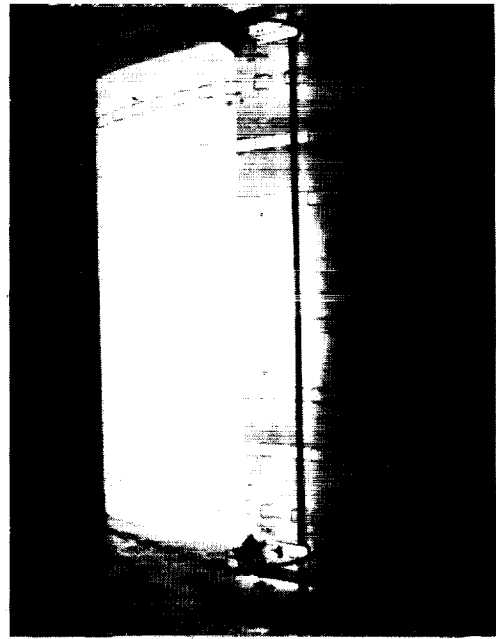
FLOW
→

(b) High angles of attack

Figure 19 - Concluded.



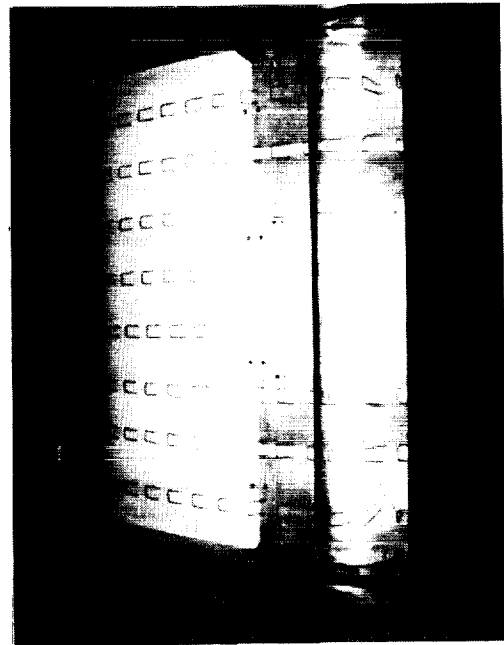
$\alpha = 0^\circ$



$\alpha = 4^\circ$



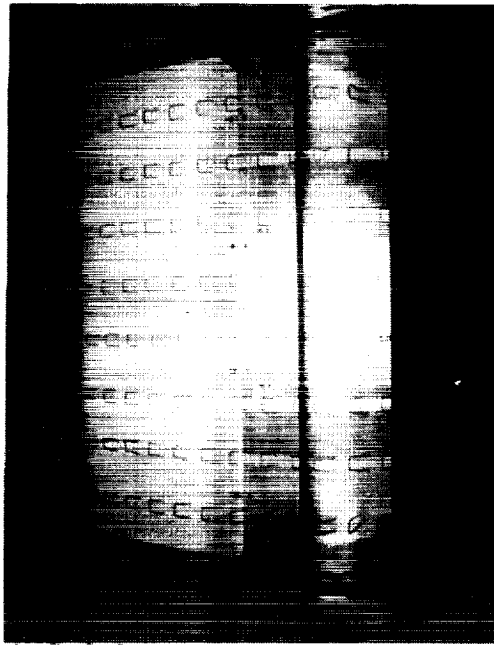
$\alpha = 8^\circ$



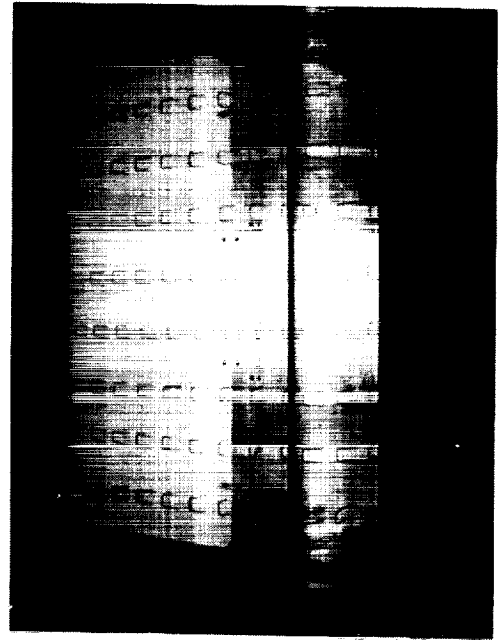
$\alpha = 10^\circ$

(a) Low angles of attack

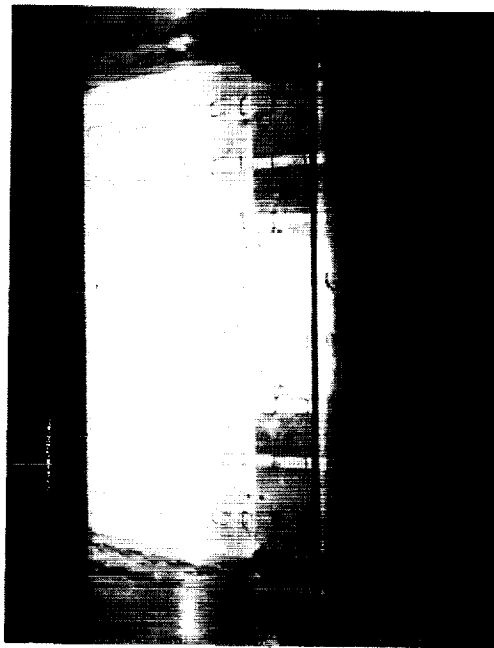
Figure 20 - Tuft Patterns with 25% Slotted Flap, 35° Flap Deflection.



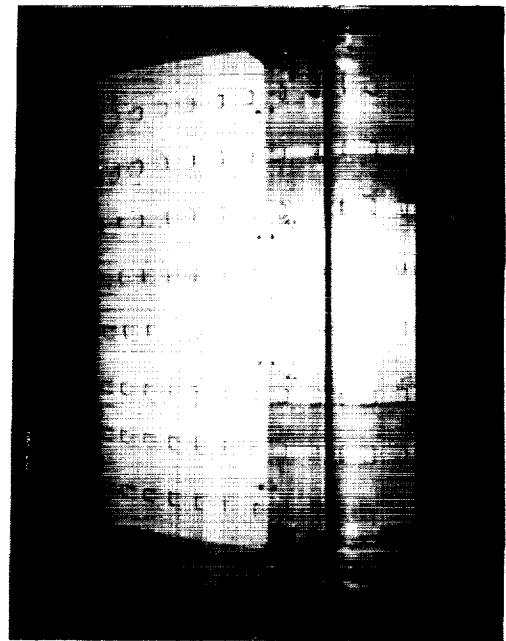
$\alpha = 12^\circ$



$\alpha = 14^\circ$



$\alpha = 15^\circ$



$\alpha = 16^\circ$

(b) High angles of attack

Figure 20 - Concluded.

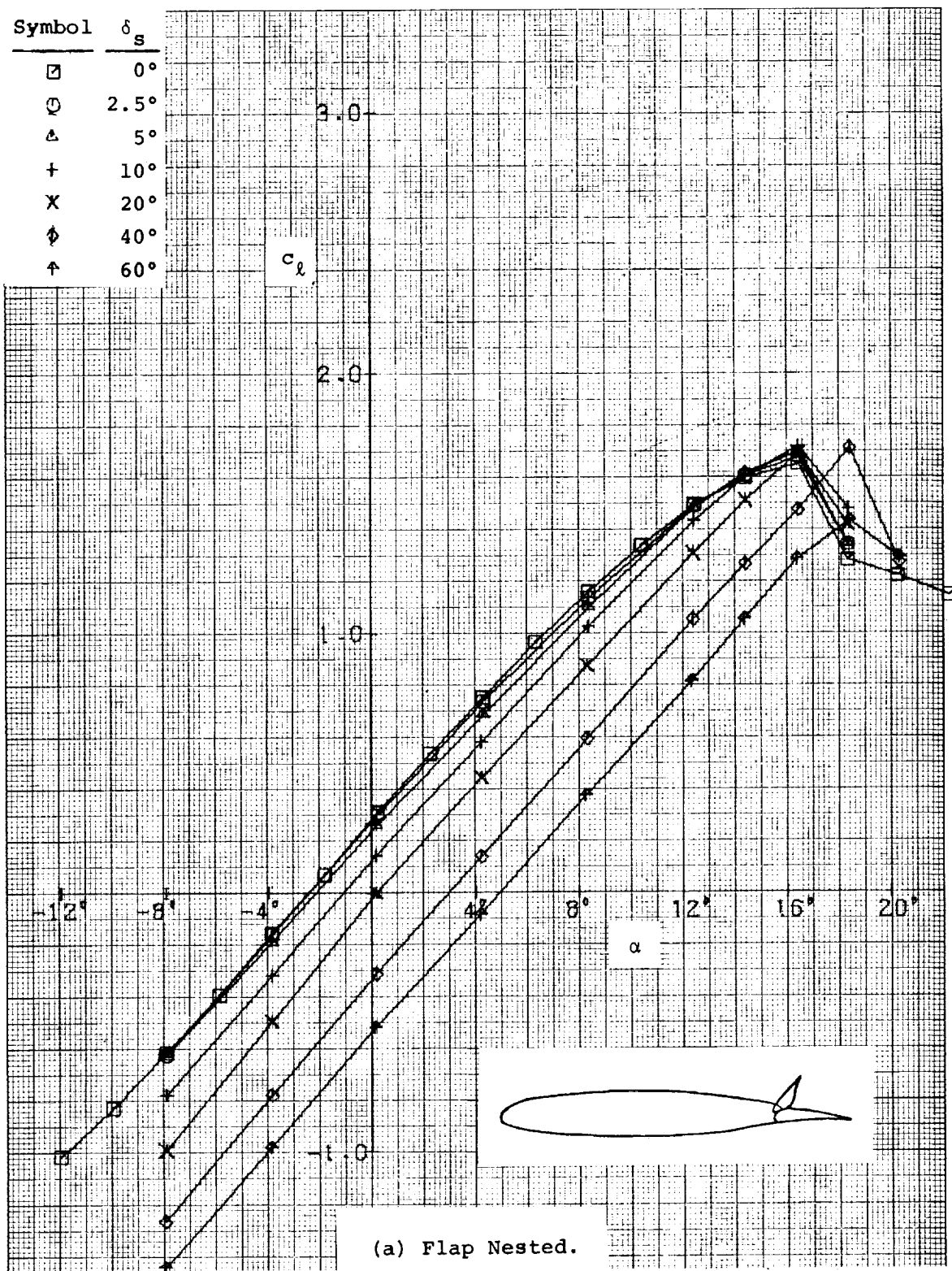
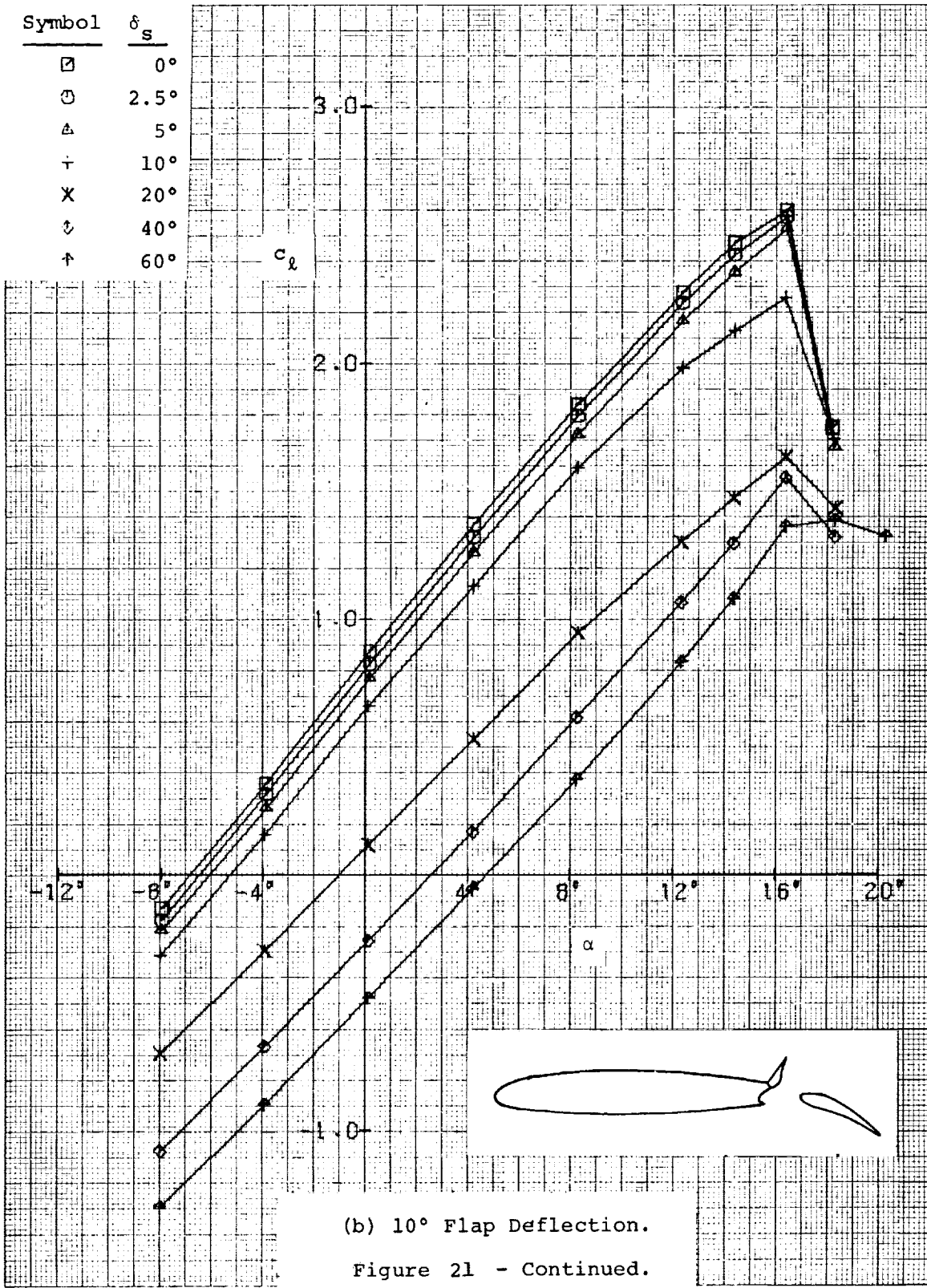
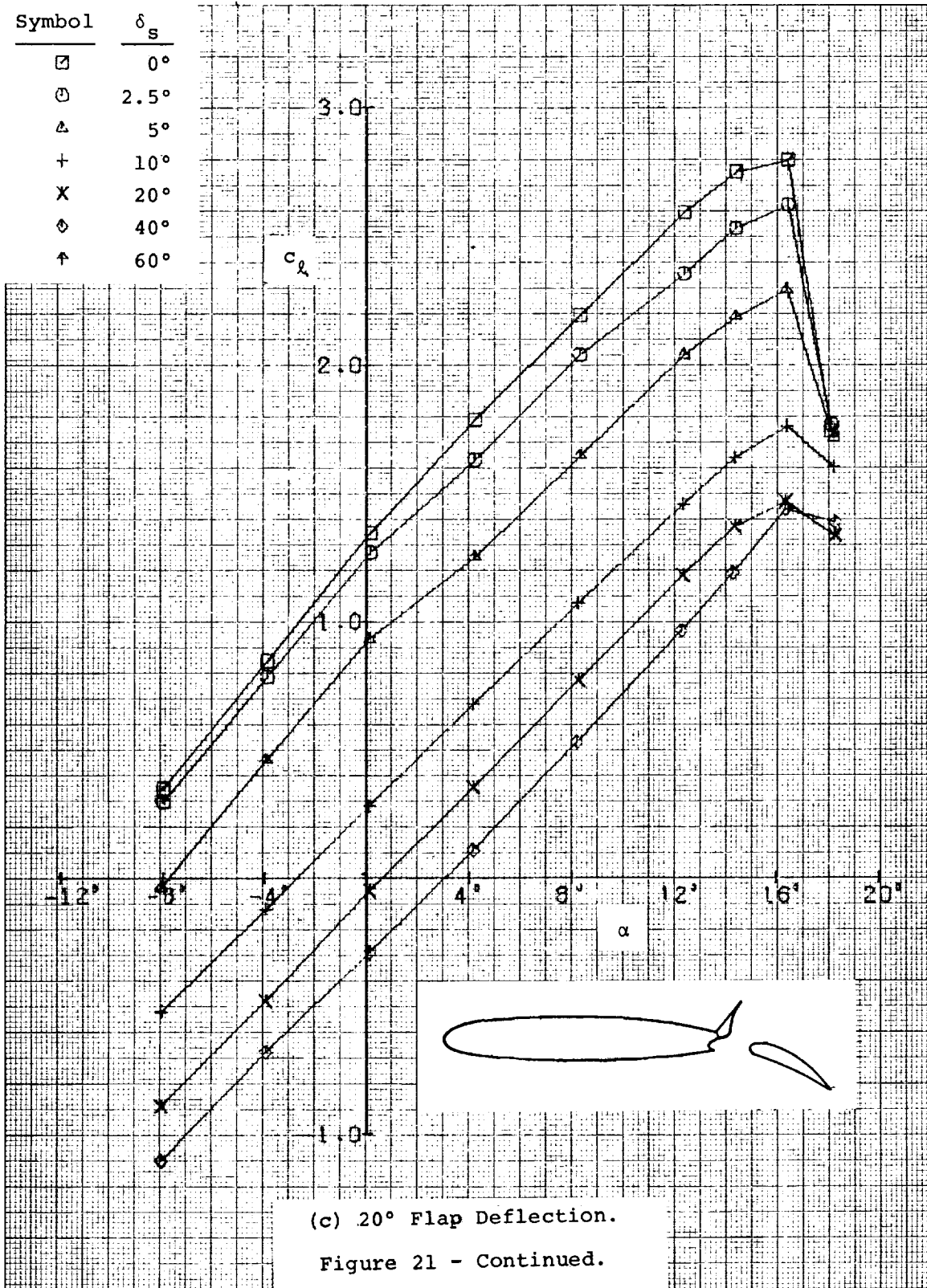


Figure 21 - Effects of Spoiler Deflection on Lift for 25% Flap.

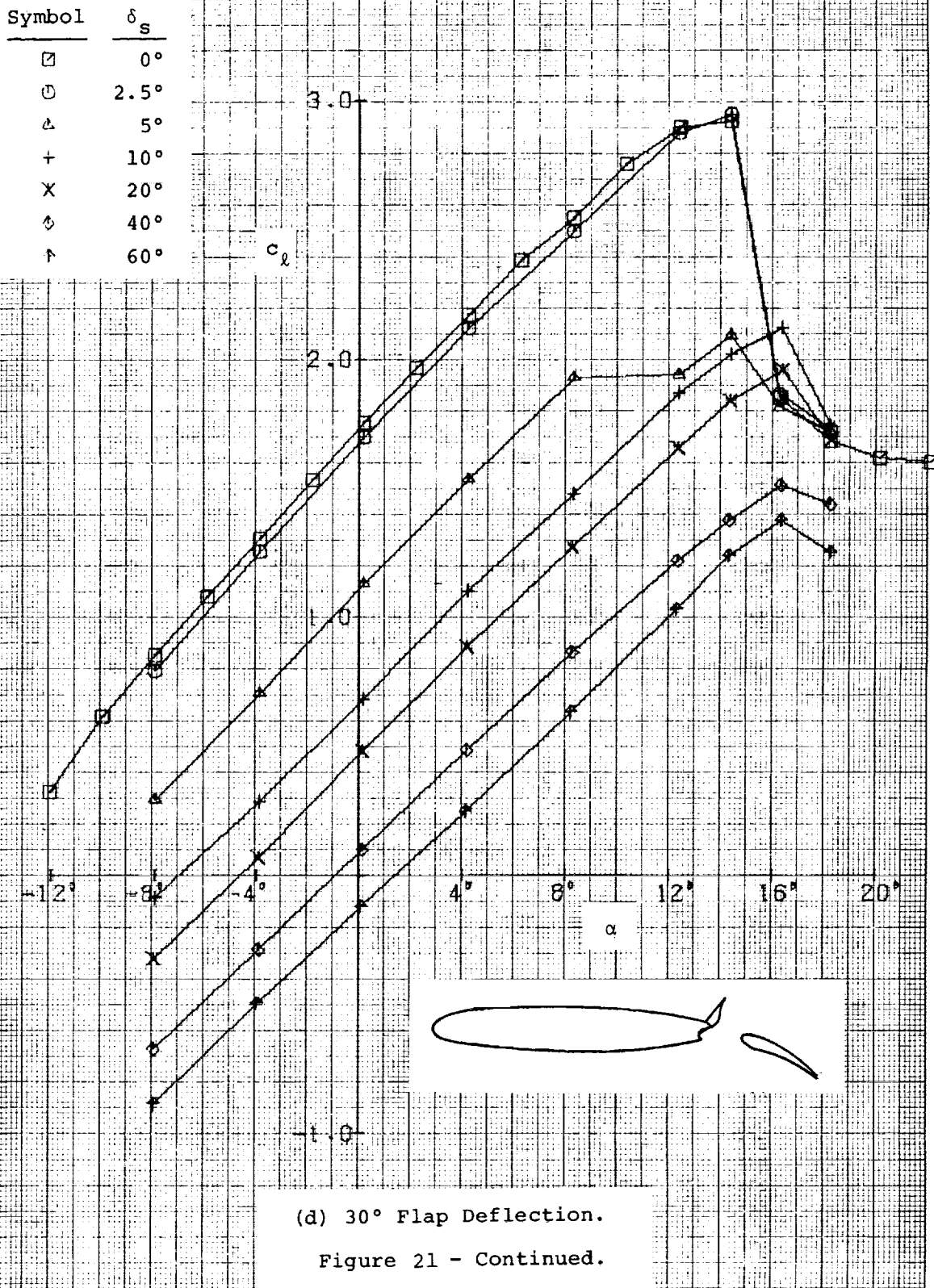


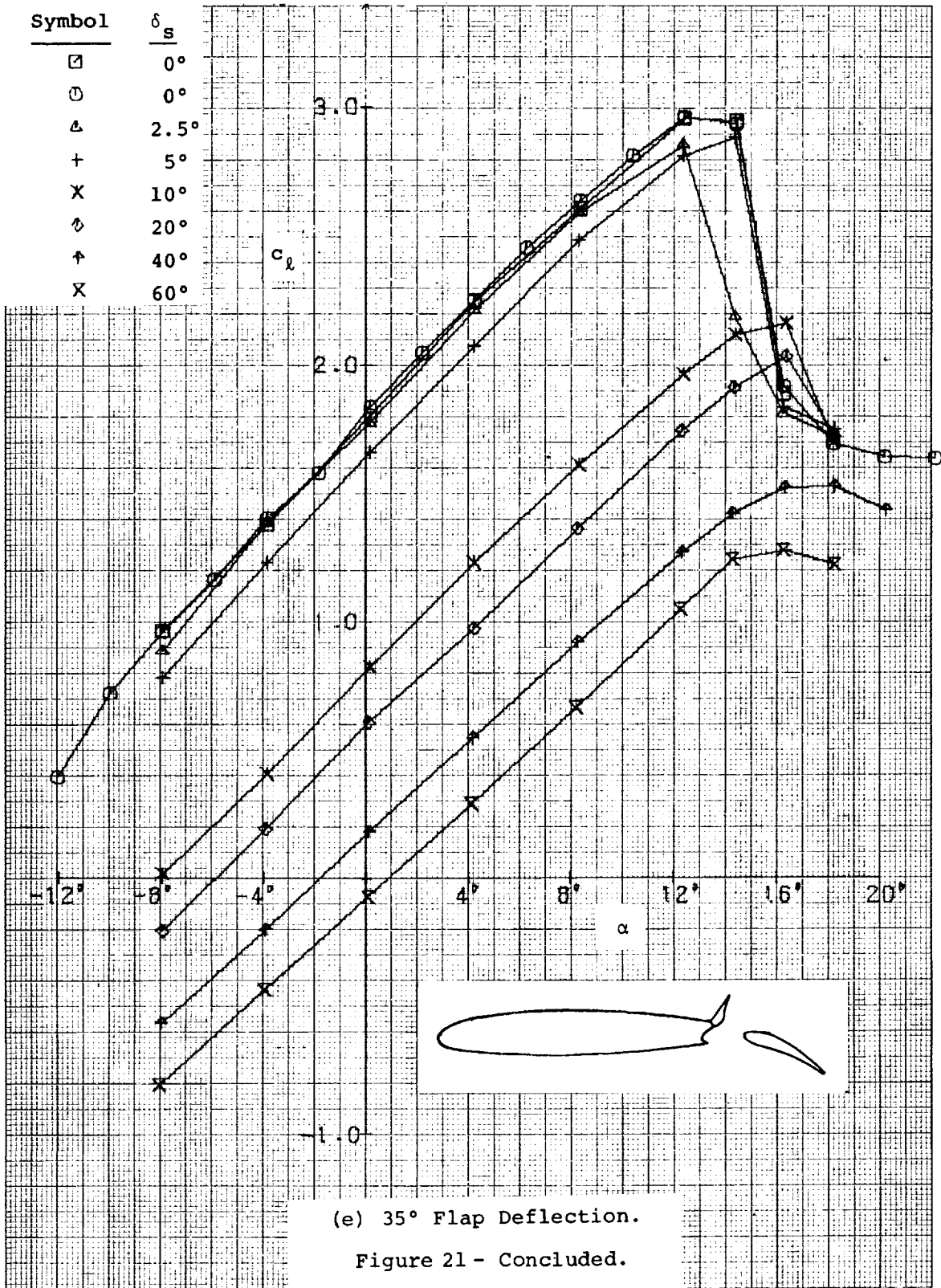
Symbol	δ_s
□	0°
⊙	2.5°
△	5°
+	10°
X	20°
◇	40°
↑	60°



(c) 20° Flap Deflection.

Figure 21 - Continued.



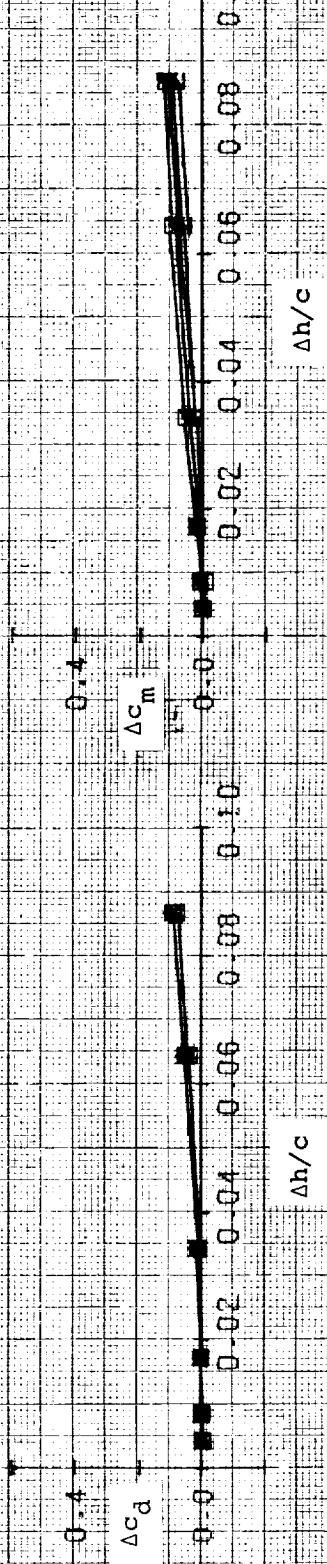


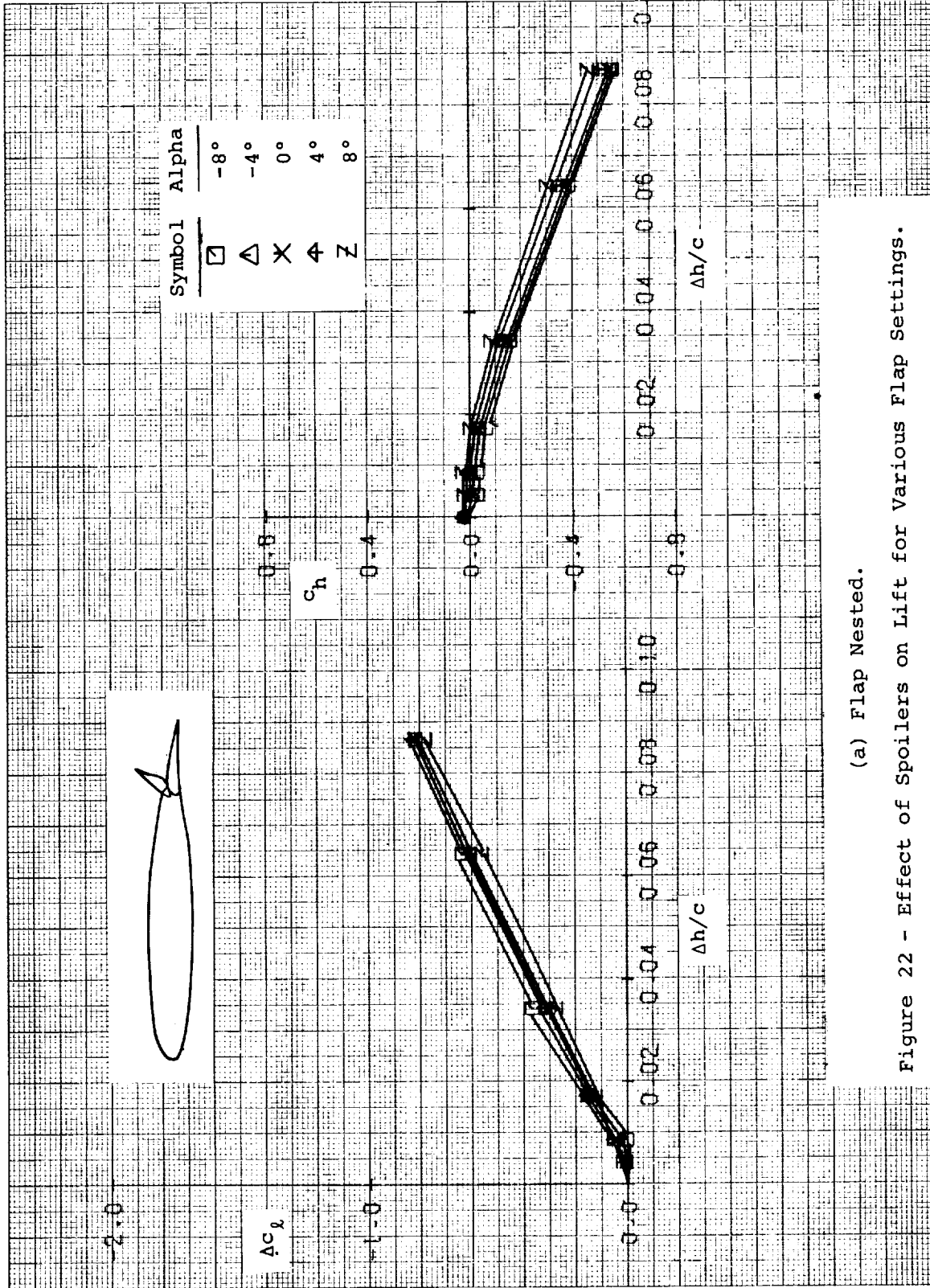
(e) 35° Flap Deflection.

Figure 21 - Concluded.



Symbol	Alpha
□	-8°
△	-4°
X	0°
+	4°
Z	8°



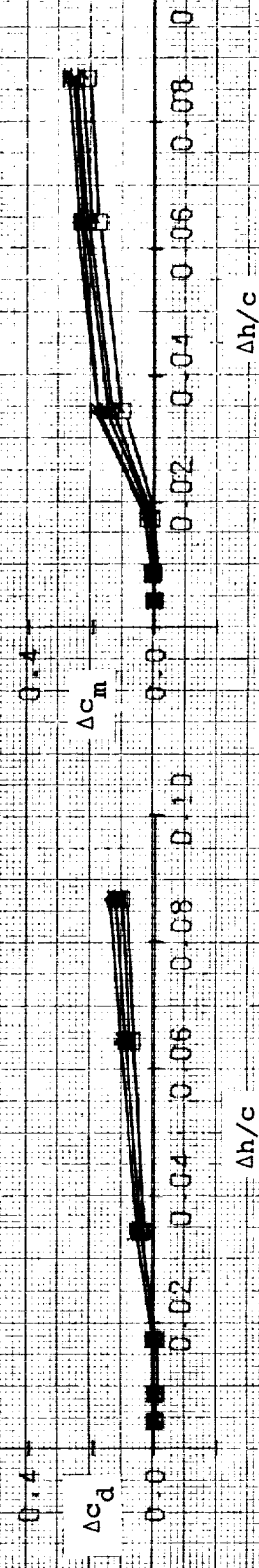


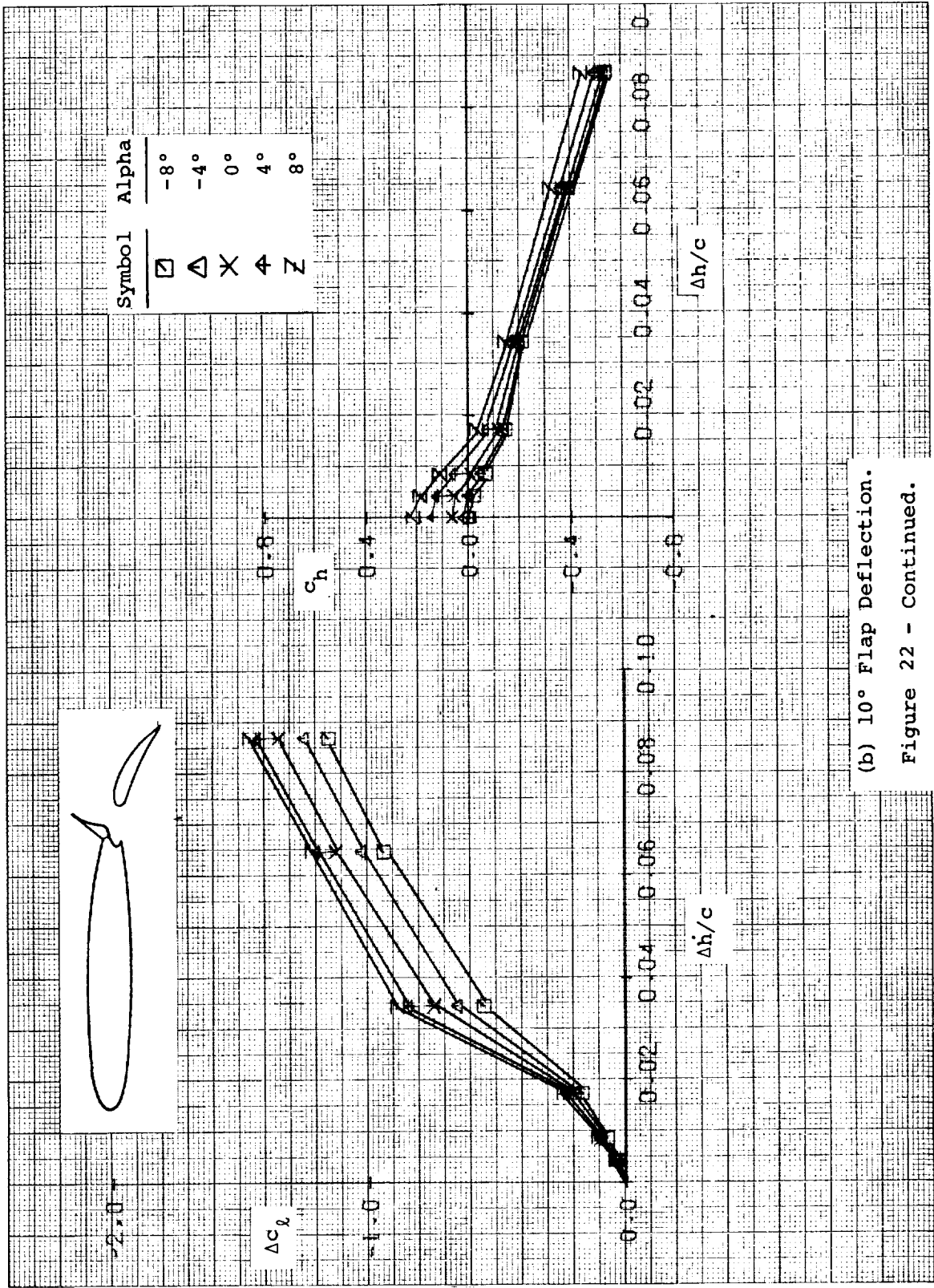
(a) Flap Nested.

Figure 22 - Effect of Spoilers on Lift for Various Flap Settings.



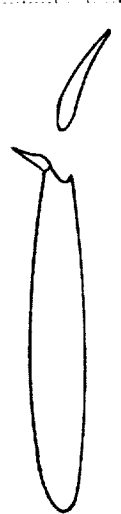
Symbol	Alpha
□	-8°
△	-4°
X	0°
⊕	4°
Z	8°



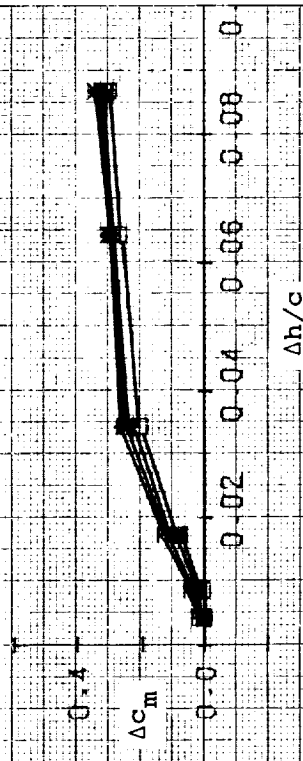
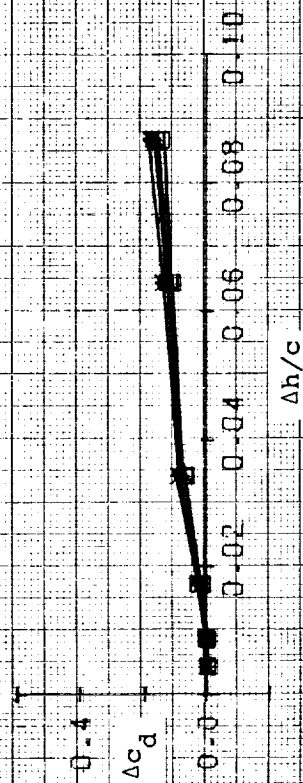


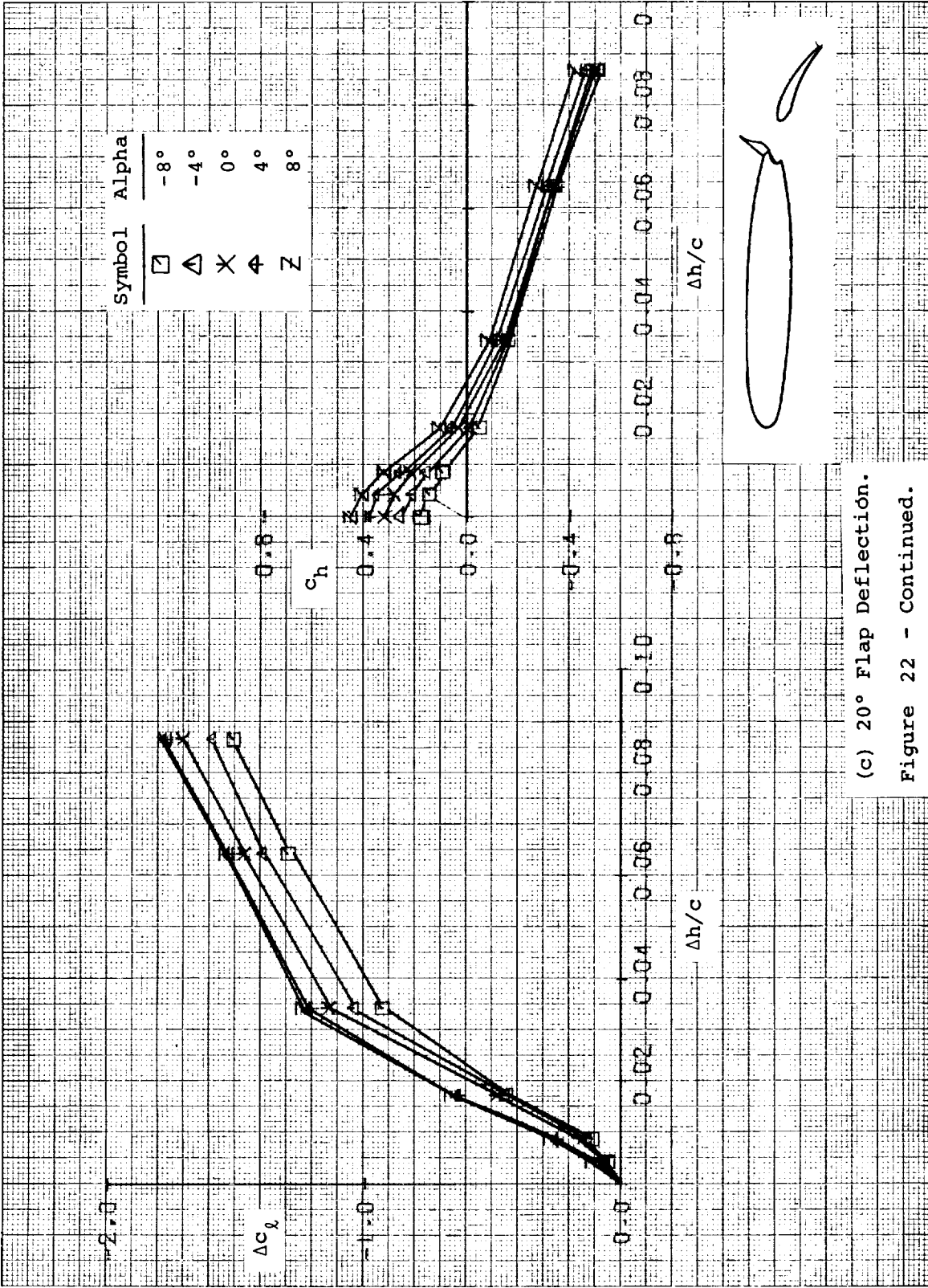
(b) 10° Flap Deflection.

Figure 22 - Continued.



Symbol	Alpha
□	-8°
△	-4°
X	0°
+	4°
Z	8°



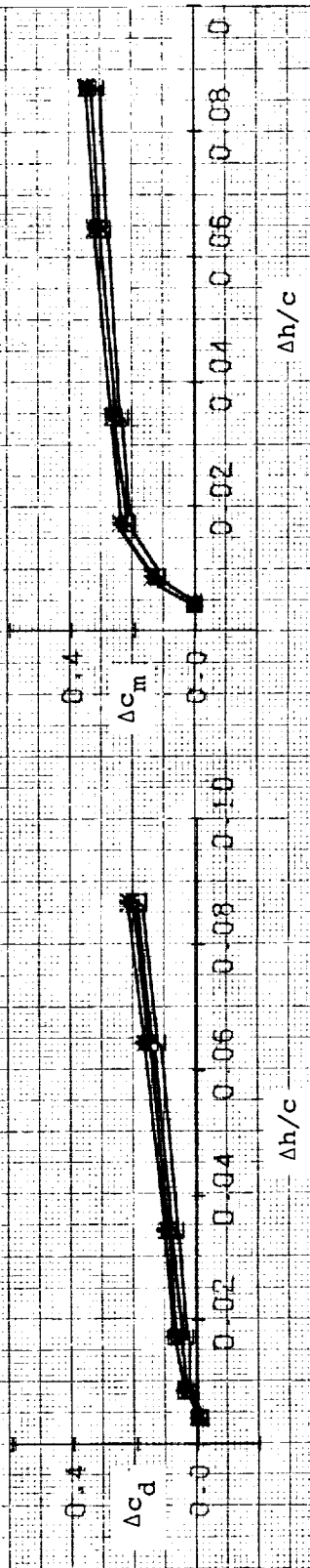


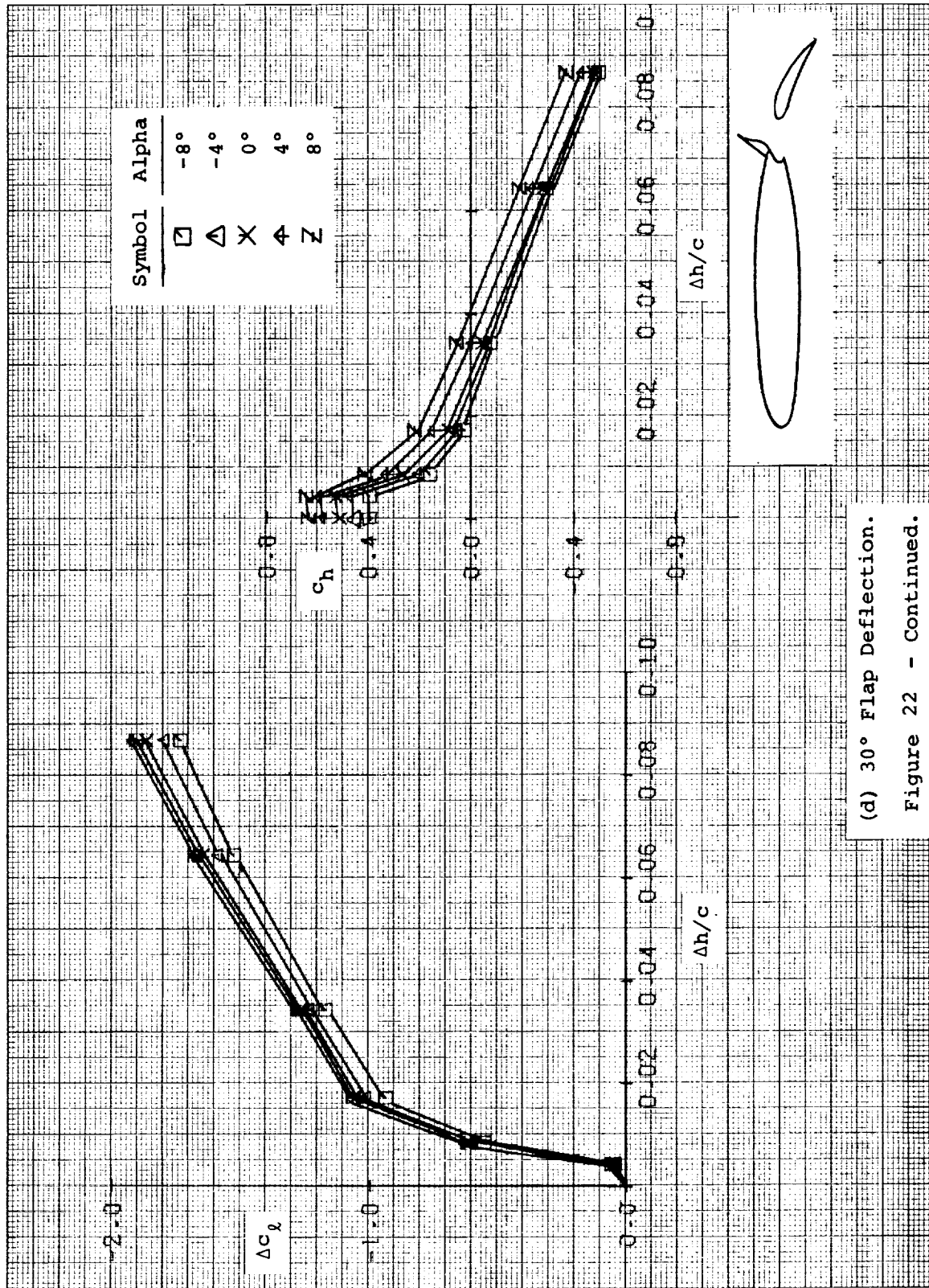
(c) 20° Flap Deflection.

Figure 22 - Continued.



Symbol	Alpha
□	-8°
△	-4°
×	0°
4	4°
Z	8°

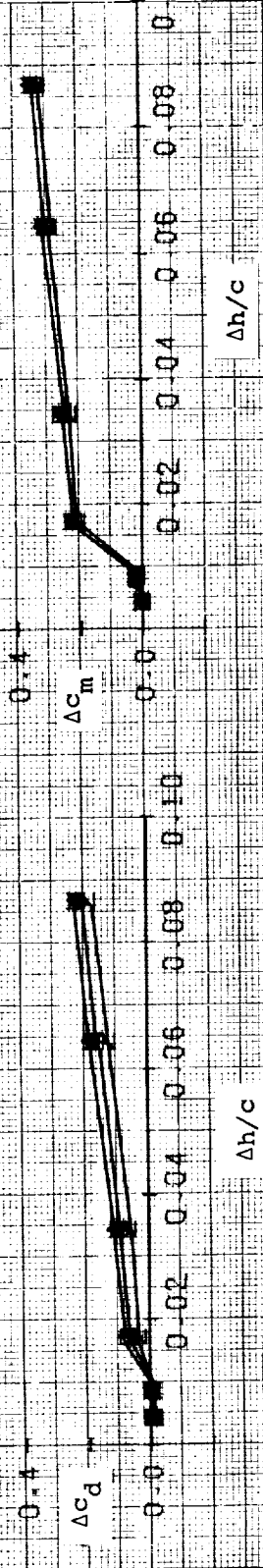


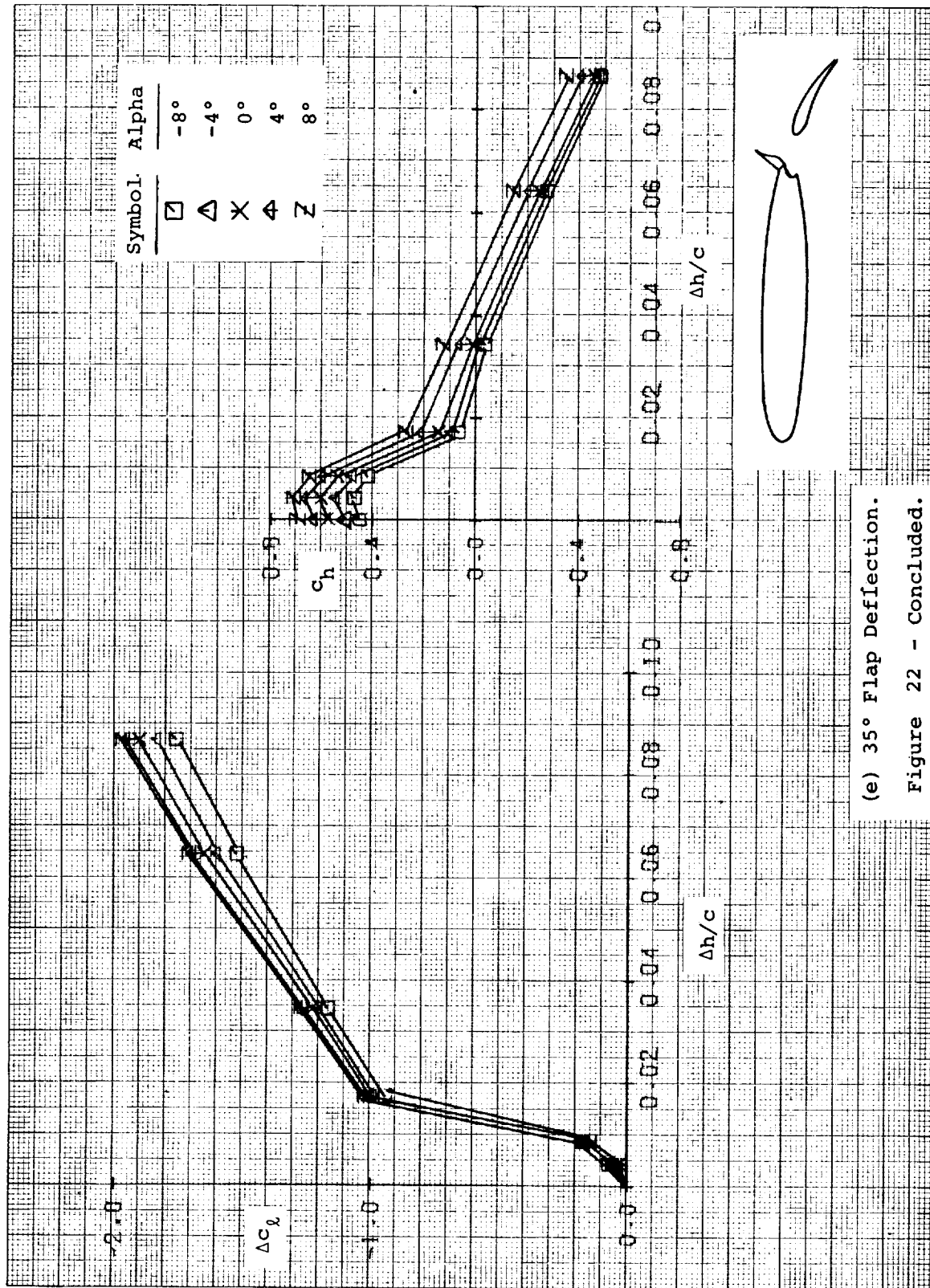


(d) 30° Flap Deflection.
Figure 22 - Continued.



Symbol	Alpha
□	-8°
△	-4°
×	0°
⊕	4°
Z	8°





(e) 35° Flap Deflection.

Figure 22 - Concluded.

1. Report No. NASA CR-3439		2. Government Accession No.		3. Recipient's Catalog No.	
4. Title and Subtitle WIND TUNNEL FORCE AND PRESSURE TESTS OF A 13% THICK MEDIUM SPEED AIRFOIL WITH 20% AILERON, 25% SLOTTED FLAP AND 10% SLOT-LIP SPOILER				5. Report Date JUNE 1981	
				6. Performing Organization Code	
7. Author(s) W. H. Wentz, Jr.				8. Performing Organization Report No. WSU AR 78-4	
9. Performing Organization Name and Address Wichita State University Wichita, Kansas 67208				10. Work Unit No.	
				11. Contract or Grant No. NSG-1165	
12. Sponsoring Agency Name and Address National Aeronautics and Space Administration Washington, D.C. 20546				13. Type of Report and Period Covered Contractor Report	
				14. Sponsoring Agency Code 505-31-33-05	
15. Supplementary Notes Langley Technical Monitor: Robert J. McGhee Topical Report					
16. Abstract Force and surface pressure distributions have been measured for a 13% medium speed (NASA MS(1)-0313) airfoil fitted with 20% aileron, 25% slotted flap and 10% slot-lip spoiler. All tests were conducted in the Walter Beech Memorial Wind Tunnel at Wichita State University at a Reynolds number of 2.2×10^6 and a Mach number of 0.13. Results include lift, drag, pitching moments, control surface normal force and hinge moments, and surface pressure distributions. The basic airfoil exhibits low speed characteristics similar to the GA(W)-2 airfoil. Incremental aileron and spoiler performance are quite comparable to that obtained on the GA(W)-2 airfoil. Slotted flap performance on this section is reduced compared to the GA(W)-2, resulting in a highest $c_{l_{max}}$ of 3.00 compared to 3.35 for the GA(W)-2.					
17. Key Words (Suggested by Author(s)) Airfoil design Control surface Pressure distributions Aerodynamic forces Flap			18. Distribution Statement RESTRICTED Subject Category 2		
19. Security Classif. (of this report) Unclassified		20. Security Classif. (of this page) Unclassified		21. No. of Pages 116	22. Price